Characterization of Silver-Polyaniline-Epoxy Conductive Adhesives

by

Sarang Gumfekar

A thesis
presented to the University of Waterloo
in fulfillment of the
thesis requirement for the degree of
Master of Applied Science
in
Chemical Engineering

Waterloo, Ontario, Canada, 2012

AUTHOR'S DECLARATION

I hereby declare that I am the sole author of this thesis. This is a true copy of the thesis, including any required final revisions, as accepted by my examiners.

I understand that my thesis may be made electronically available to the public.

Abstract

Electrical conductive adhesives (ECAs) containing silver filler and polyaniline co-filler were characterized for their electro-mechanical properties. Polyaniline is a conductive polymer and has a moderate conductivity in between those of the silver and epoxy. Incorporation of polyaniline (µm sized) in silver-epoxy facilitated the electrical conduction in ECAs and reduced the percolation threshold- a minimum volume of filler necessary to initiate the conduction. It also prevented the localization of charge carriers due to aggregation of silver filler particles. 'Bridging effect' was observed due to addition polyaniline in which the polyaniline enhanced the tunneling of electrons over the silver filler particles. We have investigated the polyaniline co-fillers as a promising alternative way to tune the mechanical and electrical properties of the ECAs and have provided a detailed analysis of the electro-mechanical properties of silver-epoxy (Ag-epoxy) and silver-polyaniline-epoxy (Ag-PANI-epoxy) system in both partially-cured/ viscoelastic and fully-cured states. Analysis of electro-mechanical properties of silver-epoxy and silver-polyaniline-epoxy also provided the insights into electrical contact resistance of ECAs under compressive force. Electro-mechanical properties of ECAs were measured '*in-situ*' using micro-indentation technique. We also synthesized the electrically conductive and highly crystalline nanotubes of polyaniline by mini-emulsion polymerization of aniline. The motivation behind the synthesis of polyaniline was to propose a potential filler/co-filler for replacement of metallic filler in ECAs. Electrical conductivity of polyaniline nanotubes was tuned by *in-situ* doping using hydrochloric acid as a dopant. Increase in dopant caused the polyaniline crystallite to grow along (400) plane. Optical, structural, electrical and thermal properties of polyaniline nanotubes are reported with varying amount of dopant. We fabricated the flexible electrically conductive coating of polyaniline tubes with uniform dispersion of polyaniline. Electrical performance of as-synthesized flexible coating is also revealed.

Acknowledgements

I owe deepest gratitude to my research supervisor, Professor Boxin Zhao, who imparted disciplines of academic research in me with significant flexibility in work. He offered his continuous advice and encouragement throughout the course of this research; especially during difficulties in getting the results. In addition to guiding this research, the opportunities Prof. Zhao provided to broaden my professional experience and prepare me for future challenges are gratefully acknowledged. His technical and editorial advice was essential to the completion of this thesis. I sincerely cannot help but express how I should credit this thesis to his constant support, encouragement and guidance. I hope that I could be as lively, hardworking, and energetic as him. It has been an honor working with him.

I am also thankful to The Natural Sciences and Engineering Research Council of Canada (NSERC) for providing financial support. I am also grateful to our industry partners- *Celestica Inc, Microbonds Inc and Research In Motion (RIM)*. They were instrumental in shaping of the project. Particularly, I am grateful to Alex Chen, John Persic and others who gave important suggestions on research work. I am thankful to the Microbonds team for introducing us to their facilities.

Besides my research supervisor, I would like to thank my fellow labmates Arun, Kuo, Hamed, Behnam, Wenjie, Brendan, Hadi, Wei, Yougun and Chong for the stimulating discussions on research work and for all the fun we had in last two years. I am also grateful to my friends Harsh, Ameya, Saurabh and Kali who made my stay 'homely' in Waterloo.

Most importantly, I am very much thankful to Prof. Shirish Sonawane and Prof. Chandrashekhar Mahajan, India for enlightening me the first glance of research. It was their kindness and open arms that convinced me to pursue higher education. No words can express how grateful I am for their encouragement to dream for bright career.

Yet among all stand my parents, grandparents and my brother Sanket, whose profound support and inspiration deserve special acknowledgement. My grandpa and late granny have been a source of unparalleled motivation and love. They have supported me in the darkest times and believed in me even when I did not believe in myself. I hope the fruitful completion of this thesis justifies the countless sacrifices on their part.

-Sarang Prakash Gumfekar

Dedication

To my beloved grandparents, parents and brother, Sanket. You truly are gifts from God.

Table of Contents

List of Figures

List of Tables

Chapter 1
Introduction

Integrated circuits are important parts of the modern electronic devices. However, it can't form a complete system unless integrated with various functional components on the system board. "Electronic packaging" plays an important role to integrate the system-level functional components with integrated circuit. Electronic packaging is defined as the bridge that interconnects the integrated circuits and other functional components into a system-level board to form electronic products [1]. The packaging is employed to serve the following functions: a medium to distribute the current, as a thermal management material and protection of the components. The challenge for the packaging material is to provide the crucial functions required by the microelectronic system without limiting the performance of an individual component. Conductive adhesive is the latest generation of packaging materials compared to surface mount technology (SMT), ball grid array (BGA), chip-scale package (CSP) and flip chip technology [2], [3]. Figure 1-1 shows the schematic of integrated circuit and functional surface mount component attached to a substrate via interconnect materials.

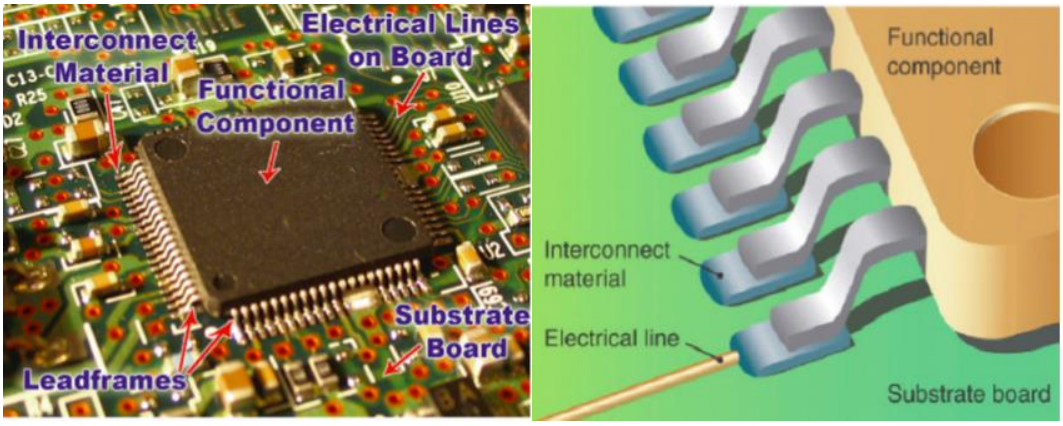

Figure 1-1: Schematic of integrated circuit and joining of functional component to a substrate via interconnect material [2] (reproduced with permission Copyright 2009, Springer)

The lead (Pb)-containing solders covered the majority of electronic packaging market in last two decades. Due to the human and environment hazard of lead-containing materials, the electronic industry is moving towards green manufacturing as a global trend. Electrical conductive adhesives (ECAs) are the promising candidates for the lead-free and environment-friendly materials. Figure 1-2 (on next page) shows the overview of materials for electrical interconnect.

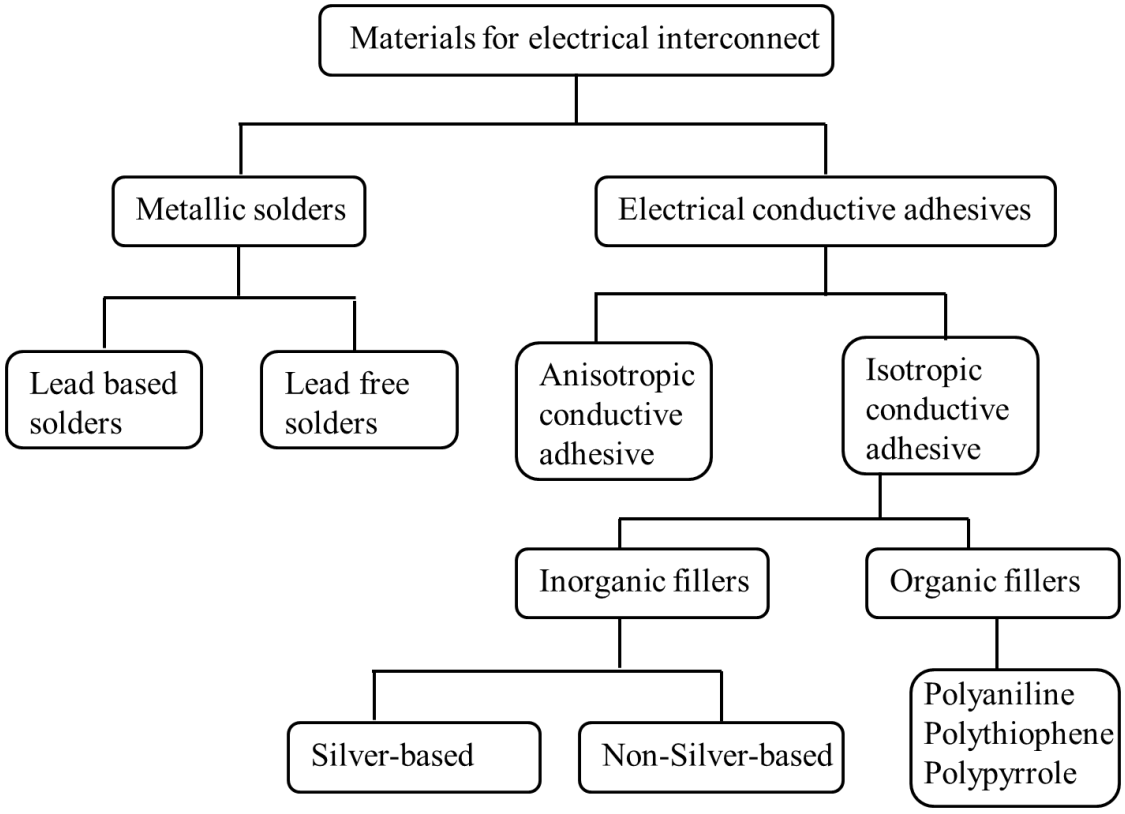

Figure 1-2: Hierarchical overview of materials for electrical interconnect

ECAs mainly consist of polymeric binder and conductive fillers. These electrically conductive compositions can tuned to a myriad of conductivity values with the proper selection of filler, its size, shape and loading concentration into its host polymeric matrix. Electronic packaging using ECA is benefited because of environmental friendliness e.g. elimination of lead, flux cleaning, mild processing conditions and fewer processing steps [2], [4], [5]. ECAs are also preferred over metallic conductors due to easy methods of applying and efficient processing. The main requirement of ECA industries is the high electrical conductivity and mechanical strength. To address this issue, use of silver as a primary filler and epoxy as a host polymer matrix is an effective solution. But, the solution to increase the conductivity can't be as simple as increasing the silver concentration in epoxy. Relatively higher cost of silver prevents its excessive use in ECAs. Physical properties such as adhesion, modulus, and impact strength also suffer due to over loading of silver. Therefore, it is important to determine the minimum volume of silver required to impart electrical conductivity to ECAs. The term "percolation threshold" refers to the minimum volume of the silver filler required to initiate the conduction. Addition of intrinsically conducting polymer co-filler such as polyaniline also

serves a better option to balance between the electrical conductivity and other physical properties of ECAs. Though polyaniline possess less conductivity compared to silver, its incorporation in silver-filled epoxy should have minimal effect on physical properties of ECAs. Following fish-bone diagram summarizes various aspects of ECAs.

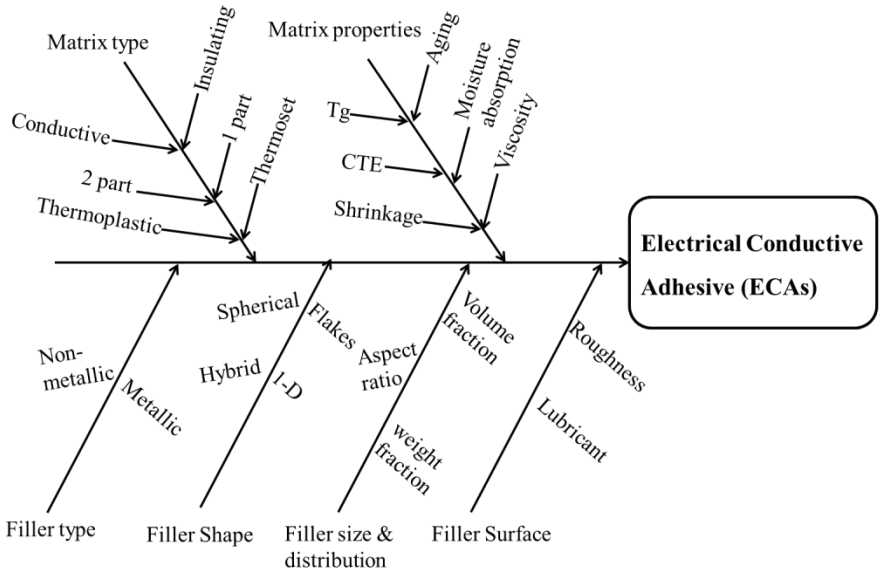

Figure 1-3: Summarization of various aspects of ECAs using fish-bone diagram

The purpose of this study is to understand the percolation threshold and electro-mechanical behavior in silver-polyaniline-epoxy conductive adhesive. We also have explored the possibility to synthesize highly crystalline polyaniline nanotubes for the use in ECAs. Potential enhancements in properties of conductive organic filler such as polyaniline can open up new possibilities to partially replace the metals in ECAs. Conductivity improvement with the use of polyaniline as a co-filler can be instrumental in cost reduction by attaining the target conductivity with less amount of silver in ECAs.

The thesis is comprised of 6 chapters. General information about the field, current status and demands, and thesis framework is highlighted in chapter 1 as introduction. Chapter 2, in detail, describes the basics of ECAs, various aspects of silver addition in ECAs and properties of polyaniline to be used as a co-filler in ECAs. It also describes the concepts of contact resistance and conduction mechanism in ECAs. In chapter 3, the percolation threshold of silver-epoxy and silver-polyaniline-epoxy conductive adhesive and corresponding mechanism will be discussed. Through this chapter, we demonstrate the novel '*in-situ*' electro-mechanical characterization technique for ECAs. Also, the electrical behavior of both systems under indentation force and stability of contact resistance will be

discussed. In chapter 4, we explain the electro-mechanical behavior of visco-elastic conductive adhesives using '*in-situ*' electro-mechanical indentation technique. Effect of polyaniline on visco-elastic behavior of silver-filled conductive adhesive is discussed, and validated using Burger's micromechanical model. In chapter 5, we demonstrate the synthesis and detailed characterization of highly crystalline and electrically conductive nanotubes of polyaniline. Additionally, the performance of polyaniline nanotubes in flexible coatings will be demonstrated. Finally, the conclusions and future trend in the field has been discussed in chapter 6. The work described in chapter 3 has been presented in 13th IEEE conference on *Electronics Packaging Technology Conference* (EPTC 2011) at Singapore which subsequently, indexed in *IEEE Xplore*® Digital Library; cited as reference [6] in this thesis. The results presented in chapter 4 are formatted for publication in the journal- *Industrial & Engineering Chemistry Research*; the manuscript is under peer review and cited as reference [7] in this thesis. The chapter 5 is formatted for publication in the journal- *Chemistry of Materials* and cited as reference [8] in this thesis. All references cited in the thesis are listed in numerical order at the end.

Chapter 2

Conventional understanding of ECAs and recent trends

In this chapter, we have recapitalized the basic terminologies and concepts in the field of electrically conductive adhesives (ECAs). The chapter describes types of ECAs and their working mechanisms. Later, we have described the properties of the materials used in ECAs; emphasis has been given to understand the various aspects of conducting fillers. Subsequently, electrically conducting polymer-polyaniline would be elaborated as an alternative conductive filler. The concept of contact resistance and conduction mechanism in ECAs will be discussed to understand our results presented in the thesis.

2.1 Electrically conductive adhesives (ECAs)

During 1950s, thermoset polymers filled with metal fillers were first patented as electrically conductive adhesives [9–11]. Nowadays, ECAs are extensively used and are vital in the assembly and packaging of electronic devices, especially in the current proliferation and mass production of electronic hardware. ECAs are used as pastes or as solid films in fabricating high-density multilayer interconnect substrates, flexible circuits, flat-panel displays, and a host of other emerging applications including optoelectronics; high-speed, high-frequency circuits; sensors; and smart cards. Due to their low cost, ease of rework, and low processing temperatures, polymeric conductive adhesives have replaced many traditional interconnect materials such as solder, eutectic alloys, and wires, especially for most commercial and consumer electronics. Following table summarizes the advantages and disadvantages of the traditional solders and polymer based conductive adhesives.

Table 2-1: Advantages and disadvantages of traditional soldering and conductive adhesives

Interconnection method	Advantages	Limitations
Traditional soldering	• Long history of use/mature process • Good electrical connection • Good thermal conduction • Batch process • Easy rework	• Need reflux • Reflux residues may cause corrosion • Contains toxic lead • Possibility of joint corrosion in humidity • Limited wetting and adhesion to some surfaces e.g. glass
Conductive adhesives	• Easy rework • Low cost	• Most require moderate to long curing time (1-2 hr)

	• Low processing temperature • Application-specific formulation • Ability to relieve stress • Excellent adhesion to substrates • Varying cure time possible • Directional conductivity possible	• Limited thermal stability • Absorption of water causes difficulty in reflow • Silver migration

Generally, ECAs are synthesized in form of paste and can be classified into two types: single-component ECAs and two-component ECAs. Single-component ECA is also called as one part system which consists of resin and cross-linking agent (hardener) altogether; but system does not cure until curing temperature has reached. Two-component ECA consists of resin and hardener, separately; when ready for use, the two parts are weighed, mixed, de-aerated, dispensed, and cured. Recently, 'snap-cure' type ECAs are being developed which cures in 3-5 min at room temperature. However, shelf-life of such systems is significantly low.

Based on working mechanism of ECAs, they can also be classified as isotropic conductive adhesives (ICAs) and anisotropic conductive adhesives (ACAs). ICAs are equally conductive in all directions while ACAs are only conductive in one direction, typically z-direction. Figure 2-1 shows the difference between traditional solder joint and two types of ECA joints.

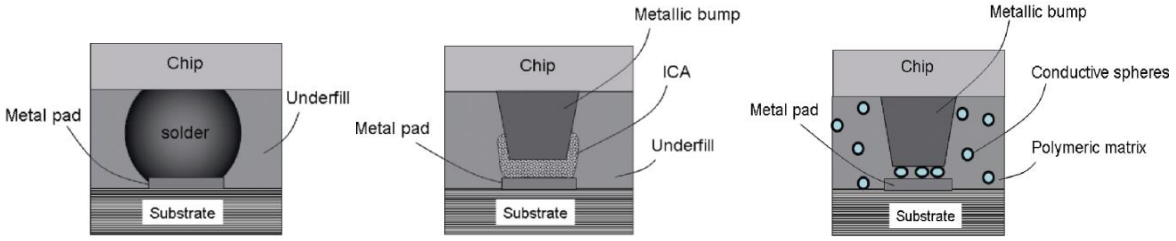

(a) (b) (c)

Figure 2-1: Different approaches for interconnects (a) traditional solder interconnect, (b) isotropic conductive adhesive (ICA) interconnect and (c) anisotropic conductive adhesive (ACA) interconnect [2] (reproduced with permission Copyright 2009, Springer)

2.1.1 Isotropic conductive adhesives (ICAs)

The most widely used electrically conductive adhesives are silver-filled epoxies. Isotropic conductive adhesives which conduct current equally in all directions are the most common and widely used in industry. They are also called as 'polymer solder'.

Figure 2-2 shows the application of ICA for joining of components with substrate.

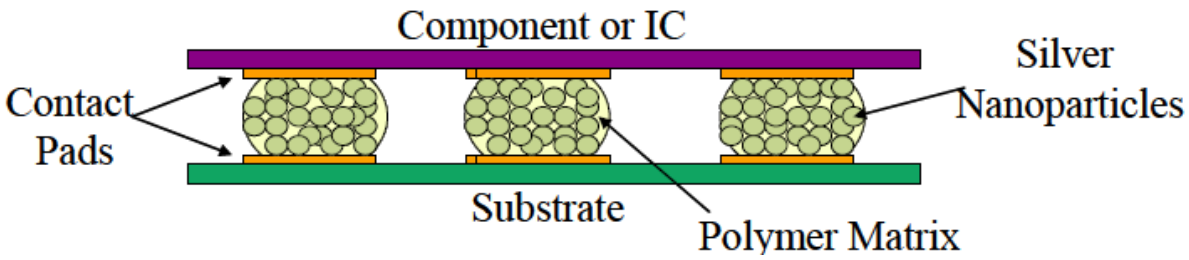

Figure 2-2: Application of ICA for joining of component with substrate [2] (reproduced with permission Copyright 2009, Springer)

Different polymers are used as binders for ICAs that include polyesters, urethanes, polyamides, phenolics, acrylics and epoxies. Epoxies clearly dominate and are likely to maintain the role because of their balance of functional properties, wide availability, moderate cost and relatively safe use. ICAs are typically filled with 1-10µm silver flakes and may have a filler volume up to 30% of total volume. The conductive fillers provide the composite with electrical conductivity through contact between the conductive particles. ICAs perform dual functions: electrical connection and mechanical bond. Specifically, electrical connection is facilitated by conductive fillers and mechanical bond is provided by polymer matrix, mostly epoxy. Excessive filler loading deteriorates the mechanical properties of the adhesive. The challenge in ICA formulations is to achieve highest possible electrical conductivity without affecting the mechanical properties. ICAs typically have low electrical conductivity before cure and their conductivity increases due to shrinkage of the epoxy matrix during the cure process. Adhesive matrix shrinkage is shown to have a strong correlation with electrical conductivity. ICAs with higher shrinkage show lower bulk resistance or better conductivity[12].

2.1.2 Anisotropic conductive adhesive (ACAs)

ACAs provide unidirectional electrical conductivity in vertical or z-axis direction. This unidirectional conductivity is achieved by using relatively low loading of conductive fillers (5-20

volume %). Low volume of conductive fillers is insufficient for inter-particle contact and prevents conductivity in the X-Y plane of the adhesive.

As shown in Figure 2-3, ACAs are applied in-between the surfaces to be connected; heat and pressure is applied simultaneously until particles connect the two surfaces.

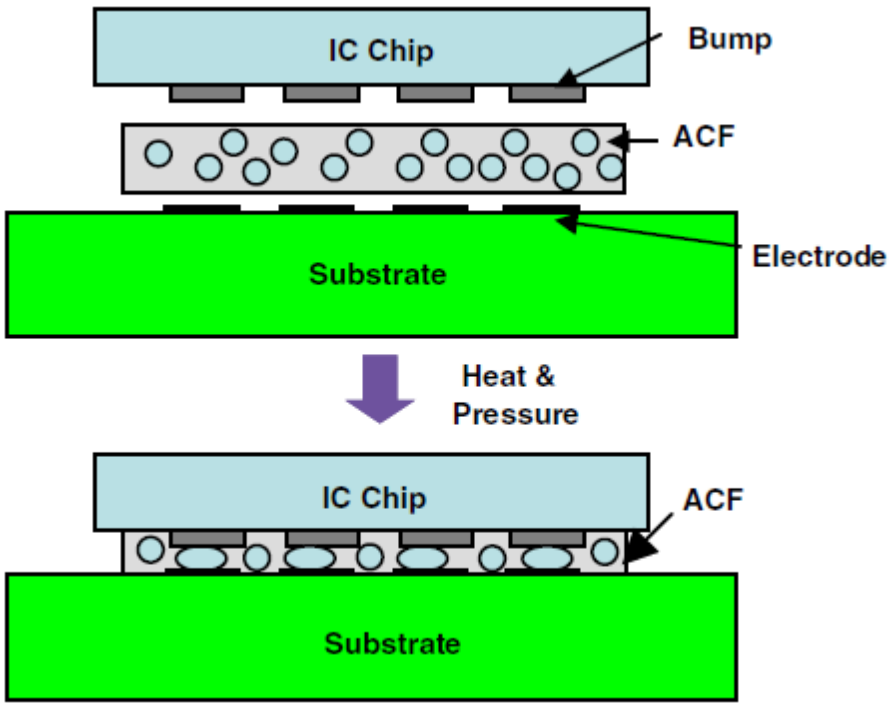

Figure 2-3: Joining of IC chip onto a substrate using ACA and with heat and pressure [13] (reproduced with permission Copyright 2006, Elsevier)

ACAs provide new material system for solder replacement besides ICAs. Anisotropic nature of these materials makes them excellent candidates for very fine pitch components [14–16], where particle density in adhesive and its dispersion consistency is extremely important to prevent open or short-circuit events. The requirement of complicated process and specific bonding equipment are the main drawbacks of these materials compared to solders and ICAs.

2.2 Materials for electrically conductive adhesives

2.2.1 Adhesive matrix

Thermoplastic adhesives

ECAs can be based on thermoplastic or thermoset adhesive or a combination of two [2], [17]. Thermoplastic binders are already polymerized and subtly used in ECAs as compared to thermoset adhesives. Thermoplastic adhesives are made by either melting or dissolving polymer resins into solvents and then adding conductive fillers. However, it is difficult to blend filler material in already polymerized thermoplastic polymers because of its exceptionally high viscosity. Solvents can be used to reduce the viscosity and facilitate higher loading of the filler. But, all thermoplastics are not soluble in common solvents; and, solvent processing has limited applicability in adhesive application due to bubble formation after solvent vaporization. Some of the commercially available thermoplastic adhesives can be used for joining of component assembly but their properties are not competitive to those of thermosets. Thermoplastics are subject to creep and significant flow above its glass transition temperature. Thermoplastic conductive adhesives are mainly used in ACAs as they do not require selective application. Therefore, thermoplastic adhesives are employed with the use of heat and pressure where it softens and bonds to adherents. Thermoplastic adhesives do not require refrigeration as there is no possibility of permanent curing of polymer matrix.

Thermoset adhesives

In thermoset adhesives, properties are permanently changed upon heating/curing. Thermoset systems are mainly used in ICAs. Epoxy is a typical thermoset polymer used to synthesize the ICAs. Their unique chemical and physical properties (i.e., excellent chemical and corrosion resistance, superior electrical and physical properties, excellent adhesion, thermal insulation, and reasonable material cost) have made epoxy resins very attractive in electronic packaging applications [18]. Epoxies, in general, exhibit exceptional and permanent adhesion to most substrates and can be tailored to survive humidity and thermal cycling. Low molecular weight, viscous epoxy is used as the primary component with co-reacting hardener. Typical epoxy cross-linking agents are amines, anhydrides, dicyanodiamides, melamine formaldehydes, urea formaldehydes, phenol-formaldehydes, and catalytic curing agents. Various types of anhydrides and amines are frequently used as curing agent to cross-link epoxy matrix. Reactivity of the epoxy formulations, curing agents determine the degree of cross-linking and the formulation of chemical bonds in the cured epoxy system. The epoxies based on the

diglycidyl ether of bisphenol-A (DGEBA), which is synthesized by reacting bisphenol-A and epichlorohydrin, are the common materials for liquid adhesives. Figure 2-4 shows the chemical structure of diglycidyl ether of bisphenol-A (DGEBA) type epoxy.

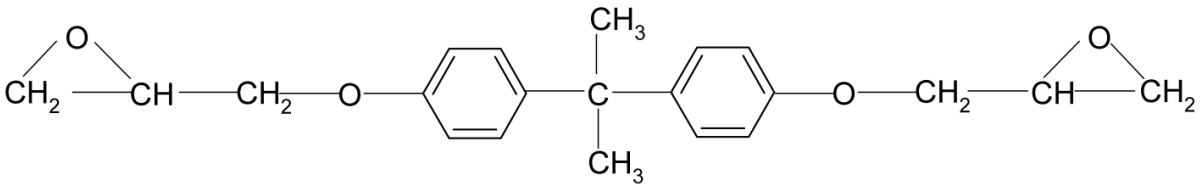

Figure 2-4: Chemical structure of diglycidyl ether of bisphenol-A (DGEBA) type epoxy

In case of ECAs, epoxy is first processed as a low viscosity monomer followed by filler blending under a shear force. Subsequent heat curing process initiates the polymerization that produces a solid three dimensional thermoset network. Heat treatment upon mixing causes components to react chemically and forms high molecular weight, cross-linked epoxy. Three-dimensional network of cross-links prevent movement of polymeric chains in thermosets. Additives can be added at low concentrations to enhance adhesion, modify rheology, enhance temperature stability and impart crack resistance [19]. Single component ECA system is preferred but it has a limited storage life unless refrigerated. Two-component system faces a serious concern of entrapment of air during the mixing process.

2.2.2 Conductive fillers

To the date, silver is most popular conductive filler; although gold, copper, nickel and carbon are used. It is considered as unique filler because both its metallic and metal oxide form is electrically conductive. On the other hand, oxides of nickel and copper are poor conductors; their conductivity decreases after aging. This effect is most significant with small size particles. Silver has the highest room temperature electrical and thermal conductivity among other frequently used fillers. The properties of ECA are affected not only by the individual phases and filler loading, but also by the filler shape, size, distribution, and orientation, state of adhesion between filler and matrix and the amount of particle agglomeration. Many commercial ECAs utilize silver with flake geometry as filler because flakes tend to have a large surface area and thus more electrical paths than spherical fillers [20]. The particle size of ECA fillers generally ranges from 1 to 20 μm. Larger particles tend to

provide the material with a higher electrical conductivity and lower viscosity [21][22]. Interestingly, silver-filled epoxies have shown improved conductivity after thermal treatment. This observation is mainly attributed to the shrinkage of epoxy matrix which brings silver flakes together to establish electrically conductive pathway. Therefore, conductivity found to be reduced after thermal treatment.

Even though silver has been a choice for the metal filler, the warning that silver is accompanied by electro-migration problems keeps on coming up. Silver migration is an electrochemical process, whereby, silver filler dispersed in insulating polymer matrix, in a humid environment and under an applied electric field, migrates from its initial location in ionic form and deposits at another location. It is considered that a threshold voltage exists above which the migration starts. Researchers have identified the electro-migration as a vital problem for ECAs [23]. However, Morris and co-workers have evidently shown that electro-migration occurs in uncured polymeric systems only [24].

Lubricant layer on silver

Silver powders are produced by three major methods: chemical precipitation, electrolytic deposition, and atomizing. Most silver flakes in the today's market are produced by a chemical precipitation method. Chemically precipitated silver powders are normally produced by reducing silver nitrate solutions, in an alkaline medium, with reducing agents such as sugars, aldehydes, hydrazine, and many others. This method typically yields powders with individual particles ranging from 0.5 to 10 μm. Silver powders are very malleable, have clean surfaces, and can cold weld easily. In order to preserve their individual character, agglomeration (welding) should be avoided. Conventionally, fatty acids such as stearic, oleic, linoleic, and palmitic acids serve the purpose. Therefore conventionally, silver flakes are coated with a mono-molecular layer of lubricant to prevent agglomeration of the flakes, improve dispersability, and impute the appropriate rheology to the epoxy resin system [25]. However, the interaction between the lubricant and silver surface, effects of this layer on electrical conductivity of ECAs, and thermal decomposition of the lubricants of the silver particles are not clear. C.P.Wong and co-workers have shown that lubricant has strong interactions with silver surface and changes its morphology from a spherical to flakes shape. Figure 2-5 shows the effect of lubricant on the morphology of silver particles [2]. Their thermal study has showed that it is not possible to remove all unused lubricant from silver surface which results in significant weight loss.

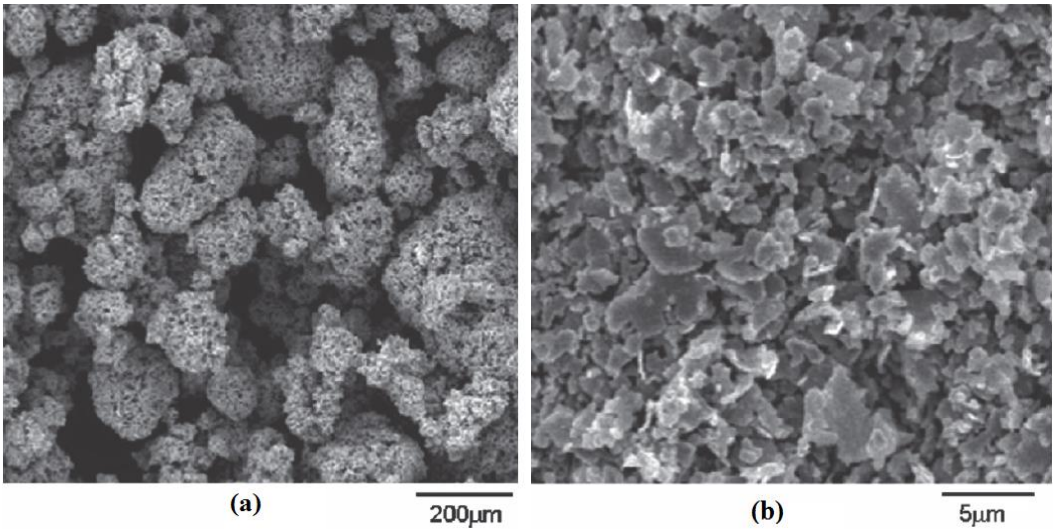

Figure 2-5: Morphology of silver particles (a) without surfactant, (b) with surfactant [2] (reproduced with permission Copyright 2009, Springer)

The organic lubricant layer on the silver surfaces is usually an insulator which affects electrical conductivity. Therefore, the conductivity can be improved if this lubricant somehow can be *in-situ* removed during the curing of ECAs. It is found that addition of short-chain acids to ECA formulations can improve electrical conductivity by removing or replacing the long-chain fatty acid lubricant on the surface of silver particles. Generally, it can be said that a thin layer of lubricant on silver surface is necessary to prevent the agglomeration; however, it is equally important to remove or replace the lubricant layer to improve its electrical conductivity. Some chemicals like short-chain acids can serve the purpose.

2.3 Polyaniline: an alternate to metallic conductive fillers

The addition of conductive fillers such as silver, copper and carbon black to conventional polymers has been the primary approach to produce easy-to-process materials having some measurable electrical conductivity. The cost of the technique is undoubtedly low, but problems can arise in the form of surface corrosion, uneven mixing, reduced mechanical properties, and incompatibility of the filler with the polymer matrix. A careful selection of materials and processing methods is required for a given application to reduce the consequences of these problems. Inherently conducting polymers such as polyacetylene, polypyrrole, polythiophene, polyaniline etc can be a potential replacement for

conventional filler-polymer systems. Table 2-2 shows the comparison of conductivity between insulators, conducting polymers and metals.

Table 2-2: Electrical conductivities of insulators, conducting polymers and metals [26] (reproduced with permission Copyright 1997, CSA)

Material	Log Conductivity (S/cm)
Cured Epoxy	-15
Diamond	-14
Glass	-10
Undoped Polyaniline	-10
Silicon	-5
Doped Polyaniline	1
Current ICAs (Ideal conditions)	4
Nanotubes/nanofibers	4
Silver-filled epoxy	4
Solder	5
Silver	6

Among all conducting polymers, polyaniline has emerged as one of the most promising inherently conducting polymer for commercialization. It conducts electricity based upon the movement of electrons along its polymer chain. Polyaniline is also called as 'synthetic metal' because, its electrical, magnetic and optical properties are typical of metals and semiconductors. Typical metallic characteristics are observed due to the conjugation of polyaniline backbone, namely a regular chain of single and double bonds [27], [28]. Polyaniline exists in 3 different oxidation states: leucoemeraldine base, penigraniline base and emeraldine base. Their chemical structures are shown in Figure 2-6.

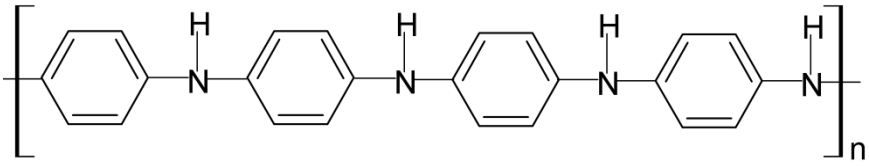

Leucoemeraldine Base

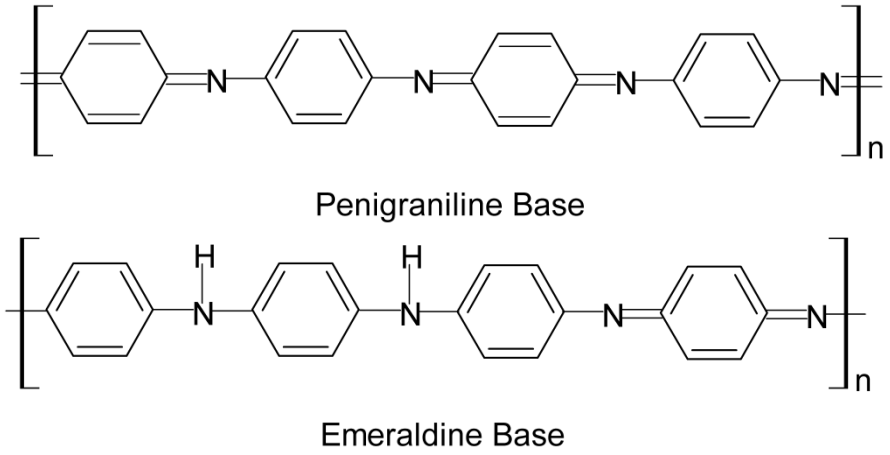

Figure 2-6: Chemical structures of different forms of polyaniline

Leucoemeraldine base is the oxidized state, penigraniline base is the reduced state, and emeraldine base is a mixture of both penigraniline base and leucoemeraldine base constituents. The conductivity boost in polyaniline occurs when the emeraldine form is doped by oxidation with a protonic acid dopant. When polyaniline is oxidized with an effective dopant, it is postulated that protonation occurs on the quinoid nitrogen where a π-electron is elevated to a level between the valence band and the conduction band and is termed as a polaron [29], [30]. The ensuing positive charge is stabilized by a local structural distortion in the polymer. Because of the close proximity of the positive charges, a rearrangement occurs where the positive-charged polaron attracts an electron from a neighboring benzene ring creating a new positive charge [31]. Thus, continuous electron transfer takes place. When charge carriers are introduced into the conduction or valence band, the electrical conductivity increases dramatically.

Polyaniline as an interconnect material

Typical conductivity levels of polyaniline measured by various researchers are comparatively lower than those of pure metals. Polyaniline has shown initial potentials in conductivity enhancement and possible implementations as an electrical contact or conductive coating. Corsat et al demonstrated the nano-imprinting of polyaniline containing thermoplastic PMMA for interconnect application [32]. Figure 2-7 shows the schematic of interconnection process utilizing polyaniline as a conducting medium. SEM image shows the polyaniline pyramid after nano-imprinting. Conductive polymer

blends and composites can be prepared by combining an insulating polymer or copolymer with polyaniline. Depending on the concentration of polyaniline and plasticizer, it is possible to adjust the conductivity of the blend and glass transition temperature. The softness (deformability) of the conductive-polymer pyramid was utilized to make the electrical contact to the metal pads of the substrate under pressure and temperature. However, the electrical testing showed that the interconnection was not functional over the full interconnect area and more work has to be done to make the interconnections fully functional.

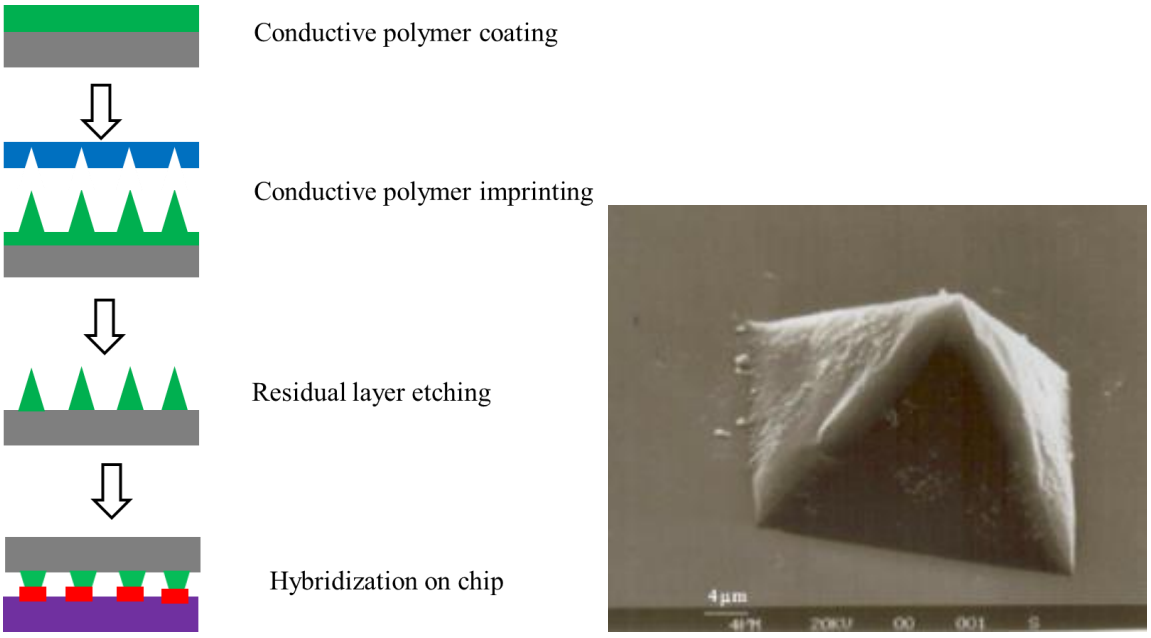

Figure 2-7: schematic of interconnection process utilizing polyaniline as a conducting medium. SEM image shows the polyaniline pyramid after nano-imprinting [32] (reproduced with permission Copyright 2006, IEEE)

Sancaktar et al studied the electrical properties of polyaniline based composite adhesive [33]. They found that 30% volume of polyaniline is necessary to initiate the conduction in insulating adhesive matrix. On the other hand, they indicated that emeraldine salt of polyaniline may catalyze the oxidation of substrates (e.g. aluminium) resulting in formation of insulating metal oxide layer such as aluminium oxide.

In our work, we have tried to develop the flexible and electrically conductive coating of polyaniline which can be used various applications but mainly as a interconnect material (chapter 5).

2.4 Concept of contact resistance in ECAs

An electrical contact is defined as the interface between the current-carrying members of electrical/electronic devices that assure the continuity of an electrical circuit. The contact resistance is the most important and universal characteristic of ECAs and is always taken into account as an integral part of overall circuit resistance. Although, it is significantly smaller as compared with overall circuit resistance, the changes in contact resistance can cause significant malfunctions in the device. This is because the contact resistance of ECA can vary significantly with the changes in the real contact area, contact pressure variations and existence of resistive film. This thesis partly, explores the changes in electrical contact resistance with force and time and also investigates the effect of co-filler, polyaniline on the same. It is the contact resistance which has been shown to be the source of electrical reliability problems in ECAs [34–36]. In case of ECAs, current-carrying members are mainly conductive fillers such as silver flakes. Uninterrupted passage of electrical current across the contact interface can be obtained if a good filler-to-filler and filler-to-substrate contact is established. The corresponding processes occurring at contact interface are complex and not completely understood within the limits of present knowledge. Fundamental phenomena in this regard include the changes in contact resistance with load, temperature and parameters associated with fillers such as coating layer, shape, size etc. It is well known that real surfaces of filler materials are not flat but comprise many asperities [37]. When contact is made between two metals, surface asperities penetrate the surface layer of filler particle establishing the localized contact and thus conductive paths. As the force on ECA, ultimately, on filler particles, increases as a result of rupturing of surface layer, contact area between filler particles increases. Therefore, the electrical properties of ECA strongly depend on applied force and changes dramatically when contact area changes. Overall, electrical resistance of ECA is a combination of intrinsic resistance of fillers and contact resistance.

Further, contact resistance consists of constriction resistance and tunneling resistance. Constriction resistance is consequence of the current flowing through ‘constricted’ conducting spots. Figure 2-8 shows schematic of constriction resistance.

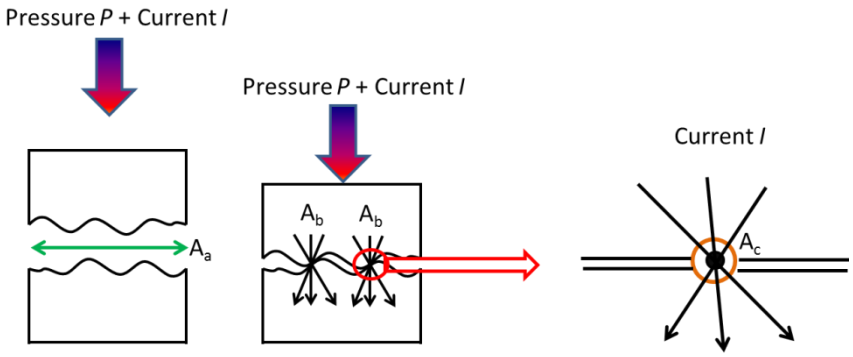

Figure 2-8: Schematic explanation for concept of constriction resistance

Tunneling resistance appears when two or more filler particles are within the range of 'tunneling' or combined thickness of their surface layer is within the range of 'tunneling' of electrons. In tunneling effect, electrons tunnel from one particle to another where they may penetrate the surface layer of filler materials. This process of penetrating the potential barrier to electron conduction is called as tunneling effect. This phenomenon is extremely sensitive to thickness of the film and force applied onto it. At higher loads, tunneling resistance can be negligible as filler-to-filler physical contact may take place. In order to obtain the stable contact resistance, Durand et al. presented a concept of poly-solder in a US patent [38]. They incorporated certain electrically conductive particles, which have sharp edges into the ECA formulations. The particles called as 'an oxide penetrating filler' need to be driven through oxide layer and held against adhered materials. This was accomplished by employing polymer binders with high shrinkage on curing.

2.5 Adhesion of electrically conductive adhesives

Generally, ECA formulations include epoxy resins which have superior adhesion capability. However, various fillers with wide chemical and structural properties are incorporated in epoxy matrix to improve its electrical conductivity. Inclusion of such fillers in the polymer matrix decreases its adhesion property and limits its applications in many fields. Inada et al studied the effect of orientation of silver flakes in epoxy matrix on adhesive strength of the composite [39]. They found that random orientation of silver flakes imparted better adhesion strength to the adhesive composite. The random orientation was also effective in preventing crack propagation. The joint strength was

improved by having large amounts of resin at the interface, instead of filler particles. Entrapment of gases (air, solvent vapors) in ECAs can badly affect the adhesive strength of the matrix. Two methodologies can be used to address this problem. When ECAs are exposed to vacuum, majority of non-bonded gases can readily escape from an adhesive matrix resulting in enhancement of adhesion. Pre-curing at low temperature can also help to eliminate the gases from ECAs. Additionally, Morris et al and Perichaud et al have shown that a brief exposure to vacuum and pre-cure heating has same effect on adhesive strength of ECAs [40], [41]. Apart from above mentioned traditional approaches, coupling agents are being used to improve the filler-polymer adhesion and ECA-substrate adhesion. This has been achieved via chemical bonds which also improves the performance of filler materials. Matienzo and co-workers showed that the use of organo-silanes as coupling agents can improve the adhesive strength also act as a corrosion inhibitor for aluminum substrate [42]. It has been also observed that silane and titanate coupling agents can improve electrical as well as mechanical properties of the epoxy based conductive adhesives [43]. In recent years, combined use of thermoplastic binders with epoxy thermoset has shown significant improvement in adhesion strength and re-workability [44]. As continuous efforts are being taken for improved filler materials, there is an increasing need to address the issues on adhesion strength of ECAs.

2.6 Conduction mechanism in ECAs

In general, ECA formulations consist of insulating polymer matrix in which conductive filler is dispersed. When a sufficient amount of conductive fillers is loaded into the insulating matrix, to form a continuous linkage of filler particles, the composite transforms from an insulator to a conductor. As the volume fraction of the conductive filler is increased, the probability of continuity increases until a critical volume fraction, beyond which the electrical conductivity is high and only increases slightly with increasing volume fraction. This critical volume fraction of conductive filler is termed as ‘percolation threshold’ and will be discussed in detail in later section.

Interestingly, ECA pastes generally have very high bulk resistance but the resistance decreases dramatically after the polymeric matrix is cured and solidified. Before curing, all the silver particles should contact each other and form continuous electrical paths. Literature reveals two distinct mechanisms of conduction development after curing. One mechanism proposes that the conductivity establishment during thermal cure is a result of removal of the lubricant and that matrix shrinkage

does not play a significant role either in the development or in the final value of conductivity [45]. Lu et al. and Wong et al investigated the conductivity establishment mechanism of ECAs by clearly studying the effects of silver flake lubricant and curing shrinkage of the polymeric resin on the conductivity establishment during curing [46], [47]. Their test device for the study of conductivity establishment is shown in Figure 2-9.

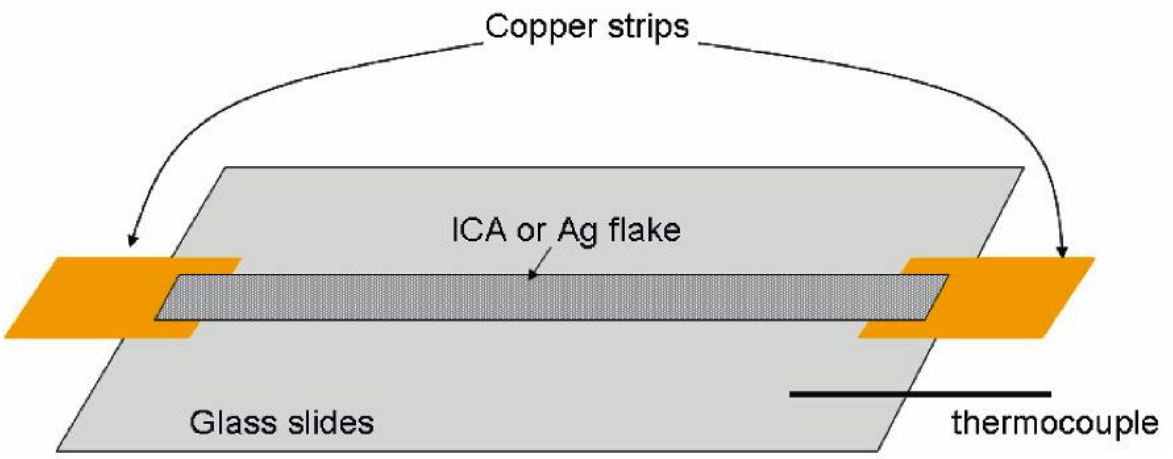

Figure 2-9: Test device for the study of conductivity establishment in ECAs during heating [2] (reproduced with permission Copyright 2009, Springer)

They observed that, without any external pressure, silver flakes can become conductive after the lubricants decomposed. It was also found that the silver particles were agglomerated together after heating. This might have caused due to removal of the lubricant on the silver flakes at high temperature. Miragliotta et al. investigated the degree of correlation between the chemical nature of the silver interface, i.e., interface conductivity, and the development of macroscopic conductivity in a metal-filled adhesive sample [48]. They performed both electrical and optical spectroscopic analysis on a silver-filled conductive adhesive, which simultaneously monitored the dynamics of sample conductivity and silver surface chemistry, respectively using surface enhanced Raman scattering (SERS). The results showed a partial decomposition of the carboxylate species and the formation of an amorphous carbon layer at the silver surface. Since amorphous carbon is highly conductive in comparison to a saturated organic hydrocarbon, this result implies a significant increase in the conductivity during thermal cure.

In other literature, a mechanism based on compressive force induced by cure shrinkage is also mentioned [49], [50]. During the cure of the ECAs, the epoxy resin shrinks. Cure shrinkage can be calculated by measuring the density before and after cure by the following relationship

$$\% \text{ Cure} = \frac{\frac{1}{d1} - \frac{1}{ds}}{\frac{1}{d1}}$$

where d_1 is the density of the liquid system before cure and d_s is the final density of the cured system. Therefore, the silver flakes in the adhesive would experience a compressive stress caused by resin shrinkage. This compressive stress would make the silver flakes closer and improve electrical conductivity. The interrelated variables such as crosslinking density, volume change, and cure shrinkage effectively contribute to the pressure on the conductive particles in the cured state. The apparatus for studying conductivity development with external pressures is shown in Figure 2-10.

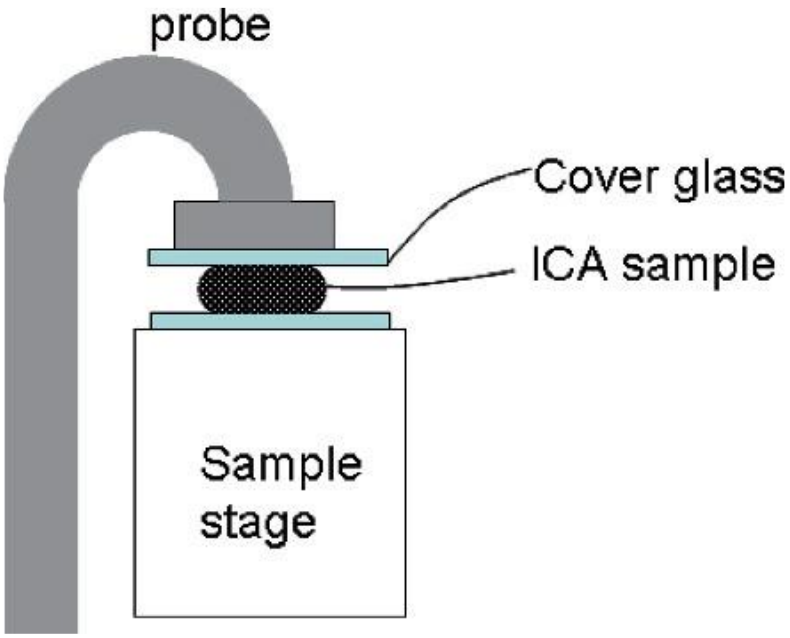

Figure 2-10: Apparatus to study conductivity development in ECAs with external pressure [2] (reproduced with permission Copyright 2009, Springer)

At the moment, it can only be said that the resin cure shrinkage plays an important role during conductivity establishment of a conductive adhesive however the possibility of removal of lubricant layer on the silver flakes can't be eliminated.

2.7 Percolation threshold

A percolation phenomenon signifies the electrical conductivity of percolating filler-polymer systems. Most polymers are electrically insulating and can be made electrically conductive by adding certain amount of conductive filler to form continuous network of conductive filler particles. When the volume fraction of conductive filler is increased, the probability of continuity between particles increases until a critical volume fraction, φ_c, or percolation threshold is reached [51]. At this volume fraction of fillers, the electrical conductivity significantly increases over a small change in filler volume, up to a maximum achievable conductivity.

Electrical conductivity of ECA equally depends on the amount of the filler and their connectivity among each other. Particle size, shape and aspect ratio influence the percolation threshold. Smaller particles with a larger aspect ratio have been found to decrease the percolation threshold [52]. Such filler materials can give a high level of electrical conductivity at lower filler volumes, which is desirable for many applications. ECAs containing small particles with a low aspect ratio result in lower electrical conductivity and high percolation volume which can be explained by fundamentals of contact resistance. Large amount of small particles with a low aspect ratio are needed to form connecting network; as number of small particles increases, subsequently, number of contact points increases resulting in high contact resistance.

Percolation theory states that a certain volume of conductive fillers is necessary to establish a continuous and percolating network which facilitates the transport of electrons. Percolation theory considers the "richness of interconnections present" in a random system and the effect of such variations in randomness [53]. When this theory is applied to ECA materials in which some conducting particles are dispersed in an insulating matrix, an insulator-to-metal transition takes place as the volume fraction of conductive filler is varied. Below the percolation threshold, the average size of conducting domains is small and conduction throughout the material does not occur [54]. However, above the critical threshold, an almost infinite chain of conducting paths is established throughout the matrix and the conductivity increases at a rapid rate as the volume fraction of the conducting particles increase [49], [55], [56]. The volume fraction at which conductive filler particles in a percolating system such as ECAs causes a transition from a non-conducting to a conducting state is a very important feature in the characterization of percolation behavior. Above and below the

threshold point, the concentration dependence of the electrical conductivity (σ) obeys scaling laws as given below:

$$\sigma = a(\varphi - \varphi_c)^t, \qquad \varphi > \varphi_c$$

$$\sigma = b(\varphi_c - \varphi)^{-s}, \qquad \varphi_c > \varphi$$

where a, b are coefficients and t, s are the electrical conductivity exponents, φ is ratio of the volume of conducting particles to that of the whole system (volume fraction) and $\varphi=\varphi_c$ at percolation transition [57][58]. For random percolation, $s=t\approx4/3$ for 2-dimensional network, while $s\approx0.75$ and $t\approx2$ for 3-dimensional network [59]. In general, $t<2$ or $t>2$ does not essentially mean a change in dimensionality; it could be a result of the influence of several parameters. These factors may include aggregation of conductive particles [60] and/or tunnelling mechanism of conduction [61], which can affect the value of t. Figure 2-11 shows insulator to conductor transition where conductivity increases sharply at the percolation threshold.

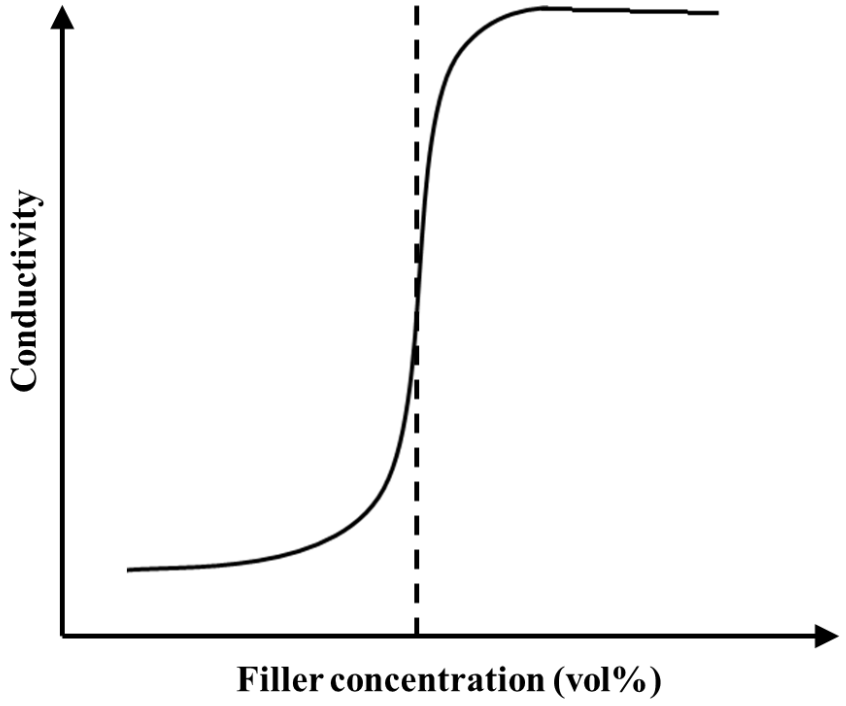

Figure 2-11: Typical percolation curve showing dramatic increase in conductivity at threshold [2] (reproduced with permission Copyright 2009, Springer)

Percolation threshold depends on shape and size of conductive particles, local variations in particle concentrations and their spatial arrangements in the polymer matrix [62]. When the conducting particle shape deviates from spherical, as in the case of elongated conducting particles, a lower percolation volume fraction (<0.16) is expected if the system is sufficiently random and isotropic [63]. Percolation volume fraction for spherical particles ranges up to 0.30 whereas it can reduce up to 0.05 for needle-like 1-dimensional particles [59].

Several techniques have been used in reducing percolation volume fraction in conductive polymeric composites. These include:

1. Minimization of the interaction between polymer and filler [64]. Higher the polarity of a polymer matrix, larger is the percolation threshold.
2. Filler shape: replacement of sphere geometry with rods [63]
3. Matrix polymer structure: Use of semi-crystalline microstructure induces preferential localization of some fillers in the amorphous regions [65]
4. Large relative difference in the particle size of polymer to filler has also been successfully applied to reduce percolation in polymer melt composites [66]

Although much work has been done with mathematical models to validate the shape of a percolation curve, predicting the magnitude of conductivity has been an elusive goal [67]. Some have found that calculation of interfacial tension between the conductive filler and the polymer matrix improves the predictability of the model [68]. Others have shown that particle size and shape are reliable predictive parameters, where smaller particles and a larger aspect ratio for the conductive particle decrease the percolation threshold [52]. Smaller particles can theoretically result in lower electrical conductivity since more high resistance particle-particle points-of-contact exist in the filler-polymer composite. Many have expressed the dependence of conductivity on pressure, where the softer conductive particles, high modulus polymer matrix, higher cure shrinkage, and larger expansion coefficient difference between filler and polymer all contribute to enhanced composite conductivity [49][50].

In conclusion, generally ECA consist of thermosetting epoxy and silver flakes in its formulation. Electrical properties of basic formulation of silver-filled epoxies are well studied in the literature and it shows the promising alternative to the lead-based solders. Improvement in properties of metallic fillers and development of novel non-metallic fillers can enhance the overall performance of ECAs. Utilization of improved or novel fillers for ECAs and subsequent enhancement in electrical conduction ultimately converges to the understanding of contact resistance in respective cases.

Chapter 3

Percolation threshold analysis of silver-polyaniline-epoxy system

3.1 Introduction

Adhesives with electrically conducting filler phase facilitate the development of electrical and micromechanical properties which are essential for electronic packaging applications. High performance conductive adhesives are designed by combining the thermosetting resin and efficient electrically conducting filler [2], [69]. Conducting fillers, typically micron sized are vital part of conductive adhesive, which provides means for the transport of electricity through the composite. Their size and shape can help to optimize the amount of filler content in a composite. Higher filler concentrations risk electrical shorting at the nearby bonding pad during electronic packaging application [70]. Micron sized fillers have high surface area to volume ratios which dramatically reduce the percolation threshold and also can control the contact resistance by minimizing the constriction resistance. Out of many combinations of polymer and filler, silver-epoxy system has a great potential to be implemented on a large volume process. Another distinctive feature of this system is the cooperative behavior of interacting particles in case of filled composites, which becomes observable at the percolation threshold [71]. Despite a large number of potential applications, this system is plagued by lack of study of fine tuning of conductivity and determination of optimal quantity of silver to obtain conductivity. To be electrically conductive, the loading of conductive fillers in insulating polymeric matrix needs to be above its percolation threshold - the minimum fraction of fillers needed to establish the conducting network. Jia et al have showed that conductivity of multicomponent conductive adhesive depends on the conductivity of individual components, their loading level and the interactions of the fillers [72].

Our research focuses on development of efficient conductive adhesives by employing functional conductive fillers such as polyaniline to the traditional silver filled epoxy system. The polyaniline (PANI) has a moderate conductivity in between the silver and epoxy; it was used to dope the epoxy matrix to minimize two problems in the ECAs: (1) localization of charge carriers because of the aggregation of the silver fillers, and (2) the interfacial polarization arising from the intrinsic difference in polarities and surface energies of fillers and epoxy. Two different methods were used to prepare the silver-polyaniline-epoxy adhesives. The first method was to add silver fillers into liquid epoxy resin, add polyaniline, and then the amine hardener. The second method was to add polyaniline

into liquid epoxy resin, add silver fillers, and then the amine hardener. Our experiments showed that silver fillers were well dispersed in cured adhesives prepared in the first method while silver fillers formed aggregates in cured adhesives prepared in second method. This chapter focuses on systematic analyses of percolation threshold of silver-epoxy (Ag-epoxy) and silver-polyaniline-epoxy (Ag-PANI-epoxy) system through an innovative study of resistance using the micro-indentation technique and morphological analyses. We also propose a mechanism of conduction based on surface properties and interactions between fillers and the epoxy matrix. Our results and analysis may help to explain the reduced percolation threshold and enhanced conductivity.

3.2 Experimental

Two-component epoxy adhesive consisting of epoxy oligomer D.E.R.™ 322 and cross-linking agent D.E.H.™ 24 (The Dow Chemical Company) was used as a polymeric matrix. Micron sized silver flakes (~10μm, Sigma) and polyaniline (Sigma) were used as conducting fillers. Isopropyl alcohol was used as a solvent to facilitate the mixing of fillers in the polymer matrix.

Preparation of composite/adhesive

Silver flakes were mixed in diluted epoxy at various weight % of the basic epoxy formulation but here, reported in volume % for the percolation threshold calculations because formation of conducting network depends on volume fraction rather than weight fraction. Addition of polyaniline to the epoxy matrix was carried out in two different methods which are summarized inFigure 3-1. To vary silver/polyaniline ratio, quantity of polyaniline was kept constant while that of silver was changed.

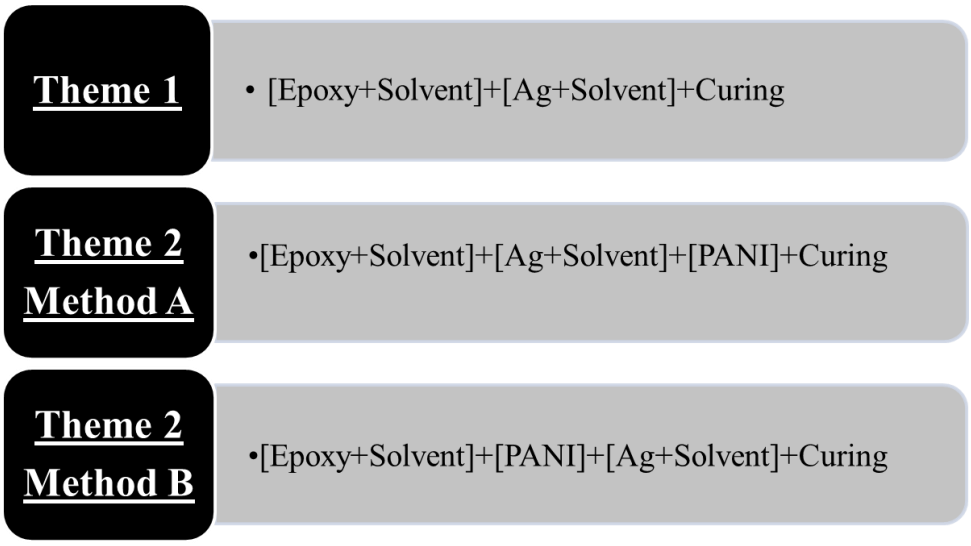

Figure 3-1: Different approaches used in the study to the synthesis of silver and polyaniline containing conductive adhesives

3.3 Characterization

Electrical contact resistance (ECR) of cured adhesives was measured using the in-built electrical sensors (range 1-100Ω) of a Universal Micro/Nano Tester (UMT) (CETR, Campbell, CA, USA) as a function of loading of silver, polyaniline and its preparation methods. UMT also enabled to measure electrical contact resistance with respect to indentation force, penetration depth and real time change of electrical contact resistance. Sample preparation included spin coating of the composite on copper substrate. The morphological properties of the composites were characterized by FE-SEM. Indentation probe was made up of the stainless steel of diameter 1.65mm. Figure 3-2 shows a setup of CETR Universal Micro/Nano Tester (UMT) and close-up view of micro-indentation test.

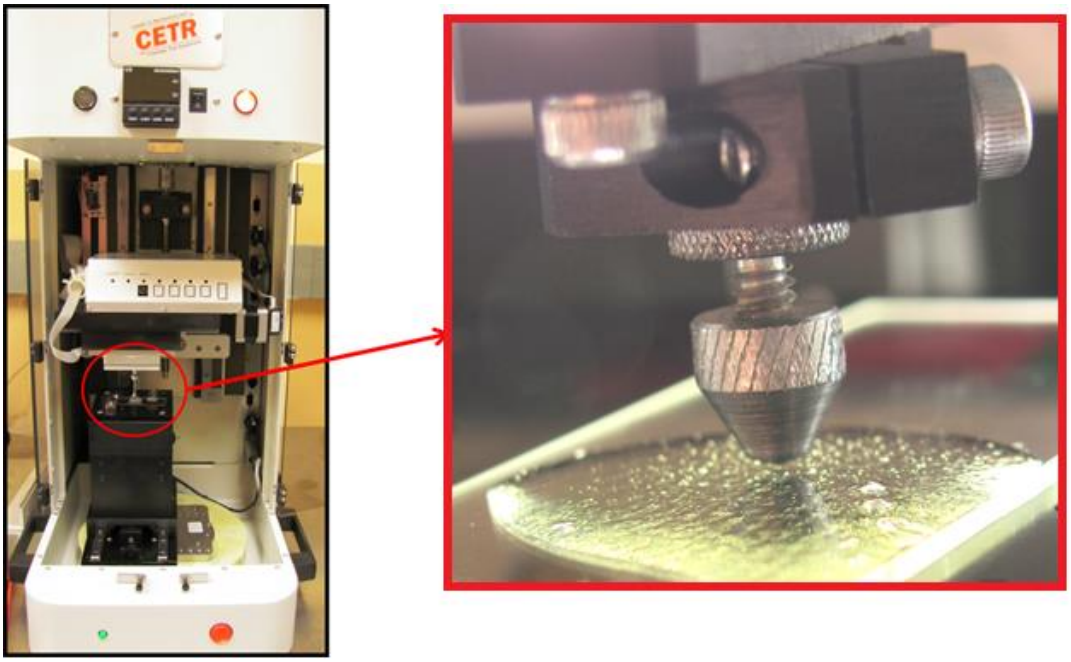

Figure 3-2: Setup of CETR Universal Micro/Nano Tester (UMT) and close-up view of micro-indentation test

3.4 Results and discussion

3.4.1 Percolation threshold

Electrical contact resistance of conductive adhesives, synthesized with various filler loadings, was obtained from UMT instrument. Figure 3-3 shows Change in resistance and contact resistance of silver-epoxy ECA with increase in silver content, as measured by 4-point probe technique and microindentation. Both techniques showed significantly similar trend within their limitations. It was also observed that after 60 wt% of silver loading, electrical conduction in the ECA significantly increases owing to the formation of conductive paths between the filler particles. Figure 3-4 shows the comparison of change in resistance of silver-epoxy and silver-polyaniline-epoxy ECAs with increasing silver content, as measured by 4-point probe technique. It was revealed that addition of polyaniline could reduce the silver content needed to obtain the same conductivity in silver-epoxy composites. This observation can be attributed the bridging effect of polyaniline.

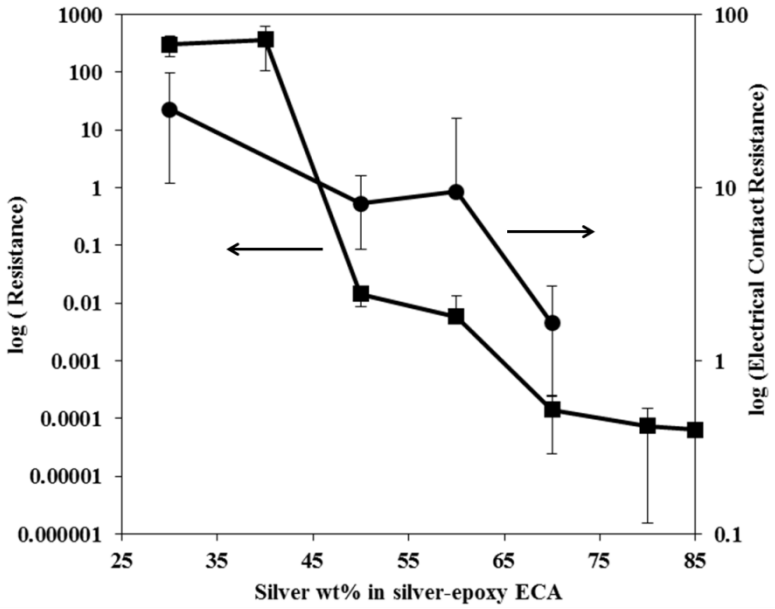

Figure 3-3: Change in resistance and contact resistance of silver-epoxy ECA with increase in silver content, as measured by 4-point probe technique and microindentation

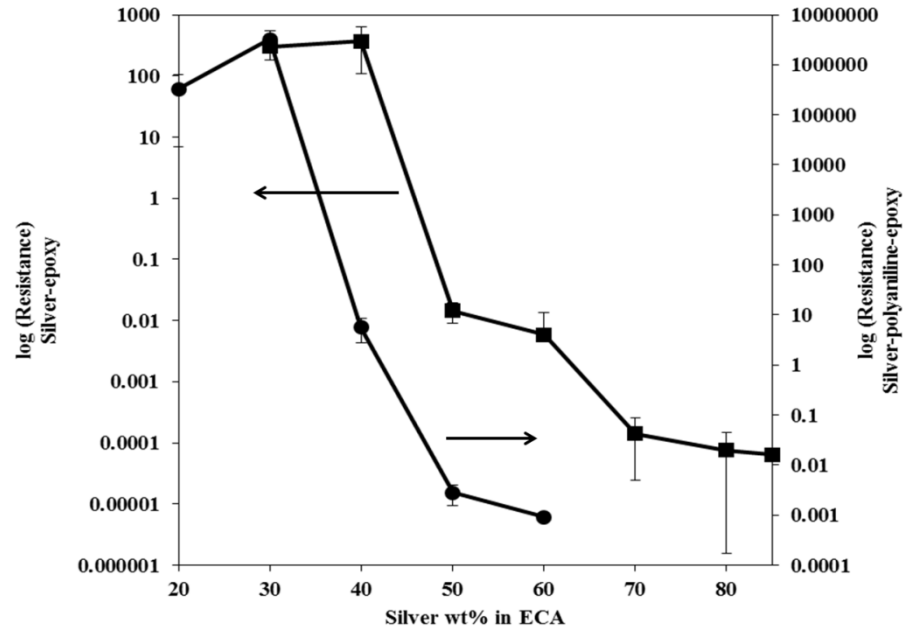

Figure 3-4: Comparison of change in resistance of silver-epoxy and silver-polyaniline-epoxy ECAs with increasing silver content, as measured by 4-point probe technique

The electrical response of the composite can be described by the percolation theory which states that the conductivity is given by, $\sigma = a(\varphi - \varphi_c)^t$ where σ is conductivity of the composite, a is coefficient, φ is volume fraction of filler and φ_c is volume fraction of the filler at percolation threshold. Conductivity can only be established when filler particles are in contact with each other or within the electron tunneling range in the composite. Detailed observation of percolation curves reveals that electrical contact resistance values at percolation threshold vary significantly than other points on the curve. In macroscopically homogeneous materials, at concentration of filler below percolation threshold a short- range percolation coherence length exists [73]. Electrical conductivity is possible for the length scales less than percolation coherence length. Thus, even if composite shows non-conductive behavior, conduction can occur within domains that are smaller than percolation coherence length. Therefore conductivity shows some fluctuations around the percolation threshold. The percolation theory predicts that no conduction occurs until one complete conductive path of filler material has been created across the composite. From Figure 3-3, approximately it can be predicted that the percolation threshold of silver-epoxy ECA lies at around 60wt%. Adding the polyaniline facilitates the formation of a continuous network of conductive fillers so as to have a reduced percolation threshold around 30wt% as observed in Figure 3-4. However, it should be noted that the overall resistance of silver-polyaniline-epoxy is significantly higher than silver-epoxy ECAs. This fact can be attributed to relatively low conductivity of polyaniline compared to silver. From these results, it is worth mentioning that a percolation threshold was reached at lower concentration of the filler, when polyaniline was added to the silver-epoxy composite. Conductivity in silver-epoxy composites can only be obtained when the silver flakes are in contact with each other or within the electron tunneling range in the epoxy resin.

3.4.2 Morphological analysis of conductive network

A morphological study of the electrically conductive adhesive below, at and above percolation threshold was carried out and images are shown in Figure 3-5. Insulating nature of the composite below the percolation threshold may be attributed to insufficient filler amount, absence of particle network and aggregation of the filler. Aggregation of filler particles results from their higher surface energy and strong interfacial interactions. At percolation threshold, Ag particles have sufficiently close contact, resulting in a continuum network.

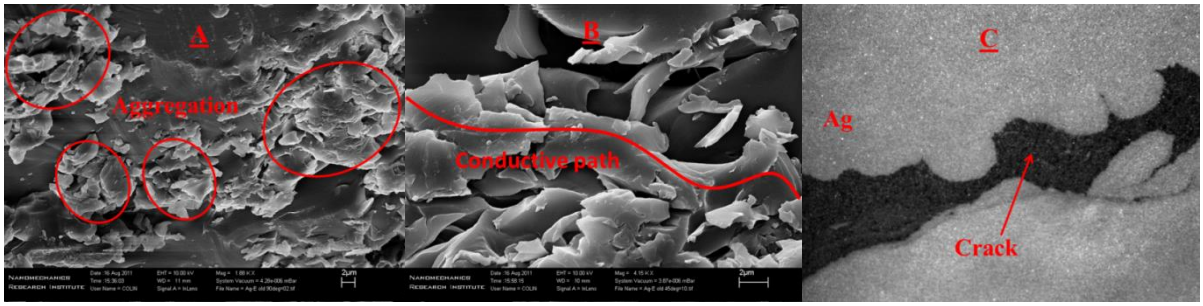

Figure 3-5: Spatial distribution of filler (A) before percolation threshold, (B) at percolation threshold and (C) above percolation threshold. A & B are SEM images (scale bar 2 µm) while C is optical image

This clearly indicates that 15.17 vol% silver leads to noteworthy insulator-to-conductor transition in silver-epoxy system. Higher filler concentration did not significantly reduce the resistance but resulted in formation of surface cracks. This behavior is common when polymer is filled with high quantity of filler material. It is observed because of decrease in impact strength which is associated with energy required to induce a catastrophic crack. Extreme loading of filler beyond the percolation threshold promotes a crack formation via stress concentration on the filler surface.

3.4.3 Force dependent contact resistance

Change in electrical contact resistance of ECAs was tracked during micro-indentation which provides a promising technique for understanding force dependent electrical contact resistance. During the testing, voltage is applied to the sample via conducting tip and resistance offered by the system was measured. This technique provides a sensitive *in-situ* means to probe the changes in the electrical signature of the material, immediately on the commencement of the loading. Change in electrical contact resistance of silver-epoxy and silver-polyaniline-epoxy systems with increase in vertically downward force/indentation force is shown in Figure 3-6 and Figure 3-7. These figures consist of the trend of electrical contact resistance on loading force and unloading force. Sudden decrease in resistance is observed in both cases which continue to decrease with increase in loading indentation force as the contact area between sample and probe increases. Here, purposefully we have shown the repetitive data electromechanical response of silver-epoxy and silver-polyaniline epoxy ECAs. Predominantly, it is observed that the electrical contact resistance of the constant composition of ECA is very unstable. There are many factors that can cause this instability which include the contact area

between probe and sample surface, filler-filler contact area. The increase in indentation force causes the change in contact area which is difficult to predict in case of irregular shaped fillers.

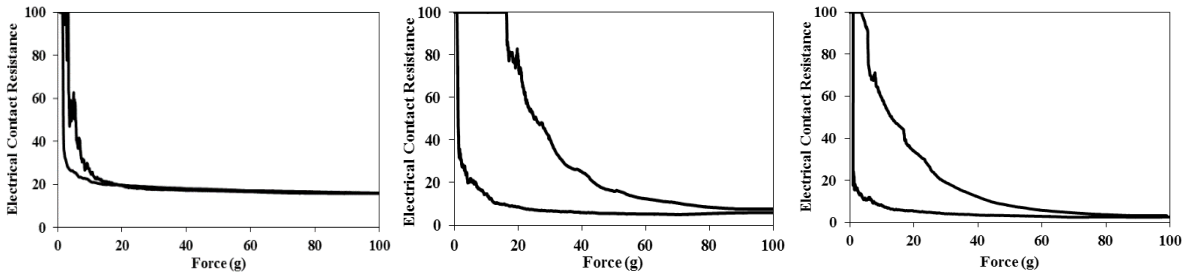

Figure 3-6: Change in electrical contact resistance of silver-epoxy ECA with increase in force. All 3 figures are repetitive measurement of single composition which show the sensitivity of electrical contact resistance with filler-filler contact area

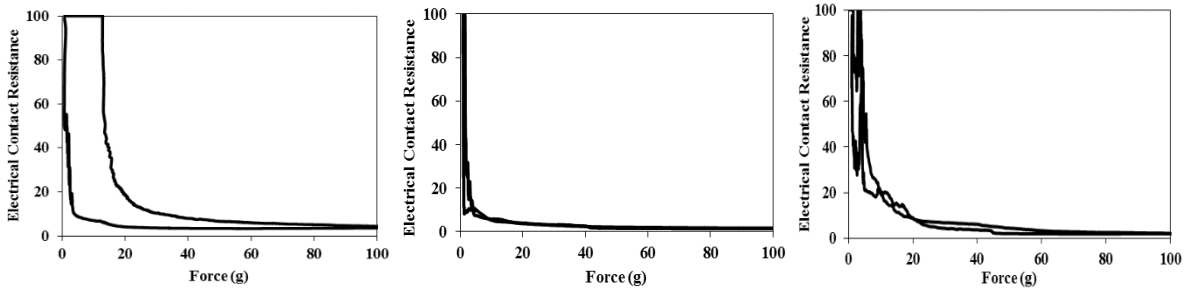

Figure 3-7: Change in electrical contact resistance of silver-polyaniline-epoxy with increase in force. All 3 figures are repetitive measurement of single composition which show an increased sensitivity of electrical contact resistance

Affinity of silver particles to epoxy matrix results in an insulating layer formation on its surface which is expected before percolation threshold. Still, tunneling effect accounts for the conduction in the composite material through insulating layer. After addition of polyaniline, comparatively less indentation force is needed to initiate the conduction. This observation can be explained by the bridging effect of polyaniline which decreases the force needed for conduction.

3.4.4 Contact resistance stability

In-situ micro-indentation enabled to test the stability of electrical contact resistance at certain depth in ECA, at percolation threshold which is crucial in case of conductive adhesives. Here, preliminary

results are quite qualitative and give valuable information about the process of packaging of electronic components. Figure 3-8 reveals the stability of electrical contact resistance at constant depth in silver-epoxy and silver-polyaniline-epoxy ECAs over a period of time. Repetitive measurements are provided to depict the sensitivity of contact resistance over a period of time. As expected, silver-epoxy system showed slow but spontaneous decrease in electrical contact resistance at certain depth in a composite. On the other hand, silver-polyaniline-epoxy system exhibited significantly constant electrical contact resistance at the same depth over the same period of time. This fact can be attributed to the establishment of physical conductive network due to the presence of polyaniline. Silver-filled conductive adhesives face a serious reliability concern such as silver migration, specifically in humid conditions. Formulation of silver-epoxy conductive system along with polyaniline can help to solve the problem of silver migration.

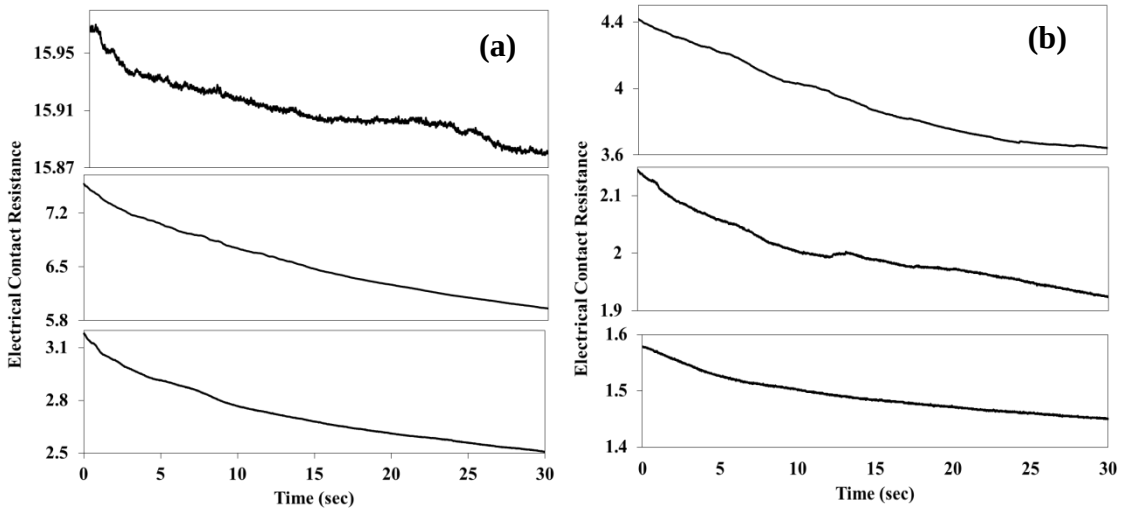

Figure 3-8: Stability of electrical contact resistance of silver-epoxy (a) and silver-polyaniline-epoxy (b) ECA over a period of time. All 3 figures are repetitive measurement of single composition which show the sensitivity of the stability of contact resistance

Though silver-epoxy composite showed conductive nature, part of the conductivity, can be attributed to tunneling effect at quasi-metallic contact where current overcomes a barrier of thin insulating layer. Addition of polyaniline gives synergetic effect towards development of conductive network, even after the complete curing. From the obtained results, we propose that silver flakes possess thin layer of stabilizer on its surface through chemical and interfacial interactions. Addition of polyaniline results in its adsorption on silver flakes through Van der Waal's forces and electrostatic interaction.

Due to the indentation force, silver and polyaniline penetrate into epoxy matrix overcoming the barrier of stabilizer layer. Schematic of this concept is shown in Figure 3-9.

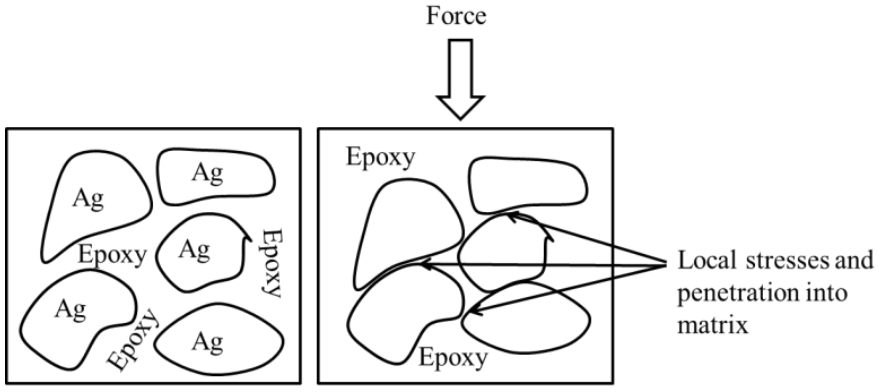

Figure 3-9: Schematic of interactions between silver and epoxy after application of indentation force

Each silver flake in the composite exhibits the finite elasticity. On the application of indentation force, adhesion between epoxy polymeric chains increases by reducing free volume. At the same time, silver particle between the polymeric chains is elastically deformed and remains intact after removal of indentation force. Therefore, indentation force may result in permanent reduction in electrical resistivity of ECAs.

3.4.5 Mechanism of conduction development

Electrical conduction in ECAs is facilitated by the establishment of contacts among conductive particles in insulating matrix. Each conductive particle can contact directly with others which depend on packaging arrangement of particles. When two filler particles make a contact, an electrical connection is created between them such that conductivity around contact region increases. In absence of conductive filler particles, conductivity is same as insulator. Electrical contact resistance at the interface between filler and polymer is contributed by intrinsic resistance of conducting particles, insulating polymer and filler-polymer boundary. In this illustration, we mean filler particles as silver flakes and insulating matrix as epoxy. Electrical contact resistance at filler-insulator interface can overcome by tunneling effect if two particles are in the tunneling vicinity of electrons. At low concentration of filler particles i.e. large separation between filler particles, tunneling may not occur resulting in increased overall resistance of the composite. In this situation, polyaniline acted as a charge carrier medium in this insulating region. Concept of constriction resistance arises due to

bending of electrical current lines at mesoscale contact area between filler particles. Polyaniline seemed to decrease the constriction resistance by establishment of contact between two filler particles. Even if polyaniline fails to establish the physical contact between two conductive particles, it occupies the interstitial space such that effective tunneling can occur. One of the important applications of conductive adhesive being as interconnects under the application of pressure and temperature where stability of resistance is a crucial issue. Addition of polyaniline to the silver-epoxy composite significantly stabilized the electrical contact resistance of the composite. Though it is believed that after complete curing of the composite silver particles can't move, the problem of silver migration and void formation in matrix, due to evaporation of solvent still exist. Incorporation of polyaniline can overcome this drawback by decreasing solvent evaporation effect and restricting significant silver movement in the polymeric matrix.

3.4.6 Conclusions

Electrical response of silver-epoxy and silver-polyaniline-epoxy ECAs have been investigated by tracing the indentation force and time dependency of resistance. Volume fraction of conductive filler required to establish the conducting network, with and without polyaniline was determined. "Bridging" effect of polyaniline helped to lower the percolation threshold and stabilize the electrical contact resistance of the ECA. Mechanism of conduction development in electrical conductive adhesive has been proposed based on physical and intrinsic properties of individual components, surface properties and interactions between fillers and epoxy matrix. It can also be concluded that silver-polyaniline-epoxy is a model system for the fine pitch applications in ECAs.

Chapter 4
In-situ electro-mechanical analysis of viscoelastic, polyaniline-tailored silver-epoxy system

4.1 Introduction

Electrical conductive adhesives (ECAs) are polymer composites filled with micron-sized conductive fillers. The polymer matrix gives strength and bonding ability to ECAs whereas the fillers facilitate with electrical conductivity. ECAs find extensive applications as interconnect materials for device assembly to meet the increasing demand of miniaturization of electronic products and portable devices [2], [4], [5], [74]. Adhesive bonding technology requires milder processing conditions, fewer processing steps, lower process cost than the conventional soldering technology, and has the fine pitch capability due to the availability of small size conductive fillers [2], [4], [5]. Silver flakes are most readily used in commercial conductive adhesives because of their high conductivity and stable contact resistance. In recent years, there is an increasing interest in the development of composites comprising of two or more filler components to improve the performance and to reduce the cost [6], [74]. Mixture of micro-scale and nanoscale particles or mixture of metallic and conductive polymer fillers have been utilized to improve the electrical conductivity of ECAs and to reduce the cost [6], [74], [75]. Conductive polymer composites have also been utilized in the development of smart materials and structures in which the conductive fillers can response to the external (electric and magnetic) fields by aligning to the field direction; the resultant anisotropic structures have a pronounced force-dependent conductivity or pizeoresistivity.

As illustrated in following, engineering applications of ECA involves a compressive pressure and/or heat during the bonding of components, where the conductivity of the resultant bonds significantly depend on the pressure and heat. Figure 4-1 also depicts the typical morphology of conductive fillers: silver flakes, polyaniline micro particles and their chemical structure. Polyaniline structure shows equal proportions of reduced and oxidized form in emeraldine base. It is well-known that the co-existence of both, reduced and oxidized form imparts electrical conductivity to the polyaniline.

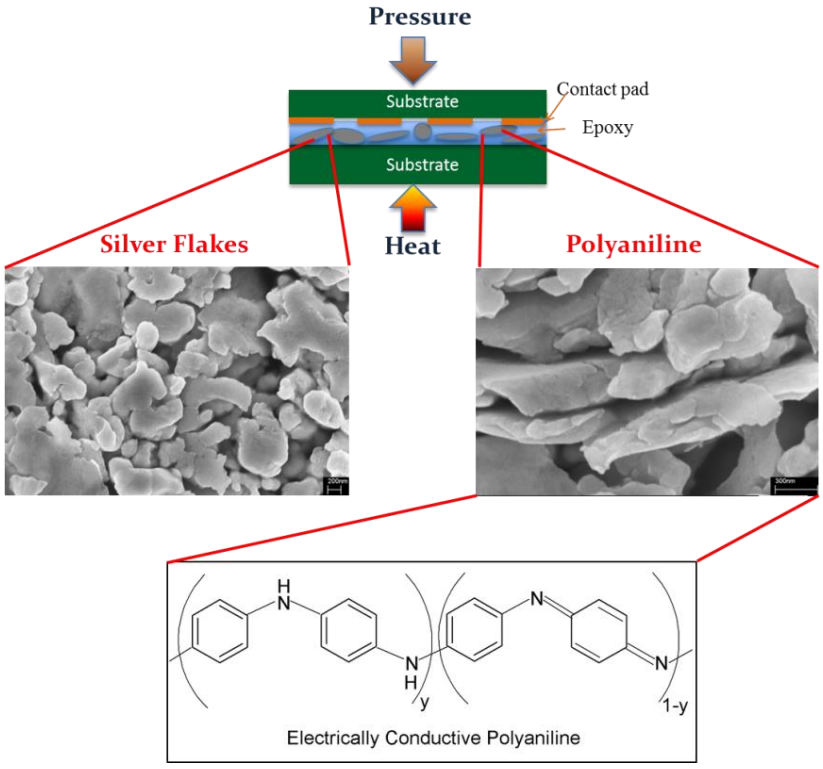

Figure 4-1: Concept of application of conductive adhesive in microelectronic packaging along with SEM images of silver flakes and polyaniline, and chemical structure of polyaniline (Scale bar: 200nm and 300nm)

The reliability of conductive bonding in terms of its contact resistance is critical for precise packaging of functional components [76], [77]. However, ECA bonds suffer from a relatively poor reliability in comparison to the conventional soldering and wire bonding. One reason might be related to the distinctive composite nature of ECA; their conductivities depend on the cooperative behavior of interacting fillers to form conductive paths, which are sensitive to the mechanical stress. Despite a large number of potential applications and many fundamental studies, the understandings of the electro-mechanical behaviors of ECAs are still very limited; the reliability of ECAs is still a major concern in practical applications [78], [79].

The ultimate objective of our research is to develop low-cost and efficient conductive adhesives by employing novel conductive fillers to the conventional silver filled epoxy adhesives. Our previous work explored the use of polyaniline (PANI) as a co-filler in silver-filled epoxy [6]. Polyaniline is a conductive polymer and has a moderate conductivity in between those of the silver and epoxy. Also, more recently, Lu et al and Zhao et al demonstrated the large-scale synthesis of polyaniline for its

potential use in electrically conductive composites [80], [81]. We used polyaniline to dope the epoxy matrix to reduce the cost by reducing the percolation threshold of silver –filled epoxy. In this study, we have investigated the polyaniline co-fillers as a potential material way to tune the mechanical and electrical properties of the ECAs and have provided a detailed analysis of the electro-mechanical properties of silver-epoxy (Ag-epoxy) and silver-polyaniline-epoxy (Ag-PANI-epoxy) system in both partially-cured/ viscoelastic and fully-cured states. The change in electrical contact resistance under varied compressive load and its evolution over contact time were investigated. In an analogy to the engineering strain, the concept of "electrical stain" is introduced to characterize the relaxation of electrical contact resistance. Adding polyaniline made the electrical strain more sensitive to engineering strain and the electro-mechanical coupling to deviate from the linear relationship. In contrast to many studies focusing only the cured system, the study of partially-cured or an intermediate stage in curing process allowed us to obtain fundamental insights into the establishment of conductive network and the particular role of polyaniline in tailoring the electro-mechanical response of the ECAs. These research findings provide insights into reliability of conductive adhesives and the way to use polyaniline to tailor the conductivity of the adhesive bonds or joints in the development of advanced functional devices.

4.2 Experimental

We used silver flakes (Sigma-Aldrich, ~10μm, resistivity 1.59 μΩ-cm) as a main filler and polyaniline (Sigma-Aldrich, 3-100 μm) as a co-filler in epoxy resin (D.E.R.^{TM} 322, Dow Chemical Co.). Triethylenetetramine (TETA) containing crosslinking agent (DEH 24, Dow Chemical Co.) was used for curing the epoxy. The polyaniline microparticles were emeraldine salts and have a dark green colour. Two different methods were used to prepare the silver-polyaniline-epoxy ECA. The first method was to add silver fillers into liquid epoxy resin, add polyaniline, and then the crosslinking agent (D.E.H.^{TM} 24, Dow Chemical Co.). The dispersion process involved the high shear mixing using vortex mixer for 45 min followed by 30 min of ultrasonication in an ultrasound bath. The similar dispersion process was followed for both of the methods described above. The second method was to add polyaniline into liquid epoxy resin, add silver flakes, and then the crosslinking agent. After adding the crosslinking agent, the entire mixture was degassed under vacuum for half an hour; and then it was spin-coated on an area of 1 x 1 cm^2 smooth copper substrate (36 gauge, Basic Copper, IL, USA) at a speed of 1100 RPM. As the thickness of ECA films at the constant RPM changes with the composition of ECAs, spinning time was adjusted to have a consistent film

thickness. As the thickness of ECA films at the constant RPM changes with the composition of ECAs, spinning time was adjusted to have a consistent film thickness. The ECA films were partially cured at 40^0C for 30 min and were fully cured at 150^0C for 2 hours. The thickness of the cured adhesive coating was measured to be 450 ± 7 µm. Preliminary experiments showed that polyaniline particles were dispersed well in the composite. However, the silver flakes were only dispersed well in epoxy composite prepared in the first method, resulting in homogenous composite samples when cured. In contrast, silver flakes formed aggregates in epoxy composites prepared in second method, giving inhomogeneous samples. This observation may be explained by the fact that the addition of polyaniline increased the viscosity of the composite and thereafter the dispersion of silver flakes was not effective. Thus, we used the first method to prepare the composite samples. Samples were prepared with a constant 70 weight % silver fraction and varied fraction of polyaniline between 0-15 weight % relative to the weight of epoxy.

4.3 Characterization

The electrical properties of the ECAs were measured in the z- or thickness direction by indenting a circular flat copper probe using a micro/nano material tester (CETR Universal Micro/nano Material Tester equipped with an electrical sensor) and in the x-y plane by a typical four-probe set-up (Keithley 2440 5A Source Meter, Keithley Instruments Inc.). Figure 4-2 shows the schematic of indentation set-up to measure force-dependant electrical contact resistance and schematic of typical four-point probe technique to measure the resistivity of ECAs.

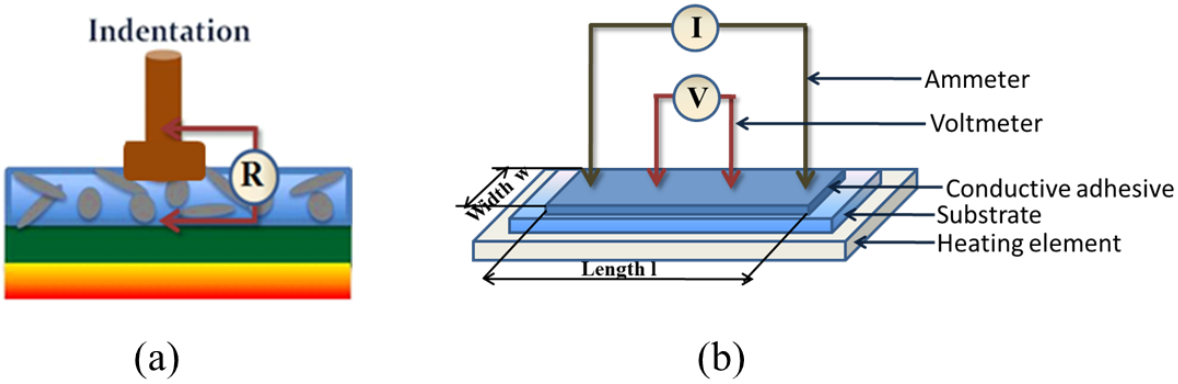

Figure 4-2: Schematic of indentation setup and typical four-point probe technique

The measurement in the z-direction is particularly useful for investigating the coupling of electrical and mechanical responses of ECAs. In this novel characterization technique the change of electrical

contact resistance was measured with respect to contact pressure and time during the loading in viscoelastic state. The circular flat probe was used for the indentation experiments instead of the frequent use of pyramidal probes for indentation of various adhesives. Thus, the contact area between probe and sample remained constant during the indentation, which minimized the efforts for measurement of contact area and reduces additional variable in the system. A compressive force up to 100g was applied on viscoelastic films; electrical contact resistance and displacement in z-direction were recorded as a function of compressive force and time. Furthermore, we explored the relaxation behavior of electrical contact resistance during creeping at a constant compressive force of 100g for 300 seconds. Scanning electron microscopy (SEM) imaging was performed on the cured ECAs for morphological characterizations. As-prepared, cured films of adhesives were surface polished to remove the insulating layer of epoxy; gold sputtering was carried out to ground the electrons and for better image quality.

4.4 Results and discussion

4.4.1 Electromechanical Behavior of Polyaniline-tailored Silver/Epoxy Conductive Composites

Polyaniline-tailored silver/epoxy conductive composite films were prepared by two different methods. The first method was to add silver fillers into liquid epoxy resin, add polyaniline, and then the curing agent. The second method was to add polyaniline into liquid epoxy resin, add silver flakes, and then the curing agent. Preliminary experiments showed the silver flakes were only dispersed well in epoxy composite prepared in the first method, resulting in homogenous composite samples when cured. In contrast, silver flakes formed aggregates in epoxy composites prepared in second method, giving inhomogeneous samples. This observation may be explained by the fact that the addition of polyaniline increased the viscosity of the composite and thereafter the dispersion of silver flakes was not effective. Thus, all the samples used in this work were prepared by the first method; they have a constant 70 wt% silver fraction and varied fractions of polyaniline between 0-15 wt% relative to the weight of epoxy resin. Figure 4-3 shows the force-dependant electrical contact resistance of partially-cured ECAs containing varied fractions of polyaniline as a function of the compressive force. The partially-cured ECAs were viscoelastic pastes, representing an intermediate stage in the curing process. Monitoring the force-dependant behaviors of these viscoelastic ECA allowed us to obtain insights into the establishment of conductive network. A sharp transition in electrical contact

resistance was observed while applying a compressive force because of the need of a critical or a minimum preload Fz_{min} to establish the conductive network of the fillers. This critical preload appeared to increase with the addition of the polyaniline because of increased viscoelasticity of the composite. After the transition, the contact resistance is constant even at higher preload, giving a steady-state value characteristic of the composition of the composite. We noticed the ECAs film became thinner at higher preload; presumably some of the ECA paste was squeezed out. Furthermore, at high compressive forces or strains, more epoxy fluids than the solid fillers might be moved out so that the local weight fraction of the conductive fillers increased to form a highly-packed continuous conductive path.

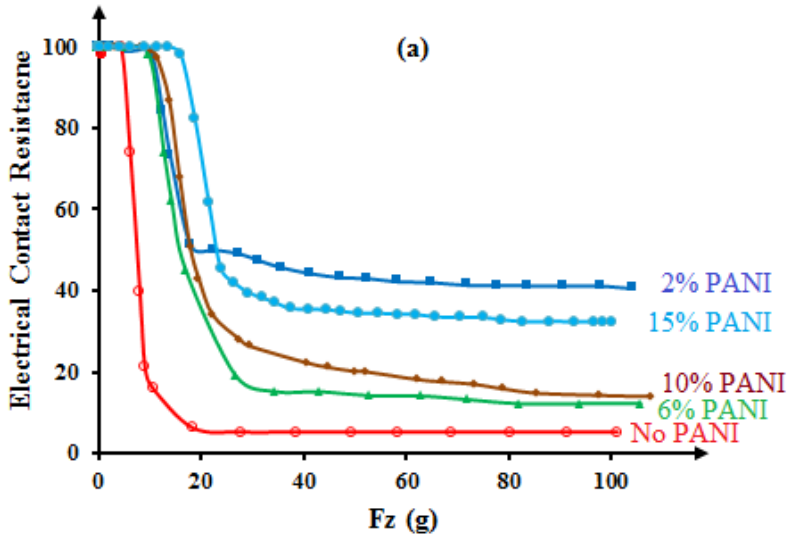

Figure 4-3: Behavior of electrical contact resistance of ECA with increase in compressive force at varying polyaniline fractions

Figure 4-4 plots the steady-state electrical contact resistance (viscoelastic state) as a function of the weight % of polyaniline. The steady-state electrical contact resistance of the composite increased with the addition of polyaniline because of its lower conductivity than that of silver flakes. We had expected a monotonic increase in electrical contact resistance with the increase of the weight fraction of polyaniline. But, the addition of 2 weight % polyaniline showed a much higher increase in the steady-state electrical contact resistance compared to the other formulations.

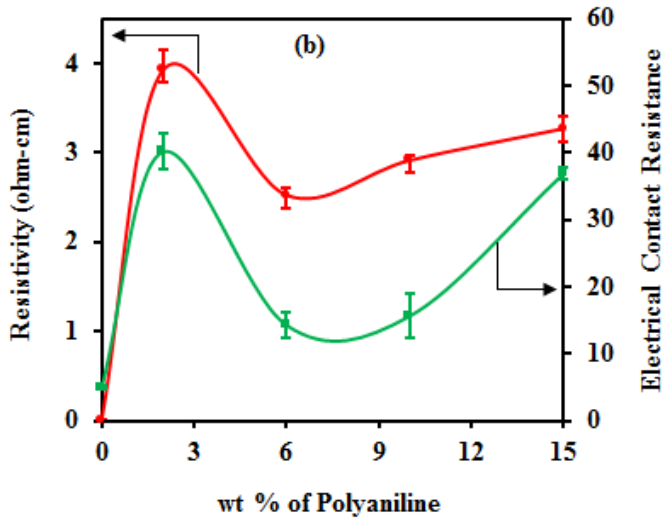

Figure 4-4: Steady state electrical contact resistance and electrical resistivity of ECA at varying weight % of polyaniline

To verify this unexpected behavior, ECA films were fully cured after the characterization of force-dependant resistance and were analyzed for electrical resistivity by a four-probe technique. Resistivity of the ECAs ρ is calculated using the equation $\rho = R_s t = \left(\frac{\pi t}{\ln 2}\right)\frac{V}{I}$ $\Omega.cm$, where *Rs* is the resistance, *t* is the thickness, *I* is the applied current, and *V* is the measured voltage. The electrical resistivity of fully cured samples is plotted as a function of the weight fraction of polyaniline in above Figure 4-4. It shows the same trend as the steady-state electrical contact resistance values. To explain this behavior, we considered the effect of packing density or concentration of PANI on electron conduction ability of the ECA. At 2 wt%, the PANI particles were dispersed sparsely in the composite and might blocked the contacts of silver particles by acting as a spacer; meanwhile, the packing density of PANI was low and not sufficient to form a continuous conductive path among them. Thus, the electrical contact resistance with the addition of 2 wt % was larger than that of other samples having higher PANI contents. In order to elucidate the unexpected increase in electrical contact resistance with the addition of 2 weight % polyaniline, we conducted morphological analysis on all the samples using SEM. Typical SEM images for samples with 2, 6 and 15 weight % are shown in Figure 4-5; the SEM images of samples with 10 weight % polyaniline are almost identical to those of samples with 15 weight %.

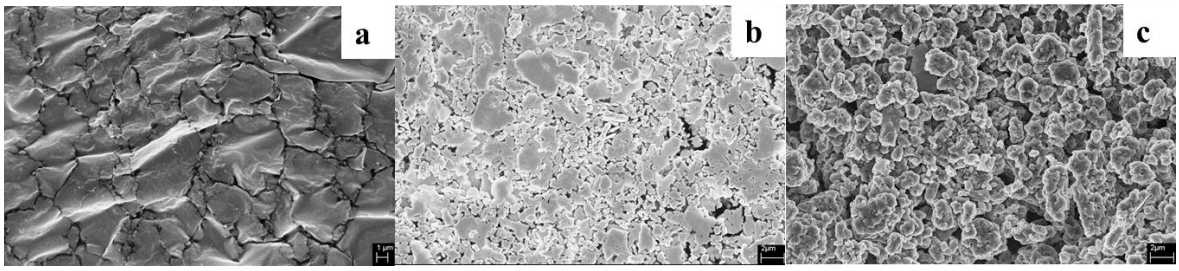

Figure 4-5: SEM images of ECAs with (a) 2% polyaniline, (b) 6% polyaniline and (c) 15% polyaniline (Scale bar: 1 µm, 2 µm and 2 µm)

It is interesting to notice the "cracked" morphology of samples of 2 weight % polyaniline. We suspect that addition of 2 weight % polyaniline resulted in infringement of conductive network due to increased resistance between silver and polyaniline flakes contacts. EDX analysis was also carried out; although silver peak was identifiable in EDX, the nitrogen of the polyaniline backbone was not distinguishable from the carbon due to their low atomic numbers. We examined many SEM images and found PANI was able to be distinguished in its shape from silver particles.

4.4.2 Evolution of the relaxation in electrical contact resistance and "Electrical Strain"

We further examined the change in the electrical resistance of ECA under a constant compressive load of 100g. As expected, the viscoelastic composites crept at that compressive load. The engineering strain was calculated by the change in thickness Z or the displacement d as

$\varepsilon = \frac{Z_0 - Z_t}{Z_0} = \frac{d}{Z_0}$, while Z_0 is thickness of the film at t = 0 and Z_t is thickness at time *t*. Figure 4-6 shows the change in both electrical resistance and engineering strain with time during the creep at the constant compressive load. The contact resistance decreased with time while the engineering strain increased. It was also observed that the values of engineering strain decreased with the increase in polyaniline fraction from the top to bottom panels in Figure 4-6. Note that the increased scale of Y-axis or the range of resistance gives better view of the change in resistance.

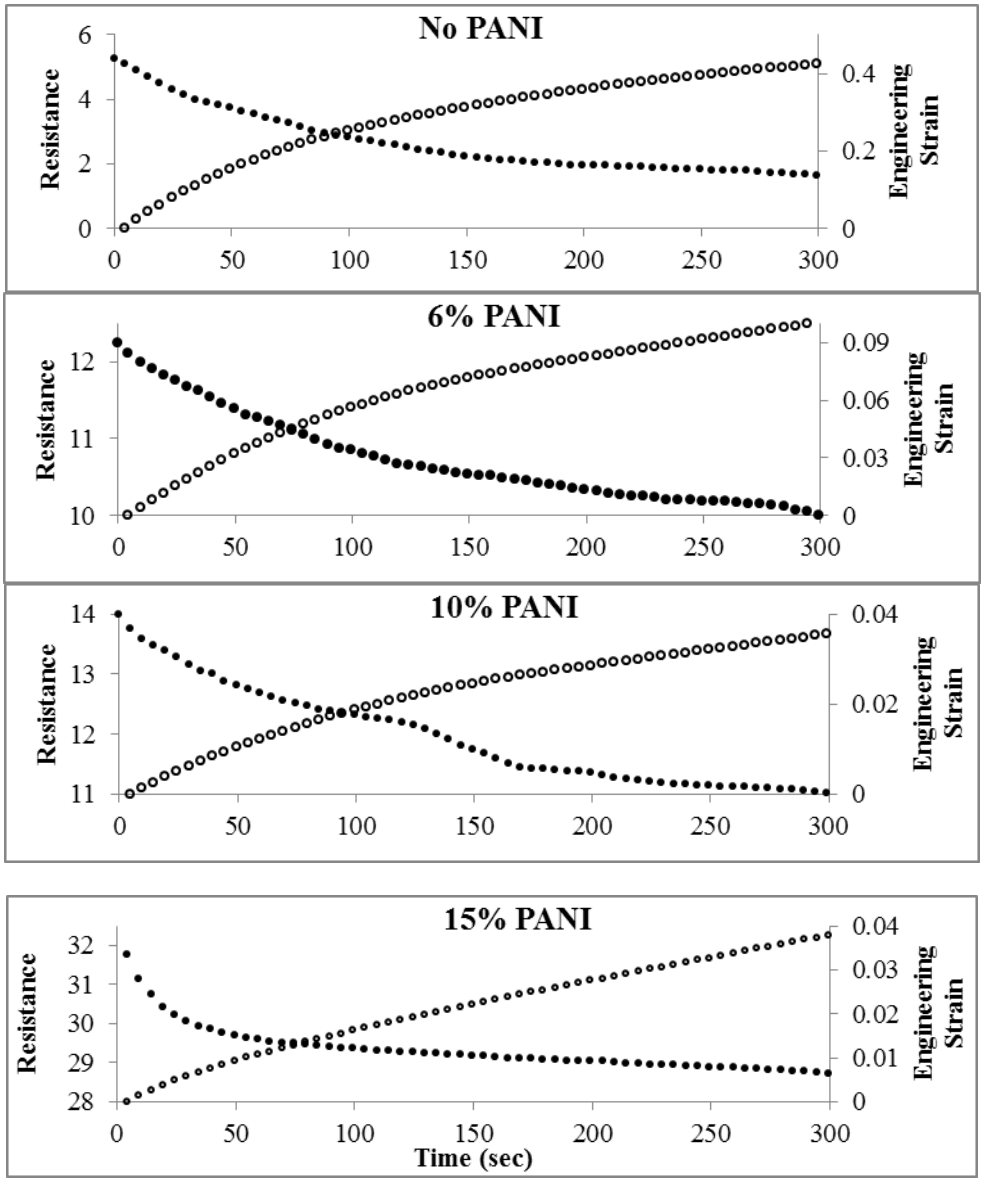

Figure 4-6: Relaxation in electrical contact resistance and increase in engineering strain of ECAs as a function of time and polyaniline concentration at a constant compressive force (●-Resistance, ○-Engineering strain)

To obtain insights about the possible linkage between the change in electrical contact resistance and that in engineering strain, we define a term called as "electrical strain"

$\varepsilon_R = \frac{R_0 - R_t}{R_0}$ which is similar to the engineering strain, $\varepsilon = \frac{Z_0 - Z_t}{Z_0}$. R_0 is initial electrical contact resistance at t = 0 and R_t is resistance at time *t*. Note that the electrical strain can also be defined in

terms of the change in electrical conductivity because of the reciprocal relationship between the electrical resistivity and conductivity. To the best of our knowledge, it is the first time that the concept of electrical strain is introduced to characterize the relaxation behavior of the electrical strain. Figure 4-7 plots the electrical strain as a function of time at varied polyaniline concentrations.

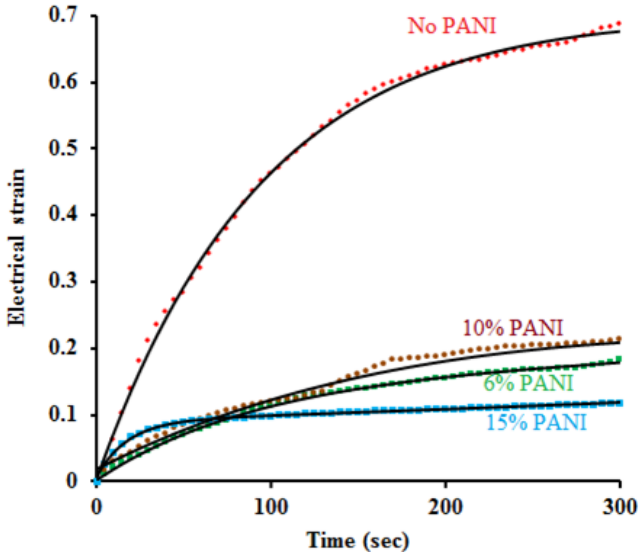

Figure 4-7: Change in electrical strain as a function of time and polyaniline concentration. Solid line shows fitted response of electrical strain using Burger's model

The electrical strain increased non-linearly with time and tended to reach a constant value if sufficient time was provided. Over the period of 300 seconds, the electrical strain of the samples without polyaniline was considerably larger than those with polyaniline; the increase in the electrical strain was also faster than the others, particularly within the first 150 seconds. Between the 150 to 300 seconds, the increases of the electrical strains were much slower for all the samples, reaching pseudo-equilibrium states. The addition of polyaniline significantly reduced the pseudo-equilibrium electrical strain of the silver-epoxy composites. The addition of 6 and 10 weight % polyaniline showed similar electrical strain curves which lied between the curves of samples without polyaniline and with 15% polyaniline. A much denser conductive network may have been formed at 15 weight % polyaniline fraction than the other two; it took about 50 seconds to reach the steady-state electrical strain after, which is much less than the other samples.

4.4.3 Modeling the "Electrical Strain" of polyaniline-tailored ECAs

We noticed the variations in electrical strain with time and polyaniline concentrations are similar in the trend to those of engineering strain. Hence, we simulated the electrical strain behavior of ECAs using Burger's micro-mechanical model. Burger's model consists of one Maxwell unit and one Kelvin unit connected in series and divides the strain of polymeric or composite material into three parts: instantaneous deformation resulting from Maxwell spring, viscoelastic deformation resulting from Kelvin units, and viscous deformation resulting from Maxwell dashpot. Mathematically, it is a linear combination of two exponential functions.

$$\varepsilon_R(t), \varepsilon(t) = A \times e^{Bt} + C \times e^{Dt}$$

where the constants A, B, C and D are comprised of viscous and elastic coefficients of the composite material [82], [83]. Following table shows the fitting parameters of the electrical strain data.

Table 4-1: Fitting parameters of Burger's model for electrical strain data

Composition	A	B	C	D
70-0	0.7316	-0.0001	-0.7263	-0.0103
70-6	0.1539	0.0006	-0.1515	-0.0110
70-10	1.0699	-0.0018	-1.0511	-0.0031
70-15	0.0907	0.0009	-0.0820	-0.0561

The Burger's model has been widely used to characterize the viscoelastic behavior of the materials [84–86], and was recently applied by Ding et al. to simulate the changes in electrical resistance of carbon-black-filled rubber composite during compression [87]. In this study, it can be seen from Figure 4-7 that the fitting lines from the Burger's model (the solid line) match the electrical strain data well.

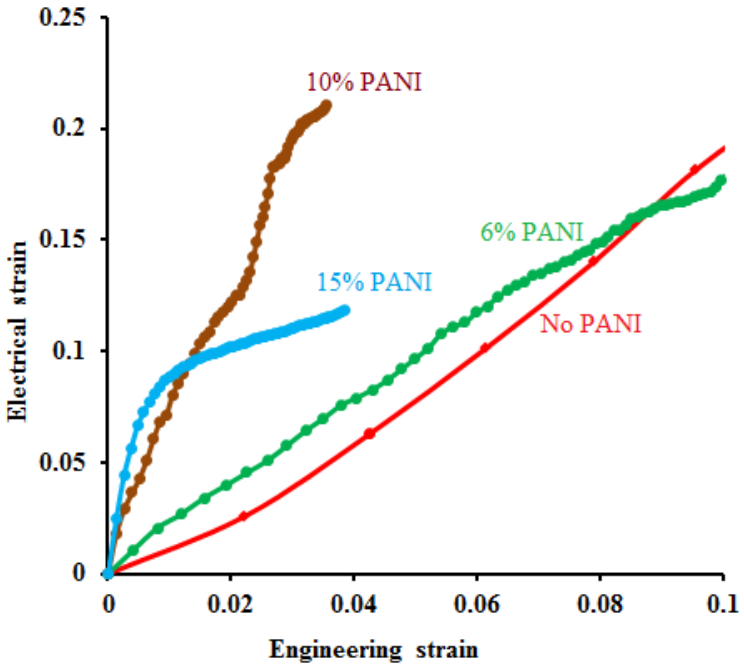

Figure 4-8: Direct dependency of electrical strain on engineering strain as a function of polyaniline concentration

Figure 4-8 shows the direct relation between the electrical strain and mechanical strain at different polyaniline concentrations. To a first approximation, the electrical strain and mechanical strain of silver-epoxy composite are linearly coupled for the strain range ε = 0-0.1. It appears that the conductive adhesive layer behaved like a homogeneous conductor at low strains. According to the classical electric theory, the electric resistance of a conductor $R = \rho l/A$ where ρ is the resistivity, l is the length and A is the cross-sectional area or the contact area of the indenter. In our measurement setup, A is a constant. The linear proportional relation between R and l suggested that the resistivity of the adhesive layer is constant at low strains. It is interesting to notice that the dependence of normalized relaxation in contact resistance on compressive strain (i.e. the initial slope of εR vs ε which is proportional to the resistivity) drastically increases with the increased polyaniline fractions. This observation is reasonable considering that the number of electrical paths increased with the compressive engineering strain so that the electrical strain increased. The addition of polyaniline significantly reduced the engineering strain but not much the electrical strain. It is interesting to notice that the dependence of electrical strain on engineering strain (i.e. the initial slope of ε_R Vs ε) drastically increases with the increased polyaniline fractions. The addition of 6 weight % polyaniline showed the linear coupling having a higher initial slope than that without polyaniline. The addition of

10 weight % polyaniline also showed a linear coupling having an even higher initial slope. The addition of 15 weight % polyaniline showed the highest initial slope but has a significant deviation from the initial linear coupling when the strain is larger than 0.005. The addition of polyaniline increased the resistivity of the Ag composite since the polyaniline is less conductive than Ag. In other words, the polyaniline bridged the silver flakes, making the adhesive composite more viscous or solid-like and more electrically resistant; thus the relaxation in contact resistance is more sensitive to the compressive strain. However, the deviation from the initial linear relationship for 10 and 15 wt% polyaniline at high compressive strains indicated stronger interaction or larger contact area among the filler particles. Since polyaniline particles are softer than silver flakes, they may undergo plastic deformation so as to increase the cross-sectional area of conductive path and give rise a lower resistivity at high compressive strains. It seems that the polyaniline bridged the silver flakes, making the adhesive composite more viscous or solid-like and creating more electrical conductive paths; thus the electrical strain is more sensitive to the engineering strain.

Overall, the dependence of the electrical strain on the mechanical strain suggested that the strain or relaxation in electrical resistance comes at least partly from the engineering strain induced during the application. Thus it is important to have a precise of control of the bonding pressure and time to have the desired electrical conductivity. Furthermore, according to the research findings of a monotonic increase in steady-state contact resistance from 6 weight % to 15 weight % polyaniline and a monotonically increase in the slope of the linear coupling between electrical strain and engineering strain, we may conclude that adding polyaniline provides a way or operating window to tailor the desired electrical conductivity of ECA. It is particularly important when well-controlled conductivity of ECAs is needed for the precision engineering application, for example, in the development of antistatic materials, electromagnetic interference shielding coatings, conducting coating materials, flexible display and many other functional devices [69], [88], [89].

4.5 Conclusions

In summary, we performed a detailed electro-mechanical study of electrically conductive adhesives filled with silver and polyaniline micro-flakes in viscoelastic state. It revealed a complex electromechanical effect of adding polyaniline to the silver/epoxy conductive adhesive composites. The addition of a small amount of PANI (2%) dramatically increased the contact resistance because it might block the contacts among silver flakes and was not able to form a continuous conductive path among them. In contrast to the 2% PANI, the addition of more PANI showed a moderate increase in

contact resistance; and the contact resistance increased with the weight fraction of PANI from 6-15%, suggesting a continuous conductive path were formed amount the PANI particles. The concept of "electrical stain" is introduced to characterize the relaxation of electrical resistance; and, the Burger's micro-mechanical model is applied and found able to simulate the change of electrical resistance with time under a constant compressive force. This study revealed a linear coupling between the electrical strain and engineering strain when the adhesives experienced low engineering strains, indicating the relaxation in electrical resistance may originate from the mechanical creep of the ECA. Furthermore, adding polyaniline to conventional silver flakes filled epoxy can be used to tailor the steady-state contact resistance and its dependence on the engineering strain. Other than reducing the cost, it may provide a novel way to control the conductivity to the adhesive bonds or joints in the assembly of portable electronic devices and in the development of advanced functional devices.

Chapter 5
Synthesis of highly crystalline and conductive polyaniline nanotubes

5.1 Introduction

Among the known electrically conductive polymers, polyaniline is one of the most promising candidates for the various electronic applications. Dimensionality and crystallinity of such a nanomaterial plays a vital role in determining its various properties. Even in case of well-studied materials, often mechanical, electrical, optical properties are improved due to its nanoscale dimensions. In addition to the dimensionality, in this work, we deal with highly crystalline nanotubes of polyaniline. Nanostructured polyaniline has attracted a great deal of interest because of tunable conductivity switching between insulator and conductor, nontoxic property, good environmental and chemical stability than their bulk counterparts [90–93]. The polymer exhibits metallic behavior in terms of electronic, magnetic and optical properties and also can retain the properties of conventional polymers such as flexibility, temperature dependant viscosity etc. It is worthwhile to note that the versatility in performance of polyaniline is because of its 'metal-like' conduction and its nano-dimensionality.

Electrical conductivity of polyaniline can be tuned from insulator-to-semiconductor-to-conductor regime by using various dopants and adjusting their degree of doping [94], [95]. The degree of doping can be controlled by acid doping or base dedoping but efforts are needed for its high precision. Fong et al demonstrated that rate of aniline polymerization significantly depends on acid concentration [96]. They also hypothesized that the formed polyaniline (oxidized) and monomer aniline exhibits the proton transfer. However, Lux et al found that high acid concentration during the synthesis of polyaniline causes significant decrease in yield [97]. Therefore, tuning of the doping is vital to control the reaction rate, yield and subsequently, the properties of polyaniline. Hydrochloric acid is widely used as a dopant for polyaniline because of its availability and simple reaction chemistry. On the other hand, bonding nature of chloride ions with polyaniline backbone chain is still unclear. Backbone structure of polyaniline emeraldine base indicating reduced and oxidized form is shown in Figure 5-1.

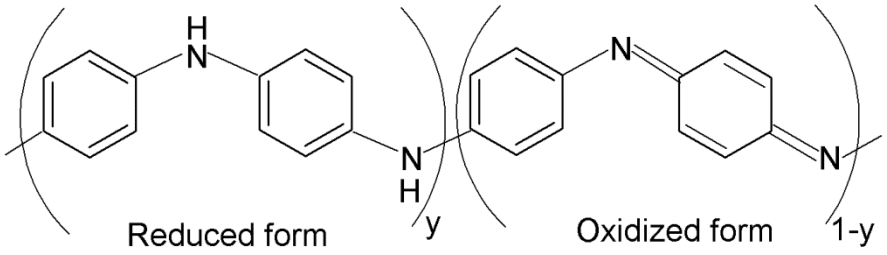

Figure 5-1: Backbone structure of polyaniline emeraldine base indicating reduced and oxidized form

Morales et al showed that the increase in substitution on polyaniline backbone decreases the electronic conjugation which resulted in decrease of conductivity [98]. Therefore, doping has to be done without affecting the backbone structure of polyaniline. Doping in polyaniline nanotubes has a deep impact on its potential applications in nano-electronics and nano-devices. It has been proved that un-doped polyaniline forms aggregates due to the hydrogen bonding between imine and amine nitrogen sites on the adjacent polyaniline molecules [99]. Such inter-chain interactions may result in gel formation and subsequent aggregation. There are still some key questions regarding the effect of doping on structural and electrical properties as well as on the device characteristics. Hence there is a considerable room for more enhanced performance of applications such as flexible electrically conductive coatings.

Different forms of polyaniline such as nanoparticles, nanotubes, nanowires can be prepared by various physical and chemical synthesis methods. Physical methods include electro-spinning [100] and various deposition techniques while chemical routes include interfacial polymerization [101], electrochemical polymerization [102] and emulsion polymerization [103], [104]. In general, polymerization of aniline has to take place in protonic acid medium which simultaneously acts as a dopant to protonate the as-synthesized polyaniline imparting the conductivity. Still, Palaniappan and co-workers carried out the polymerization of aniline without any protonic acid in the beginning of reaction [105]. Nevertheless, the choice of the best method to produce the polyaniline with desired properties remains unsolved. More recently, Antony et al reported that fibrilar polyaniline enriches the overall dispersion of polyaniline but it was difficult to determine the structure and properties of nanoscale samples because of phase separation [106]. Despite the fact that each method has its advantages and disadvantages, understanding the formation mechanism in each method and application of as-synthesized product in range of devices is still a challenge. Our research is directed

to demonstrate the formation of crystalline nanotubes of polyaniline, corresponding formation mechanism and their applications.

In order to fulfill the potential applications of our crystalline nanotubes of polyaniline, it is necessary to precisely analyse the physical and optoelectronic properties of such a one-dimensional material. Even though applications of polyaniline have been extended in various fields of electronics such as sensors [107], electromagnetic interference shielding [103], super-capacitors [92], diodes [108], limited efforts have been put to fabricate the flexible electrically conductive coatings. Insolubility of polyaniline in common solvents and its poor processability place the barrier in the development of polyaniline-based applications. Certain characteristics of polyaniline nanotubes enabled its application in the flexible electrically conductive coating i.e. nanoscale dimensions and its intrinsic anisotropic conductivity. Nanoscale dimension of polyaniline allows efficient transport of electrical carriers throughout the conductive network which is highly desired when integrated nanoscale devices involve the moving charges. To improve the electrical performance of the device, containing polyaniline, often it is incorporated with conductive metals such as silver, CNTs etc. On the contrary, we demonstrate the application of polyaniline with controlled doping level in conductive coatings. Therefore, our research has been driven by the need to replace the traditional inorganic conductive fillers and to improve the processing ability of the polyaniline nanotubes to fabricate the devices. Combination of synthesis and study of electrical properties of highly crystalline polyaniline nanotubes can offer the enticing prospect towards flexible coating applications.

In this paper, we report the experimental demonstration of the facile method for synthesis of nanotubes of polyaniline. The present approach is emphasized to synthesize polyaniline nanotubes via modified miniemulsion polymerization. Interdependent relationship in degree of doping in polyaniline, crystallinity and electrical conductivity has been extensively discussed. We also fabricated the flexible electrically conductive coating and characterized its electrical performance. In overall, we report mechanistic study of doping in crystalline polyaniline nanotubes and demonstrate its novel application in flexible electrically conductive coating.

5.2 Experimental

5.2.1 Materials

Aniline (99.9 %, corrected for water content) was purchased from J.T. Baker, USA and was stored in dark place to avoid photo-polymerization. Ammonium persulfate (98%) was procured from EMD

Chemicals which contained maximum insoluble matter of 0.005%. Polyoxyethylene sorbitan monooleate and polyvinyl alcohol (99+% hydrolyzed) of mol wt. 146,000-186,000 Da was purchased from Sigma, USA. Hydrochloric acid (37 weight %) was used as a doping agent and was purchased from Thermo Fisher Scientific. All the glassware were cleaned prior to use; they were soaked in a 1 M solution of sodium hydroxide for 24 h, neutralized with acetic acid, and then rinsed with DI water. The DI water (resistivity > 10 MΩ.cm at 25^0C; total organic carbon < 20 ppb) was obtained using the RiOs-DI Clinical system (Milli-pore Corporation).

5.2.2 Synthesis and doping of polyaniline nanotubes

Solution of 0.1M aniline was prepared in 1M HCl. Surfactant solution of polyoxyethylene sorbitan monooleate (0.08M) was prepared in ethanol. Polyoxyethylene sorbitan monooleate formed slightly hazy faint yellow solution when it was mixed with ethanol. Both, the solution of surfactant and the monomer were sonicated separately and then were mixed together. As-prepared mixture was brought to 4^0C prior to the start of reaction by circulating the coolant through jacket of the reactor. Reaction was carried out in vigorously stirred 1L reactor, equipped with temperature controlled jacket. Schematic of reaction set-up is shown in Figure 5-2.

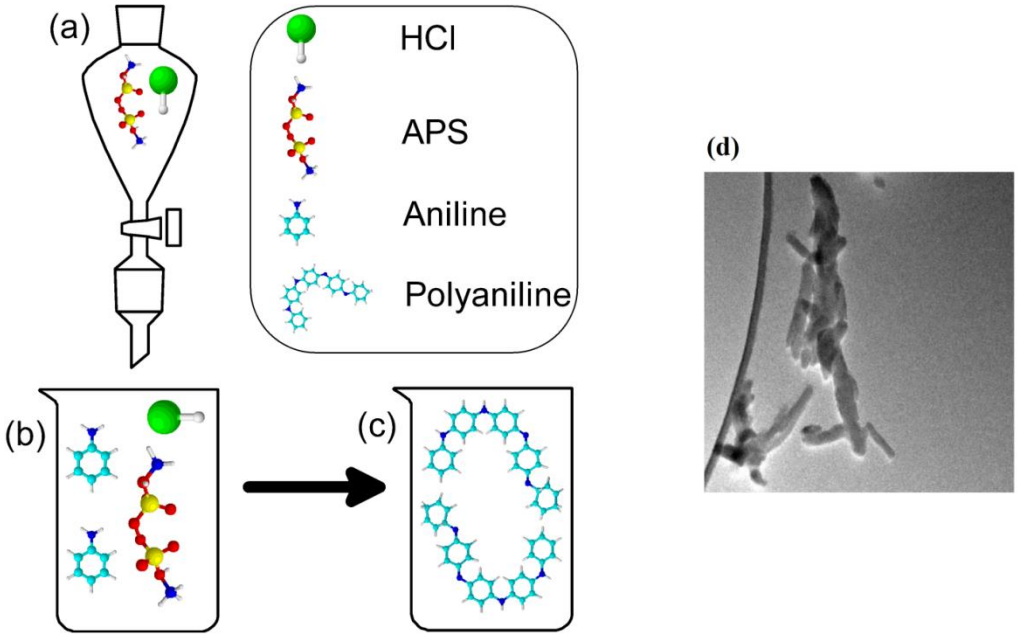

Figure 5-2: Schematic of aniline polymerization set-up (a) controlled addition of APS solution in HCl, (b) Temperature controlled jacketed reactor, (c) as-synthesized purified polyaniline nanotubes and (d) typical TEM image of polyaniline nanotubes

0.05M solution of ammonium persulfate was prepared in 1M HCl and was continuously added for half hour to emulsified mixture of aniline. The polymerization was continued for 2 hours at 4^0C and dark green color was observed at the end of reaction. Polymerization of aniline takes place according to the scheme depicted in Figure 5-3.

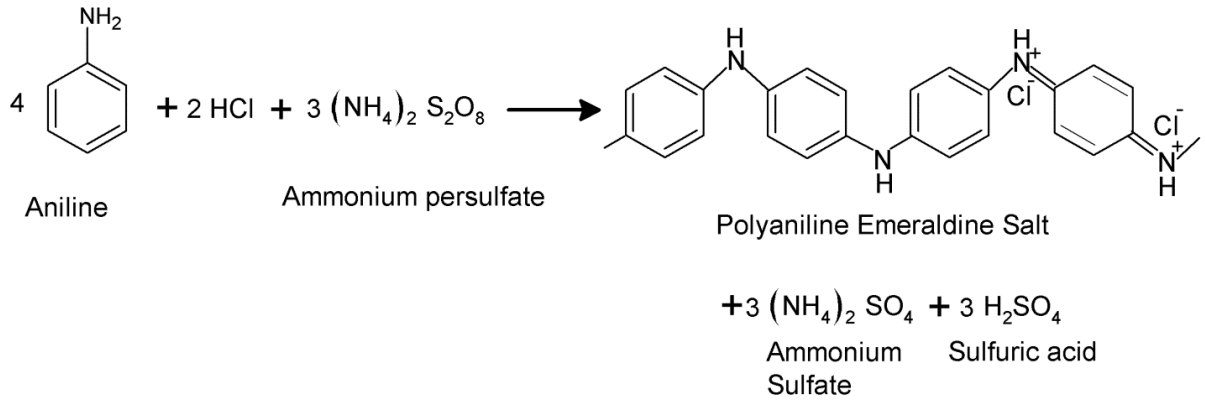

Figure 5-3: Synthesis scheme of polyaniline emeraldine salt from aniline monomer with '*in-situ*' doping of HCl in presence of ammonium persulfate. Chloride ions are attached to imine nitrogen of polyaniline backbone

Stoichiometrically, reaction produces 3 mols of sulfuric acid per 4 mols of aniline monomer. Therefore, intrinsically, reaction takes place in acidic medium and pH of reaction mixture ranges in between 2 and 4 [109]. During the course of reaction, transition of color from blue to dark green was observed, suggesting the formation of emeraldine salt of polyaniline. Depending on the dopant amount, instance of appearance of green color was changed. We noticed that increase in dopant to monomer ratio causes early stage appearance green color. Therefore, we speculate that HCl might increase the rate of polymerization of aniline. Reaction was carried out for dopant/monomer ratio of 8, 16 and 50 to study the effect of dopant.

Purification of the product was carried out by centrifugation of reaction mixture followed by washing profusely with deionized water and acetone for at least 4 times to remove the traces of surfactant, unreacted aniline and unreacted HCl. Purified polyaniline was dried under dynamic vacuum for 24 h to remove the wash solution.

5.2.3 Fabrication of flexible conductive coatings

Most of the methods reviewed in the literature for the fabrication of thin layer involve the growth of polyaniline on the substrate [91], [92], [110]. Herewith, we report the method which shows the

potential of large scale fabrication of flexible electrically conductive coatings. Solution of polyvinyl alcohol (10 wt%) was prepared by dissolving it in DI water at 80^0C in vigorously stirred environment. Special care was taken to avoid a contact with impurities in order to prevent the optical transparency of the solution. Pre-measured quantity of polyaniline nanotubes was uniformly dispersed in PVA solution under the intense sonication. Polyethylene terephthalate overhead transparency (Xerox Corporation, NY, USA) was chosen as a substrate for casting the film of PVA-polyaniline solution. Thin film of PVA-polyaniline solution was casted on the PET substrate using spin-coater at 500 RPM. As-casted conductive coating was dried in air at room temperature for 12 h to allow firm bonding of polyaniline nanotubes to the substrate. Physical observation of the conductive coating and random scratch test at considerable finger force could not peel the film off the substrate. Thus, the fabrication method demonstrated here is very robust and may lead to broad applications.

5.2.4 Characterization

Polyaniline nanotubes were characterized by several techniques to analyse its optical, structural, morphological, thermal and electrical properties. Fourier-transform infrared spectra (FTIR) of the polyaniline samples (3 repeats) were recorded using a Varian 640-IR with 100 scans per spectrum at 2 cm^{-1} resolution. The spectra were corrected for the presence of moisture and CO_2 in optical path. Wavenumber range of 2000-400 cm^{-1} was adopted for the FTIR analysis. Morphological characteristics of polyaniline nanotubes were examined at various locations by field emission scanning electron microscope (SEM) using LEO FE-SEM 1530 (Carl Zeiss NTS), operated at 10 kV. The samples were prepared by depositing one drop of the sonicated polyaniline containing solution on the conductive carbon tape and dried in air for 24 h, followed by gold sputtering for 120 s. High-angle annular dark-field (HAADF) transmission electron microscopy images combined with energy dispersive X-ray spectroscopy (Oxford EDX detector) data were acquired on a FEI Titan 80-300 TEM (FEI company, Eindhoven, The Netherlands), equipped with a CEOS image corrector and operated at 80 kV. To prepare TEM samples, one droplet of dilute dispersion of polyaniline nanotubes in methanol (1 mg/mL) was dropped on a lacey/holey carbon copper grid and dried for 1/2 h in air. Ultraviolet-visible spectroscopy (UV-Vis) (UV-2501 pc, Shimadzu) was performed (3 repeats) to confirm the formation and doping in polyaniline nanotubes. Spectra of polyaniline solution in DMF were obtained in 1.00 cm path length quartz cuvettes, and concentration of all samples was maintained at 3mg per 3 mL. The bulk resistivity of polyaniline samples (in form of compact film) was measured using a four-point probe setup consisting of a probe fixture (Cascade microtech Inc.)

and a source meter (Keithley 2440 5A Source Meter, Keithley Instruments Inc.). The sheet resistance of polyaniline nanotubes (Rs) was estimated by the drop in voltage when a constant current of 100 mA was applied. The electrical resistivity (ρ) of the film of polyaniline nanotubes was calculated using the following equation:

$$\rho = R_s \times t = \frac{\pi \times t}{\ln 2} \times \frac{V}{I}$$

where *d* is the thickness of samples; *I* and *V* are the applied current and the measured voltage, respectively. The above equation was used with following assumptions: 1) the conducting sheet infinite in the horizontal directions, 2) the thickness is < 0.4 x the spacing of the probes, 3) temperature is constant throughout the measurement, and 4) probe spacing is truly constant. Weight loss and subsequent degradation mechanism of doped polyaniline in powder form was studied using thermo-gravimetric analysis (TGA) (TA instrument, Q500-1254). Samples of about 4 mg were placed in TGA sample pan. Dynamic scan was performed from 25^0C to 800^0C with a heating rate of 10^0C/min under nitrogen atmosphere. X-ray diffraction (XRD) analysis was carried out using Bruker AXS D8 ADVANCE with Cu-Kα_1 emission and X-ray wavelength of 1.5406A^0.

5.3 Results and discussion

5.3.1 Synthesis of polyaniline nanotubes

Polyaniline nanotubes were synthesized using modified miniemulsion polymerization method. Scheme for the synthesis of polyaniline nanotubes with '*in-situ*' doping is depicted in Figure 5-3. '*In-situ*' doping reduces an extra step of doping of polyaniline emeraldine base. Therefore, aniline monomers get converted to polyaniline emeraldine salt with intermediate emeraldine base. Conventionally, it can be accounted as a type of chemical oxidative polymerization of aniline. As both, the aniline and the APS were mixed in HCl, and then reaction was carried out; polymerization of aniline took place in acidic medium. Polymerization of aniline is an exothermic process; therefore it was performed at 4^0C. We precisely controlled the rate of addition of APS solution to aniline solution which helped to maintain the temperature of reaction mixture under vigorous stirring as shown in Figure 5-2. Our preliminary experiments where all APS was added to aniline at once (without stirring) showed that formation of polyaniline results in rapid sedimentation from solution and polyaniline particles/fibers get aggregated. We hypothesized that as reaction proceeds secondary nucleation takes place on the surface of produced polyaniline which ultimately results in formation of

strong aggregates. The key step in our work involved the suppression of secondary nucleation/overgrowth of polyaniline on the already formed nanotubes of polyaniline. Use of polyoxyethylene sorbitan monooleate helped us to control the dimensions of polyaniline nanotubes by forming the soft template of uniform "reactor" size. Li et al have shown that homogeneous nucleation of polyaniline results in formation of nanotubes while heterogeneous nucleation causes formation of granular particles [111]. Our morphological analysis of powdered polyaniline using SEM (Figure 5-4) shows that polyaniline nanotubes form entangled network in bulk state.

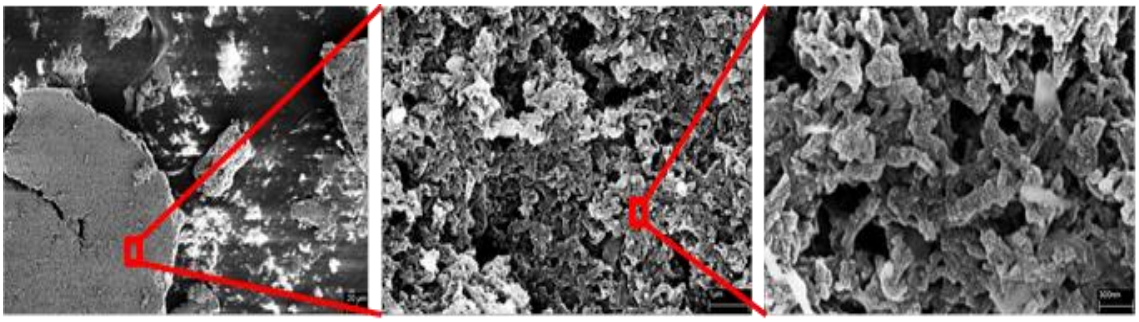

Figure 5-4: SEM images of bulk powdered polyaniline with increasing magnification, showing the close-in views of entangled polyaniline nanotubes (Scale bar: 20µm>1 µm>100nm)

Addition of APS in controlled manner caused spontaneous formation of nuclei which is a homogeneous process and vigorous stirring prevents the secondary growth of polyaniline. According to classical precipitation theory, when the concentration of small molecular aggregates exceeds the supersaturation level in solution, formation of polyaniline takes place [112]. Heterogeneous nucleation (secondary growth of polyaniline) is a predominant mechanism in formation of polyaniline. Our synthesis method could efficiently produce the high quality nanotubes of polyaniline which can be attributed to significant prevention of heterogeneous nucleation. However, TEM images at high resolution (Figure 5-5) suggest that more precise control on nucleation is needed to avoid the secondary growth of polyaniline.

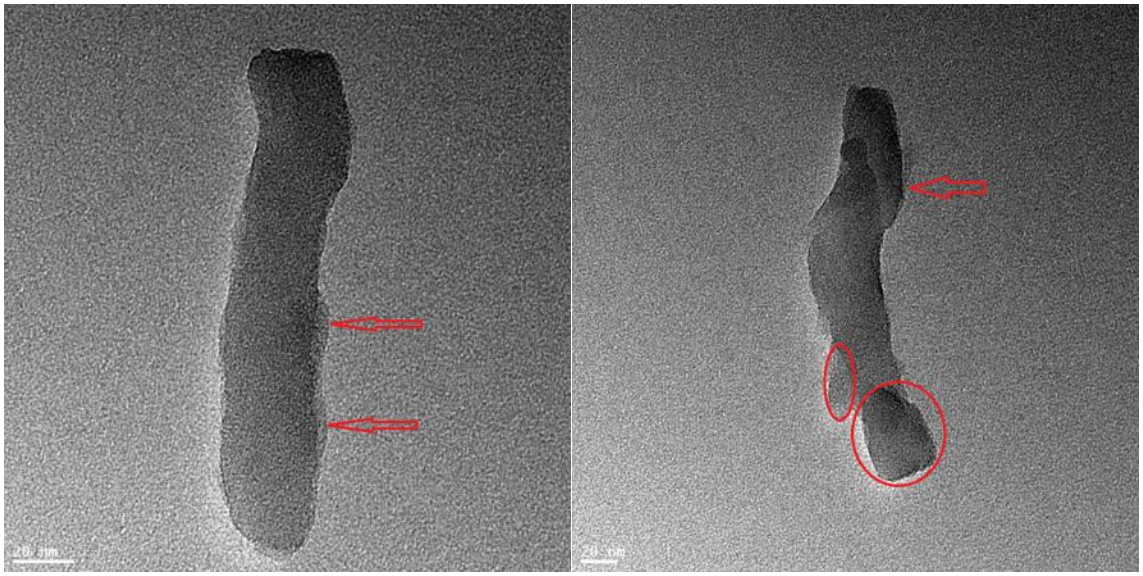

Figure 5-5: TEM images of individual polyaniline nanotubes. Arrow and circles shows probable sites of secondary nucleation

As we stated earlier, our polyaniline nanotubes bear high potential of being used as flexible electrically conductive coating. For the purpose, uniform and long-term dispersion of polyaniline is necessary. Typical obstruction in commercialization of polyaniline-based conductive coatings can be stated as the significant cost involved in dispersion and stabilization of nanodimensional polyaniline. We achieve the stable dispersion of polyaniline nanotubes, with varying degree of doping, in DMF. We ascribe this stable dispersion to the use of surfactant and dopant. Owing to homogeneous nucleation, polyaniline nanofibers form interconnecting network which is desired to obtain uniform electrical conductivity. Entanglement of polyaniline can be attributed to interchain and/or intrachain interactions. Figure 5-6 shows images of stable dispersion of polyaniline at different dopant to monomer ratios.

D/M=8 D/M=16 D/M=50

Figure 5-6: Images of the stable dispersion of polyaniline nanotubes in DMF at different dopant to monomer ratio; increasing dark green color signifies formation of emeraldine salt of polyaniline

It is clearly seen that increase in the ratio causes colour transformation form bluish green to dark green. Bluish green colour in D/M=8 implies the presence of emeraldine base along with emeraldine salt while disappearance in later two signifies the complete transformation into emeraldine salt. Increase in dopant causes increased formation of emeraldine salt of polyaniline.

5.3.2 FTIR analysis of polyaniline nanotubes

Effect of doping on chemical transformation of polyaniline nanostructures was studied by FT-IR as shown in Figure 5-7. Distinct characteristics of doped samples are associated with emeraldine salt of polyaniline. The peak at 849 cm^{-1} is related to the out-of-plane stretching vibration of 1,4-disubstituted benzenoid ring which is a para-coupling structure [113]. Complicated but vital peaks were observed in the range between 1100 and 1000 cm^{-1}. Minor peak at 1059 cm^{-1} is associated with sulfate ion stretching vibration [114], [115] while the peak at 1024 cm^{-1} was ascribed to S=O vibration; also the peak at 621 cm^{-1} is associated with S-C vibrations [109], [114], [116]. APS is considered as expected source of sulfur atoms. Appearance and subsequent increase in absorption peak at 1194 cm^{-1} is associated with vibration modes of N=Q=N in polyaniline. Increased absorption is ascribed to increase in polyaniline content with enhanced doping [103]. The peak at 1276 cm^{-1} is attributed to C-H in-plane bending mode while peak at 1359 cm^{-1} is attributed to $C\text{-}N^{+\bullet}$ stretching vibration in a polaron structure [103]. This absorption band is correlated to π-electron delocalization

induced in the polyaniline by doping process. Additionally, there are two peaks at 1535 cm^{-1} and 1520 cm^{-1}, attributed to the stretching vibration of quinoid and benzenoid ring, respectively [113], [117]. The peak at 1520 cm^{-1} undergoes slight red shift due to the dopant effect but the peak position at 1535 cm^{-1} is fixed as quinoid rings are widely separated as seen in Figure 5-1.

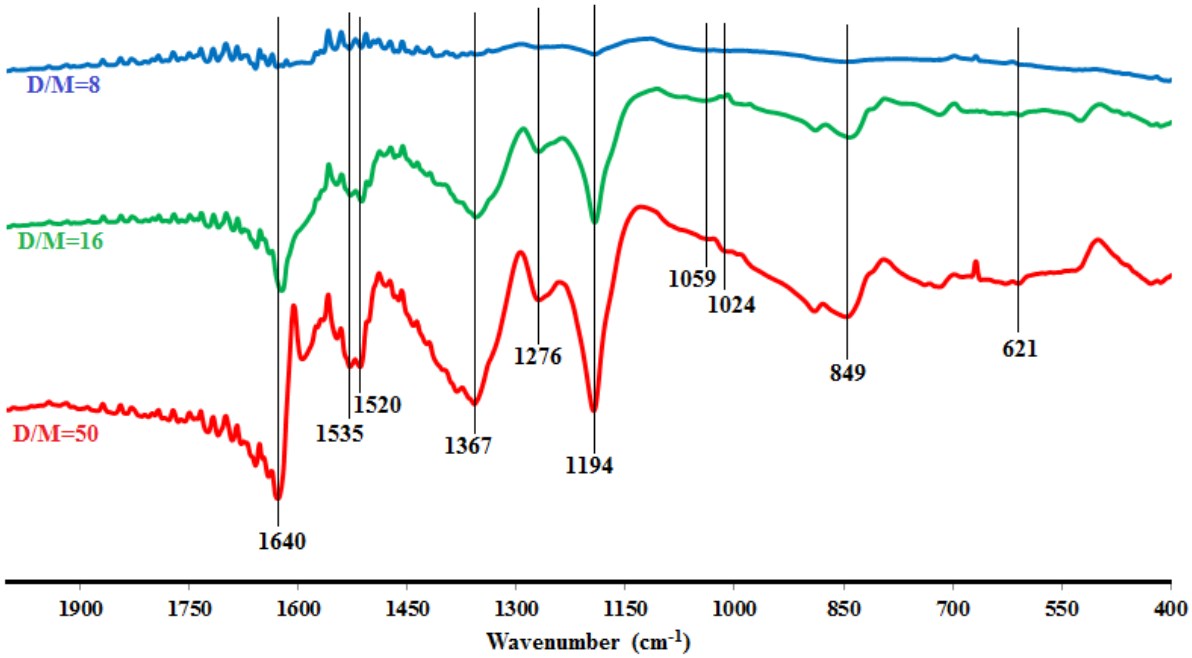

Figure 5-7: FT-IR spectra of polyaniline nanotubes with different dopant to monomer ratio

Another characteristic peak at 1640 cm^{-1} was found to appear because of stretching vibrations of C=C and it was subsequently shifted to lower wavelength with increase in dopant concentration. This shift and increased absorption was attributed to increased protonation in polyaniline due to the dopant molecules [115]. Weak features are observed at dopant to monomer ratio of 8 because polymerization is not completely triggered whereas para-coupling (849 cm^{-1}) and polaron structure (1276 cm^{-1}) peaks appear with increased ratio of dopant to monomer because of aniline polymerization towards emeraldine salt. FTIR results suggest that the dopant to monomer ratio has important role in the polymerization of aniline. Later, we also have discussed the effect of this ratio on electrical and optical properties of the polyaniline.

5.3.3 Optical characteristics of polyaniline nanotubes

UV-vis absorption spectrum (Figure 5-8) for each dopant to monomer ratio shows two distinct peaks and one "free-carrier" tail of the electron transitions which is typical absorption of the emeraldine oxidation state of polyaniline. Characteristic peak between 330-340 nm is assigned to π-π* transition of benzenoid rings and to the charge-transfer-exciton transition formed in benzenoid and adjacent quinoid ring. Another peak between 440-450 nm signifies the existence of polaron- π* transition [90], [94], [118]. The long tail at higher wavelengths is the signature of π-polaron transition.

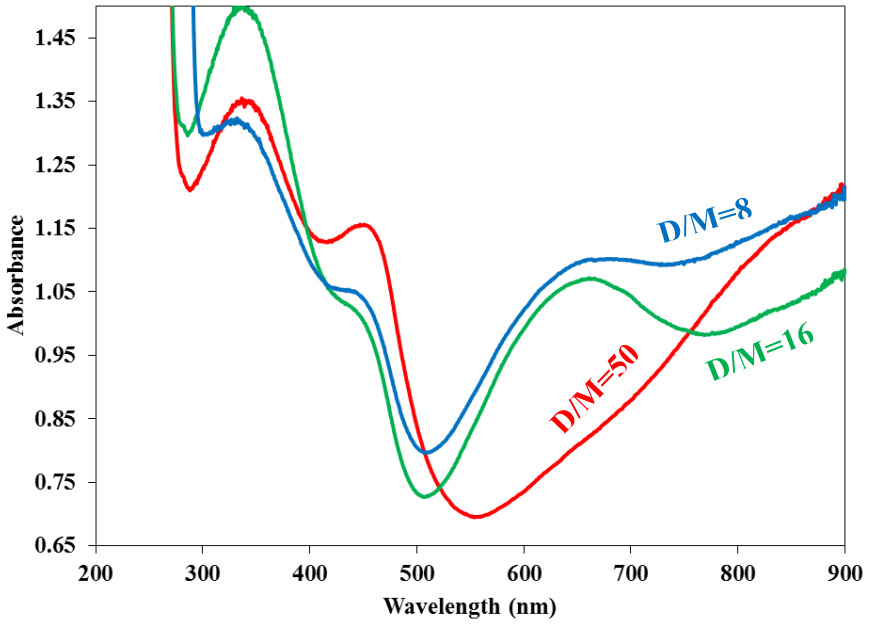

Figure 5-8: UV-visible spectra of polyaniline nanotubes showing two distinct peaks and 'free-carrier' tail

These absorption peaks of different transitions indicate the protonation of backbone of the polyaniline and its electrically conductive state. Addition of protons results in subsequent formation of polarons along the polyaniline chain which increases its electrical conductivity. It is interesting to note that the increase in dopant to monomer ratio (and subsequent increase in protonation) resulted in redshift of lower wavelength absorption peak from 328 nm-to-337 nm-to-338 nm with insignificant difference. On the other hand, irregular redshift is observed for the next peak from 443 nm-to-440 nm-to-450 nm. The redshift is attributed to the protonation of polyaniline. As higher wavelengths

correspond to lower energy, the redshift signifies the decrease in energy gap. This decrease in energy gap ultimately causes the reduction in resistivity of polyaniline. Polyaniline nanotubes exhibit two conformations i.e. “compact coil” and “extended coil” conformations. Compact coil conformation shows significantly broad (long tail) polaron absorption peak at around 650 nm while “extended coil” exhibits intense absorption in near-infrared region [119], [120]. Therefore, long tail in UV-vis spectra suggests that as-synthesized polyaniline nanofibers are in “compact coil” conformation. Our SEM observations in Figure 5-4 strongly support the above fact. However, suppression of absorption intensity of long tail with increase in dopant to monomer ratio is indicative of decreasing character of “compact coil” conformation. We hypothesize that protonation has significant effect on structural properties and found to be a vital factor for conformational changes in polyaniline nanostructures.

5.3.4 Structural characterization of polyaniline nanotubes

Dopant-polyaniline interaction and their effect on conformation were studied using XRD which is a powerful tool to probe molecular interactions in nanostructured polyaniline. Combined analysis of XRD data and electrical resistivity was used to correlate the crystallinity, solid state ordering and their effect on conductivity of polyaniline. X-ray diffractograms of polyaniline powder at different dopant to monomer ratio are shown in Figure 5-9. It is interesting to note that irrespective of dopant amount, polycrystalline polyaniline was formed which was observed through four sharp peaks in the diffractogram. Four characteristic peaks of polyaniline in emeraldine salt form were observed at 38^0, 44^0, 64^0 and 78^0 (2θ) synthesized with different dopant to monomer ratio. The crystallinity is imparted to polyaniline due to presence of Cl^- counter-ions along with protons near the nitrogen atoms (Figure 5-3). This pair of proton and counter-ion provides the electro-static force needed for a higher degree of chain ordering [121], [122].

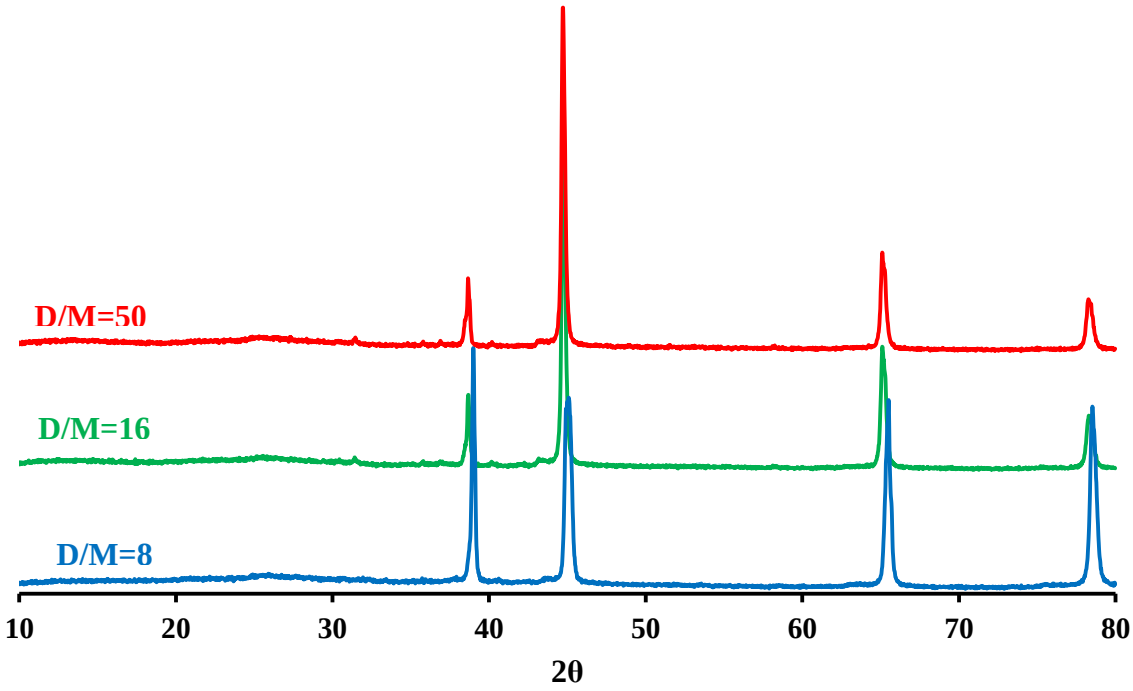

Figure 5-9: X-ray diffractograms of polyaniline showing four sharp diffraction peaks, implying the highly crystalline nature of the nanotubes

XRD pattern also confirmed the one-dimensional structure of polyaniline. The diffraction peak at around 38^0 was attributed to the periodicity parallel to the polyaniline polymer chains whereas the peak at around 78^0 was ascribed to the periodicity perpendicular to the polymer chains [123], [124]. According to Dufour et al, higher order diffraction peaks signifies the presence of lamellar structure but it was not evidenced in this case as observed in SEM and TEM [95]. Growth of small diffraction peak was observed at 32^0 with increase in dopant to monomer ratio which signifies an extended order in the chain-dopant-chain direction of polyaniline [95]. It also confirms the nanotubular structure of the polyaniline which can be justified based on our synthesis mechanism as growth of polyaniline takes place inside the micelles formed in miniemulsion polymerization. As dopant to monomer ratio was increased, micelles were stabilized because of the acidity of reaction mixture which forms tubular polyaniline, introducing peak at 32^0. HRTEM image of polyaniline (Figure 5-10) clearly shows the polycrystalline nature while it also confirms that nanotube is hollow from inside. Figure 5-10 also shows selected area electron diffraction (SAED) pattern of the respective polyaniline nanotube

revealing the distinct diffraction patterns. Well-defined and sharp peaks in XRD as well as HRTEM image confirmed that crystallinity of as-synthesized nanotubes is high.

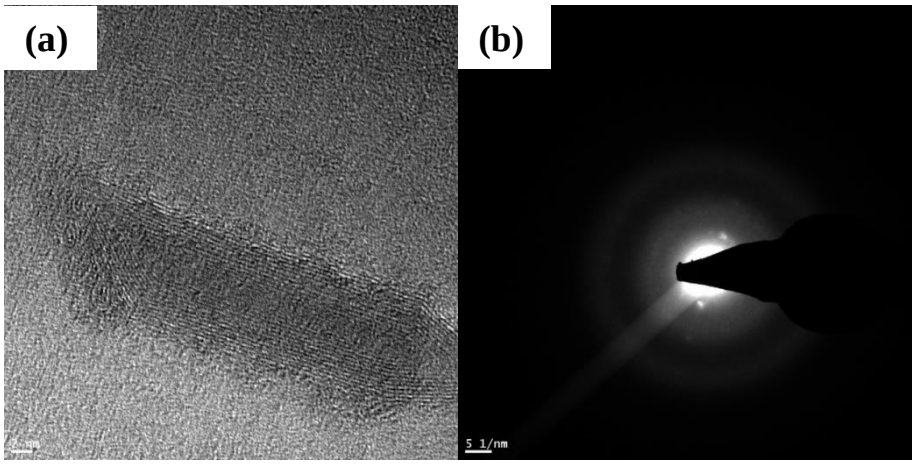

Figure 5-10: (a) HRTEM image of polyaniline nanotube at 2nm scale, showing polycrystalline structure, (b) selected area electron diffraction (SAED) pattern of the corresponding polyaniline nanotube confirming the polycrystallinity

Higher angle peak ($2\theta=78^0$) signifies the polyaniline backbone aromatic chain interactions whereas lower angle peak ($2\theta=38^0$) signifies the interdigitations of dopant molecule into the polyaniline chain lattices [99], [125–130]. The ratio of the peak intensities $I_{2\theta=38}/I_{2\theta=78}$ indicate the solid state ordering of the polyaniline. From values of the ratio shown in Table 5-1, it is clear that solid state ordering of the polyaniline increases with decrease in dopant to monomer ratio.

Table 5-1: Estimation of crystallite size from X-ray diffraction of polyaniline nanotubes and values in bracket show d-spacing of the corresponding peak. Ratio of $I_{2\theta=38}/I_{2\theta=78}$ signifies the solid state ordering in crystalline nanotubes of polyaniline

Crystallite Size (nm)					
Dopant/Monomer molar ratio	**Peak 1 (311) plane**	**Peak 2 (400) plane**	**Peak 3 (440) plane**	**Peak 4 (533) plane**	$I_{2\theta=38}/I_{2\theta=78}$
8	35.89343 ($2.322A^0$)	17.16537 ($2.021A^0$)	23.67524 ($1.429A^0$)	23.71935 ($1.219A^0$)	1.370
16	40.58081 ($2.341A^0$)	30.97336 ($2.034A^0$)	25.0199 ($1.435A^0$)	20.14775 ($1.222A^0$)	1.114
50	34.66151 ($2.340A^0$)	32.26917 ($2.034A^0$)	25.71006 ($1.435A^0$)	20.34181 ($1.222A^0$)	1.080

Our observations on solid state ordering with varying amount of dopant strongly supports the findings by Shinde et al but on the contrary to their amorphous polyaniline, we observed the

polycrystalline nanotubes of polyaniline [125]. Crystallite size along the different planes of polyaniline nanotubes was calculated using Debye-Scherrer equation as follows:

$$d = \frac{K\lambda}{\beta \cos\theta}$$

where, K is shape factor (0.9); λ is X-ray wavelength (1.5406A^0); β is full width at half maximum and θ is Bragg angle. Trend of change in crystallite size along the different planes indicates that crystal of polyaniline grows significantly along the (400) plane while minor change in crystallite size is observed along other planes. This observation strongly supports our synthesis mechanism where growth of polyaniline takes place along single direction and inside the micellar channels.

5.3.5 Thermal properties of polyaniline nanotubes

Distinct thermal features were observed in thermo-gravimetric analysis of polyaniline as shown in Figure 5-11. The temperature corresponding to weight loss was calculated from the derivative data of TGA.

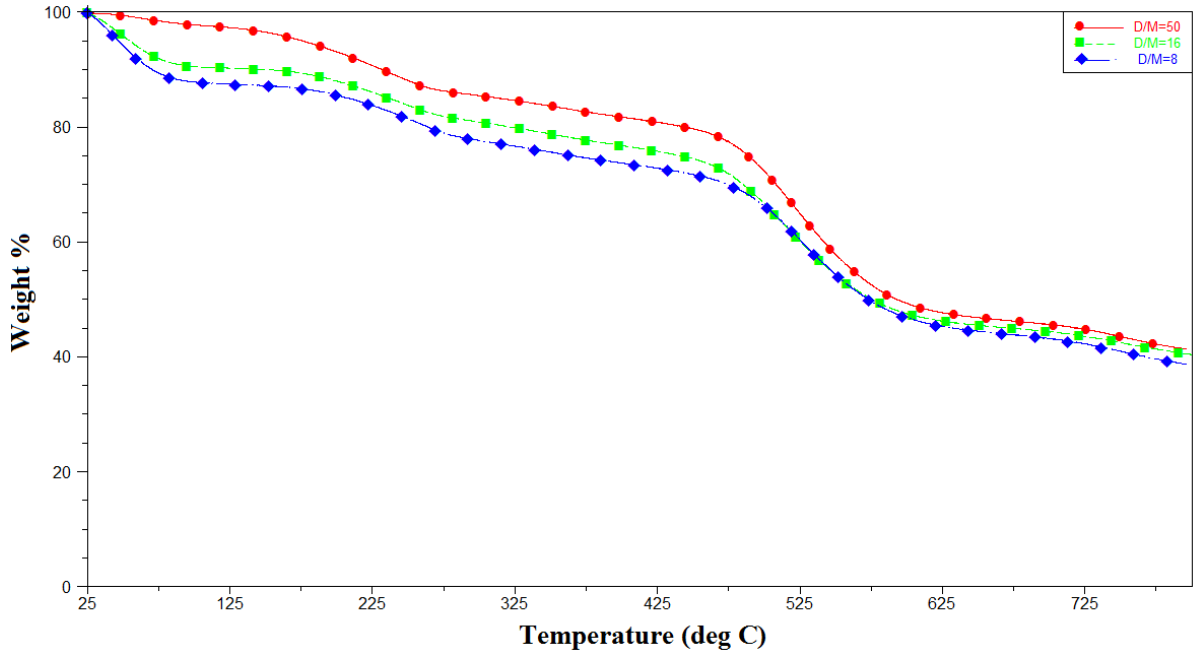

Figure 5-11: Thermogravimetric analysis of polyaniline with different dopant to monomer ratio

In general, protonation was found to cause thermal stabilization of polyaniline nanostructures. Polyaniline with dopant to monomer ratio of 8 and 16 lost significant weight below 125^{0}C. This weight loss was attributed to the expulsion of unbound water, volatile impurities and gaseous HCl

which could be physically sorbed in polymer matrix [131–133]. Interestingly, polyaniline with dopant to monomer ratio 50 did not show any weight loss below 125^0C. This observation implies that there is a strong molecular interaction between polyaniline backbone chain and chloride counter-ions which prevents the uptake of water in polymer matrix. We also hypothesize that the structural stabilization due to the increased population of chloride ions (D/M=50) contributes to the overall thermal stabilization of polyaniline. Second weight loss was observed at 250^0C in polyaniline with all dopant to monomer ratios. This reduction in weight might have caused due to the two reasons; one being removal of "linked" water to the polyaniline backbone which also act as a secondary dopant. Another reason could be the removal of many small fragments of polyaniline which decompose at lower temperature. The thermal stability observed between 100^0C and 250^0C was attributed to the cross-linking of the polymeric chains during heating [134]. We also suspect that diffusion of water and HCl in polymer matrix might have caused thermal induced doping which retains the crystallinity of polyaniline. This process does not involve significant weight loss. The final weight loss was observed at the onset of 525^0C in the polyaniline with all dopant to monomer ratios. This weight loss was occurred due to thermal decomposition of main molecular chains of polyaniline. In presence of nitrogen atmosphere, this decomposition involves removal of extended aromatic structures and formation of coke. Interestingly, the slope of the thermo-gravimetric curve between 500^0C and 600^0C was found to be steeper than that of between 200^0C and 300^0C. We assume that at elevated temperature up to 500^0C, polyaniline might have undergone the structural changes which led to the melting of crystallites and subsequent decrease in degree of crystallinity. The residue left over at 800^0C was accounted for highly carbonized materials which also includes some other thermally stable species.

5.3.6 Conduction mechanism upon doping

After discovery of the polyaniline, it is extensively showed that doping of the polyaniline increases its conductivity. Generally, it is accepted that same degree of doping is more effective in nanostructured polyaniline than its bulk counterpart. Instead of showing the transition of polyaniline from insulating to metallic regime, we demonstrate the trend of conduction in "doped/metallic" regime by precisely controlling the degree of dopant through our experimental setup. All experiments involved the use of HCl as a dopant because the structure of an anion of the acid inevitably influences the size of nanotubes. Doping scheme of the polyaniline is shown in Figure 5-3 while resistivity of the polyaniline nanotubes is shown in Figure 5-12.

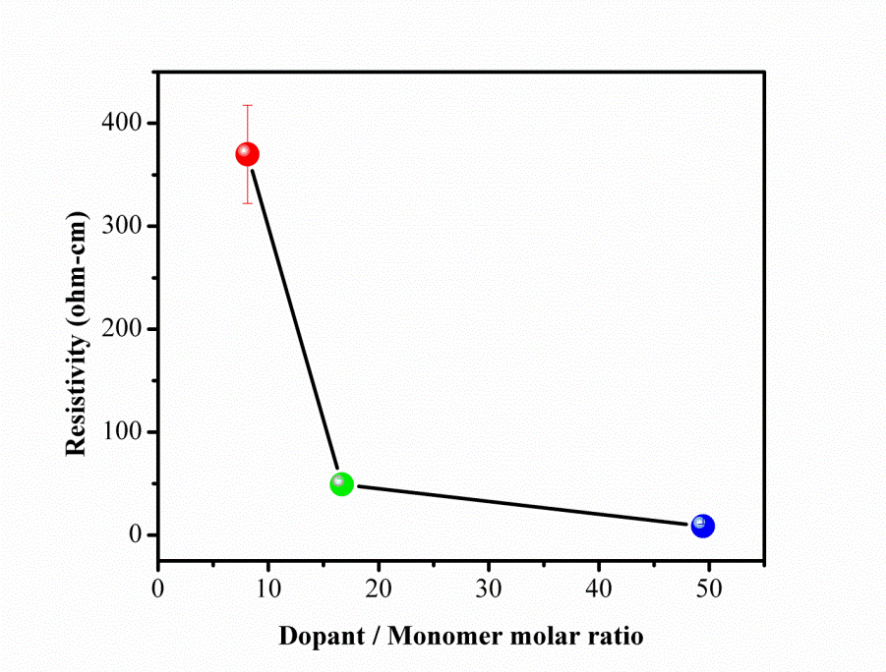

Figure 5-12: Resistivity of the polyaniline nanotubes with increasing dopant to monomer ratio

Increase in dopant to monomer ratio from 8 to 50 caused 43 times reduction in resistivity. This drastic reduction in resistivity was attributed to the increased protonation of polyaniline backbone chain. Also, the increased population of dopant along the polyaniline chains act as bridges between two neighboring chains which results in formation of stable bipolaron, enhancing the tunneling across the dopant. Conductivity of the polyaniline strongly depends on acidity of the reaction mixture in which protonation takes place. At the dopant to monomer ratio of 8, all protons are consumed to protonate the aniline monomer, resulting in formation of weakly acidic reaction mixture. On the other hand, at highest dopant to monomer ratio, acidity of the reaction mixture remains maintained even after the protonation of aniline monomer. Figure 5-13 shows molecular scenario of the reaction mixture at highest dopant to monomer ratio where majority of the aniline monomers are protonated. In such a strong acidic medium, anilinium cations are favored to form oligomers on which charge delocalization takes place after optimum conjugation. Tang et al also proved this hypothesis by monitoring the pH of reaction mixture [109].

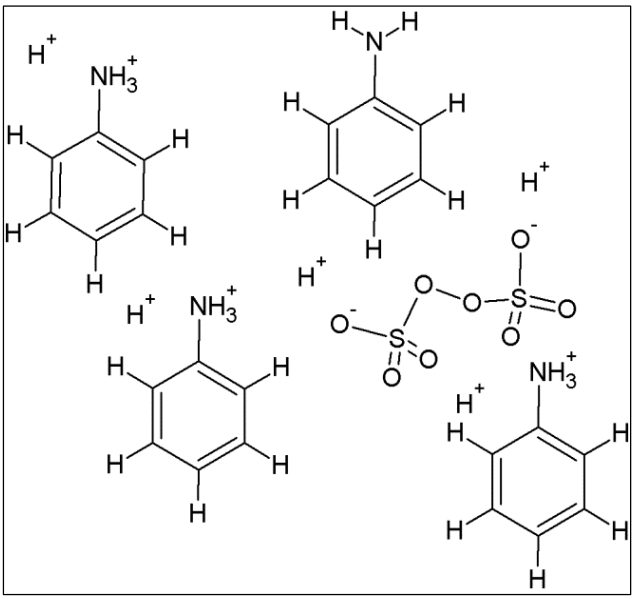

Figure 5-13: Schematic of the reacting species in reaction mixture at dopant to monomer molar ratio of 50

Reduction in resistivity with increase in dopant to monomer ratio can also be attributed to increase in conjugation and subsequent increase in interconnecting network of polyaniline. In FTIR also, it was observed that delocalization of π-electrons (1359 cm^{-1}) increases with increase in dopant to monomer ratio which might have caused to reduce the resistivity of polyaniline. Crystallinity is also a vital factor that influences the conductivity of polyaniline. Even though Bhadra et al mentioned that the decrease in d-spacing increases the probability of inter-chain hopping of the charge carriers [27] but our results from XRD suggest that polyaniline with almost constant d-spacing but increasing crystallinity causes the enhancement of conductivity. Increase in grain size along (400) plane with constant crystallinity causes increase in molecule-to-molecule hoping of charge carriers and enhancement of intramolecular mobility of charge carriers. Thus, increased conductivity can also be attributed to the enhanced mobility of charge carriers, strong dopant-polyaniline interactions and highly ordered and, crystalline nature of the polyaniline nanotubes.

5.3.7 Performance of flexible conductive coatings

The trend of decrease in resistivity of conducting coating with increase in dopant to monomer ratio is same as that of polyaniline powder. Increase in dopant to monomer ratio from 8 to 50 caused almost 150 times reduction in resistivity. Figure 5-14 shows resistivity of conductive coatings.

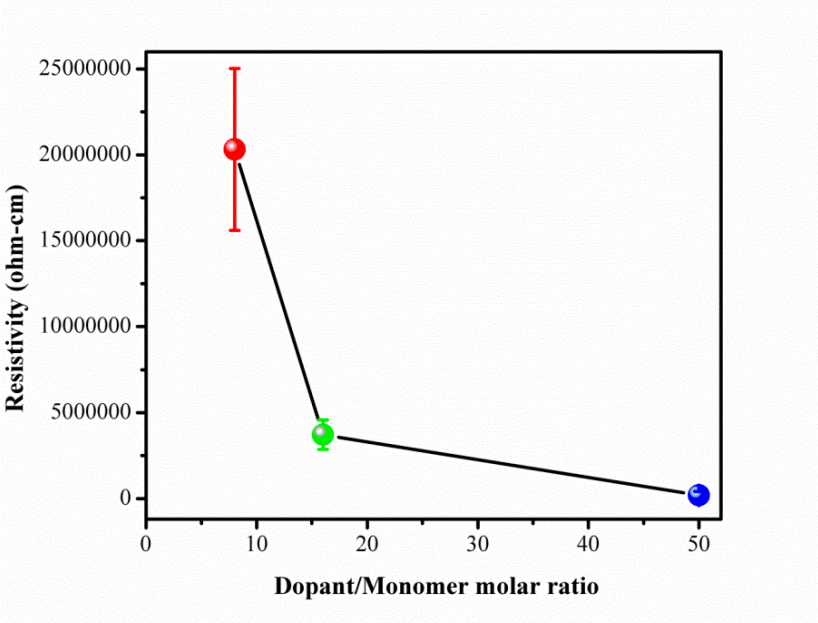

Figure 5-14: Electrical Resistivity of flexible conducting coating as-measured by four-probe technique

Two factors can be considered for such a significant reduction in resistivity: (1) formation of entangled network of polyaniline nanotubes and (2) highly uniform dispersion of polyaniline in PVA matrix. Increase in absolute resistivity of conducting coating is contributed by the presence of PVA in the system. Generally, non-uniform dispersion of filler in polymer matrix results in poor electrical performance and formation of distinct conductive domains [7], [74]. These observations can be attributed to the weak compatibility of fillers with polymer matrix and unnecessarily strong interactions between the filler particles. In the current work, we have successfully demonstrated the highly uniform dispersion of polyaniline (D/M=50) in PVA matrix. The dopant present on the backbone chain of polyaniline induces the positive charge on the backbone chain which results in electrostatic repulsion of polyaniline nanotubes in colloidal form. Li et al obtained the similar colloidal dispersion and attributed it to the sufficiently acidic pH of the solution [135] which in turn signifies the electrostatic stabilization. Morphological analysis (Figure 5-15) of dry polyaniline powder and its dispersion in PVA matrix showed that smaller aggregates may form in dry polyaniline but dispersion of its colloidal solution in PVA can be significantly uniform to fabricate the flexible conducting coating. Interestingly, we could also notice the difference that the increase in dopant to monomer ratio from 8 to 50 caused 43 times reduction in resistivity of polyaniline powder whereas 150 times reduction in case of flexible conducting coating.

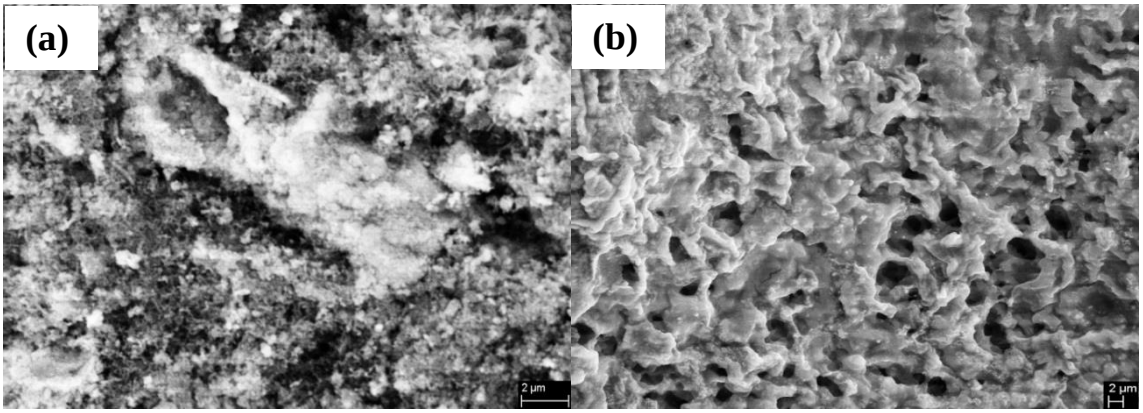

Figure 5-15: SEM image of (a) polyaniline nanotubes in powder form, (b) the flexible electrically conducting coating showing uniform dispersion and entangled network of polyaniline nanotubes

We speculate the following reason towards this technologically important observation. Resistivity of polyaniline powder was measured on compacted film (in pallet form) which consisted of physical network of smaller aggregates of polyaniline while that of conducting coating showed the resistivity of uniformly dispersed polyaniline nanotubes in PVA matrix. Resistivity of polyaniline powder also involved the contribution of excessive inter-tubular contact resistance and suppression of dopant centres which facilitate the conduction while conducting coating has uniformly spread entangled network of polyaniline nanotubes.

As-fabricated conducting coating is shown in Figure 5-16. We could also visually observe that even after 90^0 bending (Figure 5-16) no wrinkles or cracks were spotted. Therefore, we believe that these flexible electrically conducting coatings can be immediately used for various uses in flexible electronics.

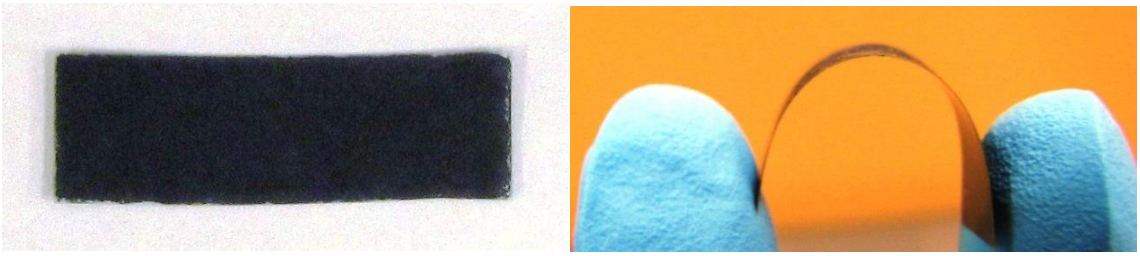

Figure 5-16: (a) an image of as-fabricated conducting coating showing uniform coverage of the coating surface and (b) an image of conducting coating showing its flexibility

5.4 Technical implications of crystalline polyaniline nanotubes

It is worth discussing the technical implications of the highly crystalline polyaniline nanotubes (emeraldine salt) as synthesized by our process, in context to various technological applications. Recently, many researchers have attempted to synthesize the crystalline polyaniline by various methods. But their product contain majority of an amorphous character with small portion of crystallinity. Probability of failure of such 'less' crystalline polyaniline in electronic applications can't be denied due to ineffective charge transport in major amorphous regions. Here, we would like to add that it is important to know, how the crystallinity is obtained. In 1992, Laridjani and co-workers introduced the concept of "amorphography-the relationship between amorphous and crystalline order" [136], [137]. It states that crystallinity of emeraldine salt obtained from emeraldine base has different physical properties than that of obtained from direct protonation during the synthesis. Therefore, the history of the crystalline polyaniline has vital impact on the performance of electronic applications. Most of the electronic applications which require the blending of crystalline polyaniline emeraldine salt with host polymer matrix involve the use of solvent, curing agent, stabilizer etc. In such cases, dedoping of crystalline polyaniline can't be denied which results in formation of amorphous domains. This dedoping and subsequent transformation from crystalline to amorphous character is more obvious in emeraldine salt synthesized from emeraldine base. In this respect, our method of synthesis provides the feasible solution from technological point of view. We have shown the control of structural properties of polyaniline nanotubes and subsequent control of physical properties. Practical application of this study has been demonstrated in form of flexible electrically conducting coating. Our work in the field of conductive adhesives [7] and electromagnetic shielding applications [138] prove the strong applicability of our process and product.

5.5 Conclusions

We demonstrated the facile method for synthesis of highly crystalline nanotubes of polyaniline. Miniemulsion polymerization with '*in-situ*' doping and controlled addition of oxidant can successfully be used to synthesis crystalline nanotubes of polyaniline. '*In-situ*' doping reduces an extra step of doping compared to conventional processes. The process suppresses the secondary growth of polyaniline nanotubes, allowing the formation of one dimensional structure. Dopant molecules and polyaniline backbone remain bonded mainly, due to electrostatic forces between them. Protonation provides the necessary electro-static force for higher degree of chain ordering. Periodicity parallel to polymer chains was found to increase with increase in dopant to monomer ratio. We also

have shown that crystallite size grows along (400) plane with increase in dopant amount. The increase in doping of polyaniline was found to enhance the electrical conductivity which was supported by the redshift of absorption peaks as observed in UV-Vis spectra. The dopant molecules induce the protonation effect which subsequently results in delocalization of π-electrons. Inter and intra-molecule mobility of charge carriers was enhanced due to the increasing dopant amount. Strong interactions between polyaniline backbone chain and dopant molecules prevent the water uptake and thermal degradation of polyaniline powder. Bulk state polyaniline exhibit entangled network of nanotubes which helped us to fabricate the robust flexible electrically conducting coating. Doped polyaniline nanotubes uniformly disperse in PVA matrix resulting in good film-forming and flexible properties. As-fabricated coating did not show any cracks after bending.

Chapter 6
Conclusions and future research

We explored the use of conducting polymer-polyaniline as a co-filler for silver-epoxy conductive adhesive system. Electrical conductivity of polyaniline is intrinsically less than that of silver metal. However, we found that less volume of total filler (silver+polyaniline) is needed to initiate the conduction in epoxy matrix. Electrical response of silver-epoxy and silver-polyaniline-epoxy ECAs was measured by tracing the indentation force and time dependency of contact resistance. "Bridging" effect of polyaniline helped to lower the percolation threshold and stabilize the electrical contact resistance of the ECA. It was also stated that silver-polyaniline-epoxy is a model system for the fine pitch applications in ECAs.

We performed a detailed *in-situ* electro-mechanical analysis of electrically conductive adhesives filled with silver and polyaniline micro-flakes in viscoelastic state, using a micro-indentation technique. We observed that electrical contact resistance of ECAs decreases over a period of time, even at constant compressive force. The concept of "electrical stain" is introduced to characterize this relaxation of electrical contact resistance; and, the Burger's micro-mechanical model is applied and found able to simulate the change of electrical resistance with time under a constant compressive force. This study revealed a linear coupling between the electrical strain and engineering strain when the adhesives experienced low engineering strains, indicating the relaxation in electrical resistance may originate from the mechanical creep of the ECA. It can also be indicated that addition of polyaniline to the conventional silver-filled epoxy can be used to tailor the steady-state contact resistance.

Furthermore, we aimed propensity of nanostructured polyaniline as alternate filler for ECAs. We demonstrated the facile method for synthesis of electrically conductive and highly crystalline nanotubes of polyaniline. Miniemulsion polymerization with '*in-situ*' doping and controlled addition of oxidant was successfully used to synthesis crystalline nanotubes of polyaniline. '*In-situ*' doping reduces an extra step of doping compared to conventional processes. The process suppresses the secondary growth of polyaniline nanotubes, allowing the formation of one dimensional structure. Dopant molecules and polyaniline backbone remain bonded mainly, due to electrostatic forces between them. Protonation provides the necessary electro-static force for higher degree of chain ordering. We also observed that crystallite size grows along (400) plane with increase in dopant

amount. The increase in doping of polyaniline was found to enhance the electrical conductivity as dopant molecules induce the protonation effect which subsequently results in delocalization of π-electrons. Inter and intra-molecule mobility of charge carriers was enhanced due to the increasing dopant amount. Strong interactions between polyaniline backbone chain and dopant molecules prevent the water uptake and thermal degradation of polyaniline powder. Bulk state polyaniline exhibited entangled network of nanotubes which helped us to fabricate the robust flexible electrically conducting coating. Doped polyaniline nanotubes uniformly dispersed in PVA matrix resulting in good film-forming and flexible properties. As-fabricated coating did not show any cracks after bending.

This thesis raises several interesting areas to be further investigated. We think that a better understanding of the issues involved would further enrich current knowledge gained from this work and open up more possibilities for future applications.

It was understood that electrical contact information between the fillers is essentially needed to establish a profound conduction mechanism. Even though indirect measurement techniques such as resistivity, thermal resistance etc can provide information about physical contact between fillers, direct measurement of the contact area between the fillers and its relation with contact resistance needs to be established. SEM was found to be supplementary and qualitative technique to study microstructure of ECAs however, sample preparation and obtaining exact contact information is still difficult. Quantitative information about ECAs such as filler dispersion and size distribution, contact dimensions etc are necessary to understand the effectiveness of process parameters.

In order to achieve the enhanced overall performance of ECAs conductive nano fillers are the major approaches in today's era. Due to nanodimensions of filler size the dispersion, rheological, mechanical and thermal mechanical properties of the ECAs change significantly. Despite of continuous efforts, the problem of non-uniform dispersion of fillers can't be neglected, which limits the fine pitch capability of the ECAs. The aggregation of nanosized filler also can affect the rheology and increase the viscosity of the ECAs which is vital for the processability. An alternative approach of *in-situ* synthesis of nanoparticles inside polymer matrix can be adopted. This can be achieved by decomposition or chemical reduction of a metallic precursor dissolved into the polymer matrix. By controlling the materials (such as polymer matrix, reducing agents, solvents, type of capping agents, etc.), the particles with desired size and distribution can be obtained with more uniform dispersion

and less agglomeration. The *in-situ* formed nano-conductive adhesives can be used for ultra-fine pitch interconnect applications.

Electrically conducting polyaniline can be considered as a potential candidate for filer or co-filler material in ECAs. However, the conductivity of polyaniline still does not approach a conductivity equivalent to that of pure silver metal. But, interestingly, polyaniline provides a unique and exciting means to attain an order of magnitude increase in conductivity. Polymerization process of aniline in presence of protonic acid can be optimized to attain the metallic conductivity of polyaniline. More compositions of polyaniline with varying dopant to monomer ratio can be analyzed. Such information will be helpful to get insights about the optimum composition of the polyaniline. Still, based on current developments in the field of conductive polymers, polyaniline is a new addition to a material researchers' toolbox that can provide the necessary conductivity boost for specific applications that need marginal conductivity improvements.

Bibliography

[1] R. R. Tummala, E. J. Rymaszewski, and A. G. Klopfenstein, *Microelectronics Packaging Handbook*, 2nd ed. Chapman & Hall, London, 1997.

[2] Y. Li, D. Lu, and C. Wong, *Electrical Conductive Adhesives with Nanotechnologies*. New York: Springer, 2009.

[3] K. J. Puttlitz, K. A. Stalter, *Handbook of Lead- Free Solder Technology for Microelectronic Assemblies*. New York, USA, 2004.

[4] I. S. Böhm, E. Stammen, G. Hemken, and M. Wagner, *Microjoining and Nanojoining*. CRC Press, USA, 2008.

[5] Y. Li, K. Moon, and C. Wong, "Electronics without lead," *Science*, vol. 308, pp. 1419–20, 2005.

[6] S. Gumfekar, A. Chen, and B. Zhao, "Silver-polyaniline-epoxy electrical conductive adhesives-a percolation threshold analysis," *13th Electronics Packaging Technology Conference*, pp. 180–184, Dec. 2011.

[7] S. Gumfekar, B. Meschi Amoli, A. Chen, and B. Zhao, "Polyaniline-tailored Electromechanical Responses of the Silver/Epoxy Conductive Adhesive Composites," *Industrial and Engineering Chemistry Research*, (under review)

[8] S. P. Gumfekar, W. Wenjie, and B. Zhao, "Highly Crystalline and Conductive Polyaniline Nanotubes: Applications in Flexible Conductive Coatings," (in-preparation)

[9] H. Wolfson and G. Elliot, "Electrically conducting cements containing epoxy resins and silver," U.S. Patent US patent 2774, 747,1956.

[10] K. R. Matz, "Electrically conductive cements and brush shunt containing the same," US patent 2849, 631,1958.

[11] D. Peck, "Printed electrical resistor," US Patent 2,866,057, 1958.

[12] C. Tison and C. P. Wong, "Fundamental understanding of conductivity establishment for electrically conductive adhesives," *52nd Electronic Components and Technology Conference 2002.*, pp. 1154–1157, 2002.

[13] M. J. Yim and K. W. Paik, "Recent advances on anisotropic conductive adhesives (ACAs) for flat panel displays and semiconductor packaging applications," *International Journal of Adhesion and Adhesives*, vol. 26, no. 5, pp. 304–313, 2006.

[14] M. Yim and K. Paik, "Design and Understanding of Anisotropic Conductive Films (ACF's) for LCD Packaging," *IEEE Transactions on Components, Packaging, and Manufacturing Technology Part A*, vol. 21, no. 2, pp. 226–234, 1998.

[15] P. Jesudoss, W. Chen, A. Mathewson, W. M. D. Wright, K. G. McCarthy, and F. Stam, "Electrical Characterization of Anisotropic Conductive Adhesive Based Flip Chip for a Direct Access Sensor," *2010 Electronic Components and Technology Conference*, pp. 369–374, 2010.

[16] L. Cao, S. Li, Z. Lai, and J. Liu, "Formulation and Characterization of Anisotropic Conductive Adhesive Paste for Microelectronics Packaging Applications," *Journal of Electronic Materials*, vol. 34, no. 11, 2005.

[17] K. A. Wilkinson and D. A. Ordonez, Eds., *Adhesive Properties in Nanomaterials, Composites and Films*. New York: Nova Science Publishers Inc., 2011.

[18] H. Li and C. P. Wong, "A Reworkable Epoxy Resin for Isotropically Conductive Adhesive," *IEEE Transactions on Advanced Packaging*, vol. 27, no. 1, pp. 165–172, 2004.

[19] A. Baldan, "Adhesively-bonded joints and repairs in metallic alloys, polymers and composite materials: Adhesives, adhesion theories and surface pretreatment," *Journal of Materials Science*, vol. 39, no. 1, pp. 1–49, 2004.

[20] J. E. Morris, *Conductive adhesives for Electronics Packaging*. UK: Electrochemical Publications Ltd , UK, pp. 36–77, 1999.

[21] S. Pandiri, "The behavior of silver flakes in conductive epoxy adhesives," *Adhesives Age*, vol. 30, pp. 31–35, 1987.

[22] L. Li, C. Lizzul, H. Kim, I. Sacolick, and J. E. Morris, "Electrical, structural and processing properties of electrically conductive adhesives," *IEEE Transactions On Components, Hybrids, and Manufacturing Technology*, vol. 16, no. 8, pp. 843–851, 1993.

[23] Y. Wei, "Electronically conductive adhesives : conduction mechanisms, mechanical behavior and durability," Clarkson University, 1995.

[24] J. Morris, C. Cook, M. Armann, A. Kleye, and P. Fruehauf, "Electrical conduction models for electrically conductive adhesives," *Proceedings of 2nd IEEE International Symposium Polymeric Electronics Packaging (PEP' 99), Gothenburg, Sweden*, pp. 15–25, 1999.

[25] D. L. Markley, Q. K. Tong, D. J. Magliocca, and T. D. Hahn, "Characterization of silver flakes utilized for isotropic conductive adhesives," *Proceedings of International Symposium on Advanced Packaging Materials*, pp. 16–20, 1999.

[26] T. McAndrew, "Corrosion prevention with electrically conductive polymers," *Trends in Polymer Science(UK)*, vol. 5, no. 1, pp. 7–12, 1997.

[27] S. Bhadra, D. Khastgir, N. K. Singha, and J. H. Lee, "Progress in preparation, processing and applications of polyaniline," *Progress in Polymer Science*, vol. 34, no. 8, pp. 783–810, 2009.

[28] S. Bhadra, N. K. Singha, and D. Khastgir, "Electrochemical Synthesis of Polyaniline and Its Comparison with Chemically Synthesized Polyaniline," *Journal of Applied Polymer Science*, vol. 104, no. 3, pp. 1900–1904, 2007.

[29] J. Chiang and A. MacDiarmid, "'Polyaniline': Protonic acid doping of the emeraldine form to the metallic regime," *Synthetic Metals*, vol. 13, pp. 193–205, 1986.

[30] P. Chandrasekhar, *Conducting Polymers, Fundamentals and Applications: A Practical Approach*. Springer, 1999.

[31] P. Tsotra and K. Friedrich, "Short carbon fiber reinforced epoxy resin/polyaniline blends: their electrical and mechanical properties," *Composites Science and Technology*, vol. 64, no. 15, pp. 2385–2391, 2004.

[32] F. Corsat, C. Davoine, A. Gasse, M. Fendler, G. Feuillet, L. Mathieu, F. Marion, and A. Pron, "Imprint Technologies on Conductive Polymers and Metals for Interconnection and Bumping Purposes," *1st Electronic Systemintegration Technology Conference*, pp. 1336–1341, 2006.

[33] E. Sancaktar and C. Liu, "Use of polymeric emeraldine salt for conductive adhesive applications," *Journal of Adhesion Science and Technology*, vol. 17, no. 9, pp. 1265–1282, 2003.

[34] J. Liu, K. Gustafsson, Z. Lai, and C. Li, "Surface Characteristics, Reliability, and Failure Mechanisms of Tin/Lead, Copper, and Gold Metallizations," *IEEE Transactions on Components, Packaging, and Manufacturing Technology—Part A*, vol. 20, no. 1, pp. 21–30, 1997.

[35] L. Li, J. Morris, J. Liu, Z. Lai, L. Ljungkrona, and C. Li, "Reliability and failure mechanism of isotropically conductive adhesives joints," *Proceedings of 45th Electronic Components and Technology Conference*, pp. 114–120, 1995.

[36] H. Botter, R. B. Van Der Plas, and A. Arunjunai, "Factors that influence the electrical contact resistance of isotropic conductive adhesive joints during climate chamber testing," *International Journal on Microelectronic Packaging Materials and Technology*, vol. 1, no. 3, pp. 177–185, 1998.

[37] R. Holms, *Electrical Contacts*. New York: Springer NY, 1979.

[38] D. Durand, D. Vieau, A. Chu, and T. Weiu, "Electrically conductive cement containing agglomerate, flake and powder metal fillers," US Patent 5,180,523, 1993.

[39] T. Inada and C. Wong, "Fundamental study on adhesive strength of electrical conductive adhesives (ECAs)," in *Proceedings of 3rd International Conference on Adhesive Joining and Coating Technology in Electronics Manufacturing*, pp. 156–159, 1998.

[40] J. E. Morris and S. Probsthain, "Investigations of plasma cleaning on the reliability of electrically conductive adhesives," *4th International Conference on Adhesive Joining and Coating Technology in Electronics Manufacturing*, pp. 41–45, 2000.

[41] M. G. Perichaud, J. Y. Deletage, D. Carboni, H. Fremont, Y. Danto, and C. Faure, "Thermomechanical behaviour of adhesive jointed SMT components," in *Proceedings of 3rd International Conference on Adhesive Joining and Coating Technology in Electronics Manufacturing*, pp. 55–61, 1998

[42] L. Matienzo, F. Egitto, and P. Logan, "The use of silane coupling agents in the design of electrically stable interfaces of 6061 T6 aluminum alloy surfaces and epoxy-based electrically conductive adhesives," *Journal of Materials Science*, vol. 38, pp. 4831–4842, 2003.

[43] F. Tan, X. Qiao, J. Chen, and H. Wang, "Effects of coupling agents on the properties of epoxy-based electrically conductive adhesives," *International Journal of Adhesion and Adhesives*, vol. 26, no. 6, pp. 406–413, 2006.

[44] S. Liong, C. P. Wong, and W. F. Burgoyne, "Adhesion improvement of thermoplastic isotropically conductive adhesive," *IEEE Transactions on Components and Packaging Technologies*, vol. 28, no. 2, pp. 327–336, 2005.

[45] S. Kuusiluoma and J. Kiilunen, "The Reliability of Isotropically Conductive Adhesive as Solder Replacement - a Case Study Using LCP Substrate," *7th Electronic Packaging Technology Conference*, vol. 2, pp. 774–779, 2005

[46] Q. K. Tong and C. P. Wong, "A study of lubricants on silver flakes for microelectronics conductive adhesives," *IEEE Transactions on Components and Packaging Technologies*, vol. 22, no. 3, pp. 365–371, 1999.

[47] C. P. Wong, D. Lu, and Q. K. Tong, "Lubricants of silver fillers for conductive adhesive applications," *Proceedings of 3rd International Conference on Adhesive Joining and Coating Technology in Electronics Manufacturing*, pp. 184–192, 1998.

[48] J. Miragliotta, R. C. Benson, and T. E. Phillips, "Measurements of electrical resistivity and Raman scattering from conductive die attach adhesives," *Proceedings. 8th International Advanced Packaging Materials Symposium*, pp. 132–138, 2002

[49] G. R. Ruschau, S. Yoshikawa, and R. E. Newnham, "Resistivities of conductive composites," *Journal of Applied Physics*, vol. 72, no. 3, p. 953, 1992.

[50] E. Sancaktar and W. Yong, "The effect of pressure on the initial establishment of conductive paths in electronically conductive adhesives," *Journal of Adhesion Science and Technology*, vol. 10, no. 11, pp. 1221–1235, 1996.

[51] C. Zhang, P. Wang, C. Ma, G. Wu, and M. Sumita, "Temperature and time dependence of conductive network formation: Dynamic percolation and percolation time," *Polymer*, vol. 47, no. 1, pp. 466–473, 2006.

[52] M. Weber and M. Kamal, "Estimation of the volume resistivity of electrically conductive composites," *Polymer Composites*, vol. 18, no. 6, pp. 711–725, 1997.

[53] R. Zallen, *The Physics of Amorphous Solids*. Weinheim, FRG: Wiley-VCH Verlag GmbH & Co. KGaA, pp. 135–146, 1983

[54] F. Carmona, R. Canet, and P. Delhaes, "Piezoresistivity of heterogeneous solids," *Journal of Applied Physics*, vol. 61, no. 7, pp. 2550–2557, 1987.

[55] R. Strumpler and Glatz-Reichenbach J, "Conducting polymer composites," *Journal of Electroceramics*, vol. 3, no. 4, pp. 329–346, 1999.

[56] Y. Chekanov, R. Ohnogi, S. Asai, and M. Sumita, "Electrical properties of epoxy resin filled with carbon fibers," *Journal of Materials Science*, vol. 34, pp. 5589–5592, 1999.

[57] N. Lebovka, M. Lisunova, Y. P. Mamunya, and N. Vygornitskii, "Scaling in percolation behaviour in conductive–insulating composites with particles of different size," *Journal of Physics D: Applied Physics*, vol. 39, no. 10, pp. 2264–2271, 2006.

[58] V. G. Shevchenko, A. T. Ponomarenko, and N. S. Enikolopyan, "Anisotropy effects in electrically conducting polymer composites," *International Journal of Applied Electromagnetics in Materials*, vol. 5, no. 4, pp. 267–277, 1994.

[59] D. Stauffer and A. Aharony, *Introduction to percolation theory*. London: Taylor and Francis, London, 1992.

[60] J. K. W. Sandler, J. E. Kirk, I. A. Kinloch, M. S. P. Shaffer, and A. H. Windle, "Ultra-low electrical percolation threshold in carbon-nanotube-epoxy composites," *Polymer*, vol. 44, no. 19, pp. 5893–5899, 2003.

[61] B. E. Kilbride, J. N. Coleman, J. Fraysse, P. Fournet, M. Cadek, A. Drury, S. Hutzler, S. Roth, and W. J. Blau, "Experimental observation of scaling laws for alternating current and direct current conductivity in polymer-carbon nanotube composite thin films," *Journal of Applied Physics*, vol. 92, no. 7, p. 4024, 2002.

[62] D. S. McLachlan, K. Cai, and G. Sauti, "AC and dc conductivity-based microstructural characterization," *International Journal of Refractory Metals and Hard Materials*, vol. 19, no. 4–6, pp. 437–445, 2001.

[63] I. Balberg and N. Binenbaum, "Scher and Zallen criterion: Applicability to composite systems," *Physical Review B*, vol. 35, no. 16, pp. 8749–8752, 1987.

[64] K. Miyasaka, K. Watanabe, E. Jojima, H. Aida, M. Sumita, and K. Ishikawa, "Electrical conductivity of carbon-polymer composites as a function of carbon content," *Journal of Materials Science*, vol. 17, no. 6, pp. 1610–1616, 1982.

[65] F. J. Balta Calleja, R. K. Bayer, and T. A. Ezquerra, "Electrical conductivity of polyethylene-carbon-fibre composites mixed with carbon black," *Journal of Materials Science*, vol. 23, no. 4, pp. 1411–1415, 1988.

[66] A. Malliaris, "Influence of Particle Size on the Electrical Resistivity of Compacted Mixtures of Polymeric and Metallic Powders," *Journal of Applied Physics*, vol. 42, no. 2, p. 614, 1971.

[67] M. L. Clingerman, J. a. King, K. H. Schulz, and J. D. Meyers, "Evaluation of electrical conductivity models for conductive polymer composites," *Journal of Applied Polymer Science*, vol. 83, no. 6, pp. 1341–1356, 2002.

[68] B. Wessling, "Electrical conductivity in heterogeneous polymer systems. V (1): Further experimental evidence for a phase transition at the critical volume concentration," *Polymer Engineering & Science*, vol. 31, no. 16, pp. 1200–1206, 1991.

[69] I. Novák, I. Krupa, and I. Chodák, "Electroconductive adhesives based on epoxy and polyurethane resins filled with silver-coated inorganic fillers," *Synthetic Metals*, vol. 144, no. 1, pp. 13–19, 2004.

[70] S. K. Anuar, M. Mariatti. A. Azizan, N. C. Mang, and W. T. Tham, "Effect of different types of silver and epoxy systems on the properties of silver / epoxy conductive adhesives," *Journal of Materials Science: Materials in Electronics*, vol. 22, no. 7, pp. 757-764, 2011.

[71] M. Rong, M. Zhang, H. Liu, and H. Zeng, "Synthesis of silver nanoparticles and their self-organization behavior in epoxy resin," *Polymer*, vol. 40, pp. 6169–6178, 1999.

[72] W. Jia, R. Tchoudakov, R. Joseph, M. Narkis, and A. Siegmann, "The conductivity behavior of multi-component epoxy, metal particle, carbon black, carbon fibril composites," *Journal of Applied Polymer Science*, vol. 85, no. 8, pp. 1706–1713, 2002.

[73] G. M. Tsangaris, N. Kouloumbi, G. C. Psarras, E. Manolakaki, G. Ponticopoulos, and D. Tsekouras, "Conductivity and percolation in polymeric particulate composites of epoxy resin and conductive fillers," in *Seventh International Conference on Dielectric Materials, Measurements and Applications*, pp. 100–102. 1996

[74] B. M. Amoli, S. Gumfekar, A. Hu, Y. N. Zhou, and B. Zhao, "Thiocarboxylate functionalization of silver nanoparticles: effect of chain length on the electrical conductivity of nanoparticles and their polymer composites," *Journal of Materials Chemistry*, vol. 22, no. 37, p. 20048, 2012.

[75] W.-J. Jeong, H. Nishikawa, D. Itou, and T. Takemoto, "Electrical Characteristics of a New Class of Conductive Adhesive," *Materials Transactions*, vol. 46, no. 10, pp. 2276–2281, 2005.

[76] W. Liu, M. Lee, M. Pecht, and R. Martens, "An investigation of the contact resistance of a commercial elastomer interconnect under thermal and mechanical stresses," *IEEE Transactions on Device and Materials Reliability*, vol. 3, no. 2, pp. 39–43, 2003.

[77] H. K. Kim and F. G. Shi, “Electrical reliability of electrically conductive adhesive joints : dependence on curing condition and current density,” *Microelectronics Journal*, vol. 32, pp. 315–321, 2001.

[78] A. Lovinger, “Development of electrical conduction in silver-filled epoxy adhesives,” *The Journal of Adhesion*, vol. 10, pp. 1–15, 1979.

[79] Z. Mo, X. Wang, T. Wang, S. Li, Z. Lai, and J. Liu, “Electrical Characterization of Isotropic Conductive Adhesive under Mechanical Loading,” *Journal of Electronic Materials*, vol. 31, no. 9, 2002.

[80] X. Lu, W. Wu, J. Chen, P. Zhang, and Y. Zhao, “Preparation of Polyaniline Nanofibers by High Gravity Chemical Oxidative Polymerization,” *Industrial & Engineering Chemistry Research*, vol. 50, no. 9, pp. 5589–5595, 2011.

[81] Y. Zhao, W. Wu, J. Chen, H. Zou, L. Hu, and G. Chu, “Preparation of Polyaniline/Multiwalled Carbon Nanotubes Nanocomposites by High Gravity Chemical Oxidative Polymerization,” *Industrial & Engineering Chemistry Research*, vol. 51, no. 9, pp. 3811–3818, 2012.

[82] B. Moginger, “The determination of a general time creep compliance relation of linear viscoelastic materials under constant load and its extension to nonlinear viscoelastic behavior for the Burger model,” *Rheologica Acta*, vol. 32, no. 4, pp. 370–379, 1993.

[83] F. Akyildiz, R. S. Jones, and K. Walters, “On the spring-dashpot representation of linear viscoelastic behaviour,” *Rheologica Acta*, vol. 29, no. 5, pp. 482–484, 1990.

[84] N. E. Marcovich and M. A. Villar, “Thermal and mechanical characterization of linear low-density polyethylene/wood flour composites,” *Journal of Applied Polymer Science*, vol. 90, no. 10, pp. 2775–2784, 2003.

[85] A. J. Nunez., N. E. Marcovich, and M. I. Aranguren, “Analysis of the creep behavior of polypropylene-woodflour composites,” *Polymer Engineering and Science*, vol. 44, no. 8, pp. 1594–1603, 2004.

[86] B. A. Acha, M. M. Reboredo, and N. E. Marcovich, “Creep and dynamic mechanical behavior of PP–jute composites: Effect of the interfacial adhesion,” *Composites Part A: Applied Science and Manufacturing*, vol. 38, no. 6, pp. 1507–1516, 2007.

[87] T. Ding, L. Wang, and P. Wang, “Changes in electrical resistance of carbon-black-filled silicone rubber composite during compression,” *Journal of Polymer Science: Part B: Polymer Physics*, vol. 45, pp. 2700–2706, 2007.

[88] Y. Wang and X. Jing, “Intrinsically conducting polymers for electromagnetic interference shielding,” *Polymers for Advanced Technologies*, vol. 16, no. 4, pp. 344–351, 2005.

[89] R. Zhang, K. Moon, W. Lin, J. C. Agar, and C. P. Wong, "A simple, low-cost approach to prepare flexible highly conductive polymer composites by in situ reduction of silver carboxylate for flexible electronic applications," *Composites Science and Technology*, vol. 71, no. 4, pp. 528–534, 2011.

[90] S. Jafarzadeh, E. Thormann, T. Rönnevall, A. Adhikari, P-E. Sundell, J. Pan, and P. M. Claesson, "Toward homogeneous nanostructured polyaniline/resin blends," *ACS Applied Materials & Interfaces*, vol. 3, no. 5, pp. 1681–91, 2011.

[91] Y.-Z. Long, M.-M. Li, C. Gu, M. Wan, J.-L. Duvail, Z. Liu, and Z. Fan, "Recent advances in synthesis, physical properties and applications of conducting polymer nanotubes and nanofibers," *Progress in Polymer Science*, vol. 36, no. 10, pp. 1415–1442, 2011.

[92] X. Lu, W. Zhang, C. Wang, T. C. Wen, and Y. Wei, "One-dimensional conducting polymer nanocomposites: Synthesis, properties and applications," *Progress in Polymer Science*, vol. 36, no. 5, pp. 671–712, 2011.

[93] D. Li, J. Huang, and R. B. Kaner, "Polyaniline nanofibers: a unique polymer nanostructure for versatile applications.," *Accounts of chemical research*, vol. 42, no. 1, pp. 135–45, 2009.

[94] B. J. Polk, K. Potje-Kamloth, M. Josowicz, and J. Janata, "Role of Protonic and Charge Transfer Doping in Solid-State Polyaniline," *The Journal of Physical Chemistry B*, vol. 106, no. 44, pp. 11457–11462, 2002.

[95] B. Dufour, P. Rannou, D. Djurado, H. Janeczek, M. Zagorska, A. De Geyer, J. Travers, and A. Pron, "Low Tg , Stretchable Polyaniline of Metallic-Type Conductivity : Role of Dopant Engineering in the Control of Polymer Supramolecular Organization and in the Tuning of Its Properties," *Chem. Mater.*, vol. 15, no. 8, pp. 1587–1592, 2003.

[96] Y. Fong and J. Schlenoff, "Polymerization of aniline using mixed oxidizers," *Polymer*, vol. 36, no. 3, pp. 639–643, 1995.

[97] F. Lux, "Properties of electronically conductive polyaniline: a comparison between well-known literature data and some recent experimental findings," *Polymer*, vol. 35, no. 14, pp. 2915–2936, 1994.

[98] G. Morales, M. Llusa, M. Miras, and C. Barbero, "Effects of high hydrochloric acid concentration on aniline chemical polymerization," *Polymer*, vol. 38, no. 20, pp. 5247–5250, 1997.

[99] W. Zheng, M. Angelopoulos, A. J. Epstein, and A. G. MacDiarmid, "Experimental Evidence for Hydrogen Bonding in Polyaniline : Mechanism of Aggregate Formation and Dependency on Oxidation State," *Macromolecules*, vol. 30, no. 10, pp. 2953–2955, 1997.

[100] J. H. Jun, K. Cho, J. Yun, K. S. Suh, T. Kim, and S. Kim, "Enhancement of electrical characteristics of electrospun polyaniline nanofibers by embedding the nanofibers with Ga-doped ZnO nanoparticles," *Organic Electronics*, vol. 9, no. 4, pp. 445–451, 2008.

[101] J. Li, Q. Jia, J. Zhu, and M. Zheng, "Interfacial polymerization of morphologically modified polyaniline : from hollow microspheres to nanowires," *Polymer International*, vol. 57, no. 2, pp. 337–341, 2008.

[102] A. Watanabe, K. Mori, A. Iwabuchi, Y. Iwasaki, Y. Nakamura, and O. Ito, "Electrochemical polymerization of aniline and N-alkylanilines," *Macromolecules*, vol. 22, no. 9, pp. 3521–3525, 1989.

[103] M. A. Dar, R. K. Kotnala, V. Verma, J. Shah, W. A. Siddiqui, and M. Alam, "High Magneto-Crystalline Anisotropic Core–Shell Structured $Mn_{0.5}Zn_{0.5}Fe_2O_4$ /Polyaniline Nanocomposites Prepared by in Situ Emulsion Polymerization," *The Journal of Physical Chemistry C*, vol. 116, no. 9, pp. 5277–5287, 2012.

[104] E. Marie, R. Rothe, M. Antonietti, and K. Landfester, "Synthesis of Polyaniline Particles via Inverse and Direct Miniemulsion," *Macromolecules*, vol. 36, no. 11, pp. 3967–3973, 2003.

[105] S. Palaniappan and A. John, "Polyaniline materials by emulsion polymerization pathway," *Progress in Polymer Science*, vol. 33, no. 7, pp. 732–758, 2008.

[106] M. J. Antony and M. Jayakannan, "Molecular template approach for evolution of conducting polymer nanostructures: tracing the role of morphology on conductivity and solid state ordering.," *The Journal of Physical Chemistry. B*, vol. 114, no. 3, pp. 1314–24, 2010.

[107] J. Janata and M. Josowicz, "Conducting polymers in electronic chemical sensors.," *Nature Materials*, vol. 2, no. 1, pp. 19–24, 2003.

[108] S. E. Bourdo, V. Saini, J. Piron, I. Al-Brahim, C. Boyer, J. Rioux, V. Bairi, A. S. Biris, and T. Viswanathan, "Photovoltaic device performance of single-walled carbon nanotube and polyaniline films on n-Si: device structure analysis.," *ACS Applied Materials & Interfaces*, vol. 4, no. 1, pp. 363–8, 2012.

[109] S.-J. Tang, A.-T. Wang, S.-Y. Lin, K.-Y. Huang, C.-C. Yang, J.-M. Yeh, and K.-C. Chiu, "Polymerization of aniline under various concentrations of APS and HCl," *Polymer Journal*, vol. 43, no. 8, pp. 667–675, 2011.

[110] A. Pud, N. Ogurtsov, A. Korzhenko, and G. Shapoval, "Some aspects of preparation methods and properties of polyaniline blends and composites with organic polymers," *Progress in Polymer Science*, vol. 28, no. 12, pp. 1701–1753, 2003.

[111] D. Li and R. B. Kaner, "Shape and aggregation control of nanoparticles: not shaken, not stirred.," *Journal of the American Chemical Society*, vol. 128, no. 3, pp. 968–75, 2006.

[112] D. Li and R. B. Kaner, "How nucleation affects the aggregation of nanoparticles," *Journal of Materials Chemistry*, vol. 17, no. 22, p. 2279, 2007.

[113] H. Ding, J. Shen, M. Wan, and Z. Chen, “Formation Mechanism of Polyaniline Nanotubes by a Simplified Template-Free Method,” *Macromolecular Chemistry and Physics*, vol. 209, no. 8, pp. 864–871, 2008.

[114] M. Trchová, I. Seděnková, E. N. Konyushenko, J. Stejskal, P. Holler, and G. Cirić-Marjanović, “Evolution of polyaniline nanotubes: the oxidation of aniline in water.,” *The Journal of Physical Chemistry. B*, vol. 110, no. 19, pp. 9461–8, 2006.

[115] C. Chen, C.-F. Mao, S.-F. Su, and Y.-Y. Fahn, “Preparation and characterization of conductive poly(vinyl alcohol)/polyaniline doped by dodecyl benzene sulfonic acid (PVA/PANDB) blend films,” *Journal of Applied Polymer Science*, vol. 103, no. 5, pp. 3415–3422, 2007.

[116] J. Stejskal, I. Sapurina, M. Trchová, and E. N. Konyushenko, “Oxidation of Aniline: Polyaniline Granules, Nanotubes, and Oligoaniline Microspheres,” *Macromolecules*, vol. 41, no. 10, pp. 3530–3536, 2008.

[117] Z. D. Zujovic, L. Zhang, G. A. Bowmaker, P. A. Kilmartin, and J. Travas-Sejdic, “Self-Assembled, Nanostructured Aniline Oxidation Products: A Structural Investigation,” *Macromolecules*, vol. 41, no. 9, pp. 3125–3135, 2008.

[118] T. Abdiryim, Z. Xiao-Gang, and R. Jamal, “Comparative studies of solid-state synthesized polyaniline doped with inorganic acids,” *Materials Chemistry and Physics*, vol. 90, no. 2–3, pp. 367–372, 2005.

[119] R. Sainz, W. R. Small, N. A. Young, C. Vallés, A. M. Benito, W. K. Maser, and M. in het Panhuis, “Synthesis and Properties of Optically Active Polyaniline Carbon Nanotube Composites,” *Macromolecules*, vol. 39, no. 21, pp. 7324–7332, 2006.

[120] Y. Xia, J. Wiesinger, and A. G. MacDiarmid, “Camphorsulfonic acid fully doped polyaniline emeraldine salt: conformations in different solvents studied by an ultraviolet/visible/near-infrared spectroscopic method,” *Chemistry of Materials*, vol. 7, no. 3, pp. 443–445, 1995.

[121] J. P. Pouget, M. E. Jozefowicz, a. J. Epstein, X. Tang, and a. G. MacDiarmid, “X-ray structure of polyaniline,” *Macromolecules*, vol. 24, no. 3, pp. 779–789, 1991.

[122] P. Kahol, N. Pinto, E. J. Berndtsson, and B. J. McCormick, “Electron localization effects on the conducting state in polyaniline,” *Journal of Physics: Condensed Matter*, vol. 6, pp. 5631–5638, 1994.

[123] L. Zhang, Y. Long, Z. Chen, and M. Wan, “The Effect of Hydrogen Bonding on Self-Assembled Polyaniline Nanostructures,” *Advanced Functional Materials*, vol. 14, no. 7, pp. 693–698, 2004.

[124] Y. Moon, Y. Cao, P. Smith, and A. Heeger, “X-ray scattering from crystalline polyaniline.,” *Polymer Communications*, vol. 30, no. 7, pp. 196–199, 1989.

[125] S. D. Shinde and M. Jayakannan, “Probing the Molecular Interactions at the Conducting Polyaniline Nanomaterial Surface via a Pyrene Fluorophore,” *The Journal of Physical Chemistry C*, vol. 114, no. 36, pp. 15491–15498, 2010.

[126] P. Anilkumar and M. Jayakannan, “A novel supramolecular organogel nanotubular template approach for conducting nanomaterials.,” *The Journal of Physical Chemistry. B*, vol. 114, no. 2, pp. 728–36, 2010.

[127] P. Anilkumar and M. Jayakannan, “Self-assembled cylindrical and vesicular molecular templates for polyaniline nanofibers and nanotapes.,” *The Journal of Physical Chemistry. B*, vol. 113, no. 34, pp. 11614–24, 2009.

[128] P. Anilkumar and M. Jayakannan, “Fluorescent Tagged Probing Agent and Structure-Directing Amphiphilic Molecular Design for Polyaniline Nanomaterials via Self-Assembly Process,” *Journal of Physical Chemistry C*, vol. 111, no. 9, pp. 3591–3600, 2007.

[129] T. Jana and A. K. Nandi, “Sulfonic Acid-Doped Thermoreversible Polyaniline Gels: Morphological, Structural, and Thermodynamical Investigations,” *Langmuir*, vol. 16, no. 7, pp. 3141–3147, 2000.

[130] T. Jana and A. K. Nandi, “Sulfonic Acid Doped Thermoreversible Polyaniline Gels. 2. Influence of Sulfonic Acid Content on Morphological, Thermodynamical, and Conductivity Properties,” *Langmuir*, vol. 17, no. 19, pp. 5768–5774, 2001.

[131] A. Wolter, P. Rannou, J. Travers, B. Gilles, and D. Djurado, “Model for aging in HCl-protonated polyaniline: Structure, conductivity, and composition studies,” *Physical Review B*, vol. 58, no. 12, pp. 7637–7647, 1998.

[132] P. Rannou and M. Nechtschein, “Aging studies on polyaniline : conductivity and thermal stability,” *Synthetic Metals*, vol. 84, no. 1–3, pp. 755–756, 1997.

[133] Y. Weir, G. Jang, K. F. Hsueh, E. M. Scherr, A. G. Macdiarmid, and A. J. Epstein, “Thermal transitions and mechanical properties of films of chemically prepared polyaniline,” *Polymer*, vol. 33, no. 2, pp. 314–322, 1992.

[134] S. Bhadra and D. Khastgir, “Extrinsic and intrinsic structural change during heat treatment of polyaniline,” *Polymer Degradation and Stability*, vol. 93, no. 6, pp. 1094–1099, 2008.

[135] D. Li and R. B. Kaner, “Processable stabilizer-free polyaniline nanofiber aqueous colloids.,” *Chemical communications*, no. 26, pp. 3286–8, 2005.

[136] J. P. Pouget, M. Laridjani, M. E. Jozefowicz, A. J. Epstein, E. M. Scherr, and A. G. MacDiarmid, “Structural aspects of the polyaniline family of electronic polymers,” *Synthetic Metals*, vol. 51, no. 1–3, pp. 95–101, 1992.

[137] M. Laridjani, J. P. Pouget, E. M. Scherr, A. G. MacDiarmid, M. E. Jozefowicz, and A. J. Epstein, “Amorphography - the relationship between amorphous and crystalline order. 1. The structural origin of memory effects in polyaniline,” *Macromolecules*, vol. 25, no. 16, pp. 4106–4113, 1992.

[138] Wenjie Wang, S. P. Gumfekar, Q. Jiao, and B. Zhao, “Synthesis and Characterizations of Ferrite-on-Polyaniline Nanocomposites for Electromagnetic Absorbing Application,” *Journal of Materials Chemistry (under review)*.